21127

NATIONAL LIBRARY
OTTAWA

CANADA

BIBLIOTHÈQUE NATIONALE
OTTAWA

NAME OF AUTHOR.....CHIN-FONG (FRANK) TSONG

TITLE OF THESIS..STUDIES OF URANIUM-LEAD SYSTEMATICS BY VOLATILIZATION AND THE EVOLUTION OF THE YELLOWKNIFE AREA, N.W.T.

UNIVERSITY....OF ALBERTA, EDMONTON, CANADA

DEGREE FOR WHICH THESIS WAS PRESENTED.....PH.D.

YEAR THIS DEGREE GRANTED......1974

Permission is hereby granted to THE NATIONAL LIBRARY OF CANADA to microfilm this thesis and to lend or sell copies of the film.

The author reserves other publication rights, and neither the thesis nor extensive extracts from it may be printed or otherwise reproduced without the author's written permission.

(Signed)..F. C. F. Tsong

PERMANENT ADDRESS:

1496-5A AVE N.E.
MEDICINE HAT, ALBERTA

DATED...Feb 11.........1974

NL-91 (10-68)

THE UNIVERSITY OF ALBERTA

STUDIES OF URANIUM-LEAD SYSTEMATICS BY VOLATILIZATION AND THE EVOLUTION OF THE YELLOWKNIFE AREA, N.W.T.

by

© CHIN-FONG (FRANK) TSONG B.Sc., M.Sc.

A THESIS

SUBMITTED TO THE FACULTY OF GRADUATE STUDIES AND RESEARCH

IN PARTIAL FULFILMENT OF THE REQUIREMENTS FOR THE DEGREE

OF DOCTOR OF PHILOSOPHY

DEPARTMENT OF PHYSICS

EDMONTON, ALBERTA

SPRING, 1974

THE UNIVERSITY OF ALBERTA

FACULTY OF GRADUATE STUDIES AND RESEARCH

The undersigned certify that they have read, and recommend to the Faculty of Graduate Studies and Research, for acceptance, a thesis entitled "Studies of uranium-lead systematics by volatilization and the evolution of the Yellowknife area, N.W.T." submitted by Chin-Fong (Frank) Tsong, B.Sc., M.Sc., in partial fulfilment of the requirements for the degree of Doctor of Philosophy.

G.L. Cumming
Supervisor

H. Baadsgaard

R.M. Farquhar
External Examiner

November, 1973

ABSTRACT

Studies of uranium-lead systematics in eight plutonic rocks indicate that the western granodiorite which intrudes the Yellowknife volcanics has whole rock and mineral isochron ages of 2700 ± 85 m.y. and 2550 ± 70 m.y. respectively. Some new sulfide and galena data from the Yellowknife volcanics and the sediments suggest a mineralization age of close to 2630 m.y.. Fractional removal of lead from one southeast granodiorite rock sample yields a mineral isochron age of 2660 ± 45 m.y.. There is a strong indication that the most acidic phase of the Stock Lake intrusive was remobilized at about 1880 ± 75 m.y..

The volatilization technique with an induction furnace was used for extractions of most of the lead samples studied in this thesis and this technique was found to be highly satisfactory.

Some experimental data on mass discrimination suggest that different positioning of the sample filaments between runs may produce appreciable mass dependent errors in the measured isotopic ratios.

ACKNOWLEDGMENTS

The writer wishes to express his sincere appreciation to Dr. G. L. Cumming for his enthusiastic supervision and constant assistance which made this thesis possible. The writer is also deeply indebted to Dr. H. Baadsgaard of the Department of Geology who helped the writer so often and in so many ways with his skilled analytical techniques.

Lead-free water and other repurified acids for lead extraction purposes were made available to the writer by the Department of Geology through the courtesy of Dr. Baadsgaard and his associates and is very much appreciated.

The automatic digital mass spectrometer designed by Dr. Cumming was maintained during this project by the able technicians Mr. M. Burke, Mr. H. McCullough and Mr. W. Williams. Considerable improvements in the design of the cold finger and vacuum evacuation system used for volatilization were made by Mr. D. Kristic.

Financial assistance was provided by the University of Alberta in the form of a Graduate Teaching Assistantship (1968-69) and a University of Alberta Dissertation Fellowship (1969-70) and is greatly appreciated.

TABLE OF CONTENTS

CHAPTER PAGE

I. INTRODUCTION 1

Introduction 1

Sample locations 2

Radiometric dating 8

Mass spectrometry 9

II. DETERMINATION OF U, Th AND Pb 10

Determination of U and Th 10

Neutron activation 11

Comparison of chemical and neutron activation methods for U and Th determinations 13

Method used for U and Th determinations 14

Extraction of Pb from rock sample 16

Extraction of Pb by volatilization 17

Mass spectrometric measurement and data reduction 18

Least squares polynomial fitting 19

Internal errors and external reproducibility.. 26

Test runs on standard samples and mass dependent errors 28

III. VOLATILIZATION 33

Introduction 33

Furnaces 34

Analytical procedures 37

Loading PbS on the filament 38

Blanks 39

IV. MASS DISCRIMINATION IN A MASS SPECTROMETER 42

Introduction 42

Measuring error and fractionation due to
the positioning of the filament 44

Focusing effects on the isotope ratios 45

Conclusions on the mass discrimination
experiments 50

V. WHOLE ROCK DATA AND U/Pb AGES 53

Whole rock Pb, U and Th determinations 53

Uranium-lead radiometric method 56

Whole rock lead-lead and uranium-lead ages .. 68

Possible three or higher-stage system 73

Second whole rock ratios 74

VI. ISOTOPIC COMPOSITION OF FRACTIONALLY VOLATILIZED
LEAD AND THE TEMPERATURE ISOCHRON 78

Introduction 78

Temperature isochron 82

Two-stage model temperature isochron ages ... 98

Mineral and whole rock isochrons 100

Some implications 105

Temperature isochron of southeast granodiorite 107
VII. MINERAL LEAD COMPOSITION AND THE MINERAL ISOCHRON 110
Introduction and mineral separation 110
Mineral lead composition and the mineral isochron 111
Sulfide mineral isochron of the Yellowknife volcanics 117
An indication of the age of the Yellowknife metasediments 125
VIII. SUMMARY AND CONCLUSIONS 126
Introduction 126
Interpretation and comparison with other results 126
Mass discrimination 129

****

REFERENCES CITED 131
APPENDIX I. SOME FORMULAS ON VECTOR DIFFERENTIATION 136
APPENDIX II. COMPUTER PROGRAMS FOR DATA REDUCTION BY IBM 360 137
APPENDIX III. DITHIZONE EXTRACTION PROCEDURES 162
VITA 164

LIST OF TABLES

Table	Description	Page
1	Isotopic ratios of "Broken Hill" galena	31
2	Isotopic ratios of "NBS Equal Atom #982" lead	32
3	Blanks test runs on combined volatilization and dithizone purification of lead	40
4	Ratios of a lead sample continously run for six hours	46
5	Ratios of a lead sample (same sample as that used in Table 4)	47
6	Ratios of a lead sample (same sample as that used in Table 4)	48
7	Fractionation test of different focusing made on different isotopes	51
8	Whole rock lead isotopic ratios	54
9	Pb, U, Th concentrations and U-Pb ages	55
10	Comparison of U and Th concentration determinations by isotope dilution and neutron activation methods	57
11	Comparison of whole rock Pb ratios between the first and second heatings	75
12	Pb ratios of fractionally volatilized lead	83
13	Slope ages of the temperature isochrons	99

14 Ratios of the volatilized lead of the southeast granodiorite 108
15 Mineral lead ratios of the western granodiorite 112
16 Slope ages and μ values of the mineral isochrons 118
17 Pb ratios of sulfide samples from the Yellowknife volcanics 119
18 Pb ratios of galena samples from the Yellowknife volcanics 121

LIST OF FIGURES

Figure		Page
1.	Geological map of the Yellowknife area	3
2.	Schematic geological model of the Yellowknife area	4
3.	Sample locations	5
4.	Sample locations	6
5.	Neutron-induced fission cross-section as a function of energy	12
6.	Time series of a mass spectrum	20
7.	Polynomial fitting of points	27
8.	Time series of raw and smoothed data	29
9.	Schematic diagram of the high temperarure brick furnace	35
10.	Schematic diagram of the sample assemblage in place in the coil of the induction furnace	36
11.	The development of lead in a two stage system and the lead-lead diagram	61
12.	The development of lead in a three stage system and the lead-lead diagram for lead that has	

evolved according to a three stage f_1=constant history 63
13. Lead-lead diagram for lead that has evolved according to a three stage f_2=constant history 65
14. Modified concordia plot for a two stage evolution of lead 67
15. Modified concordia diagrams for lead that has evolved according to a three stage f_1 and f_2 constant history 69
16. Whole rock lead isochron 70
17. Modified concordia plot of samples from western granodiorite 72
18. Whole rock lead isochron (second heating) 77
19. Temperature isochron of YKWG #1 90
20. Temperature isochron of YKWG #2 91
21. Temperature isochron of YKWG #3 92
22. Temperature isochron of YKWG #4 93
23. Temperature isochron of YKWG #5 94
24. Temperature isochron of YKWG #6 95
25. Temperature isochron of YKWG #7 96
26. Temperature isochron of YKWG #8 97
27. All temperature isochron 101

28. Effect of metamorphism on the change in the Sr^{87}/Sr^{86} with time in a rock and its constituent minerals 103

29. Variation in Sr^{87}/Sr^{86} vs. Rb^{87}/Sr^{86} for whole rock and the effect on the constituent minerals by a metamorphic event at time, t_m 104

30. Lead-lead diagram for whole rocks and minerals showing a two-event history 107

31. Temperature isochron of the southeast granodiorite 109

32. Mineral isochron of YKWG #1 114

33. Mineral isochron of YKWG #4 115

34. Mineral isochron of YKWG #5 116

35. Mineral isochron of the Yellowknife volcanics 122

36. Lead-lead diagram of galena samples from the Yellowknife volcanics 124

37. Age measurements of the Yellowknife area 128

CHAPTER I

INTRODUCTION

1.1. Introduction

As part of a continuing investigation of the geological evolution of the Yellowknife area, this thesis presents the results and interpretations of a study of lead-uranium systematics on several plutonic rock samples of this area.

All the leads studied in this thesis are extracted from rocks and minerals by volatilization. It was felt that the volatilization technique for the removal of trace amounts of rock lead for radiometric dating purposes may have some advantages over other methods, and that a closer study of this technique might be fruitful in an area well investigated geochronologically.

Yellowknife is located on the north shore of Great Slave Lake, approximately 700 miles north of Edmonton. The area surrounding Yellowknife has been well studied by investigators using various radiometric methods (Keevil et al (1942), helium method; Folinsbee et al (1956), K/Ar; Folinsbee (1955), radiation dosage; Cumming et al (1955), model lead ages on galena; Burwash and Baadsgaard (1962), K/Ar; Van Breeman (1965), Rb/Sr; Robertson and Cumming (1968), model lead ages on galena; Green et al (1968), Rb/Sr; Green and Baadsgaard (1971), U/Pb in zircons; Gates and Hurley (1973), Rb/Sr on dykes). Besides checking the volatilization technique for whole rock radiometric dating, it is hoped that the addition of a whole rock lead-uranium study will yield a more complete picture of the geological evolution of the area.

1.2. Sample locations

Figure 1 shows a map of the Yellowknife area. The regional geology has been described in detail by Green (1968) and is not repeated in this thesis. A schematic geological model of this area is illustrated by Figure 2 with some of the relevant age measurements on the rocks indicated. The Yellowknife group consists of acidic to basic volcanics overlain by a thick sequence of sedimentary rocks and is intruded by three major plutonic bodies. The southeast granodiorite intrudes the sediments from the southeast, the Prosperous Lake granite intrudes the sediments around Prosperous Lake and the western granodiorite intrudes the volcanics from the west. One of the problems posed at the beginning of the investigation was the determination of the age of the western granodiorite by means of whole rock lead-uranium systematics in order to compare it with the ages obtained by Green et al(1968, Rb/Sr) and others.

Eight rock samples were collected in the summer of 1969 from the body of the western granodiorite. These rocks have been dated by the whole rock Rb/Sr method by Green et al (1969) who obtained an age of 2610 ± 58 m.y. ($\lambda_{Rb} = 1.39 \times 10^{-11}$ yr^{-1}) in excellent agreement with similar data on the volcanics themselves. Some of the samples were collected from the same localities as the material used by Green et al (1968).

Twenty-three sulfide and five galena samples collected by A. P. Leech of the Department of Geology and one whole rock sample from the southeast granodiorite obtained from the collection in the Department of Geology were also analysed.

The locations from which samples were obtained from the western granodiorite are shown in greater detail in Figures 3 and 4 and are

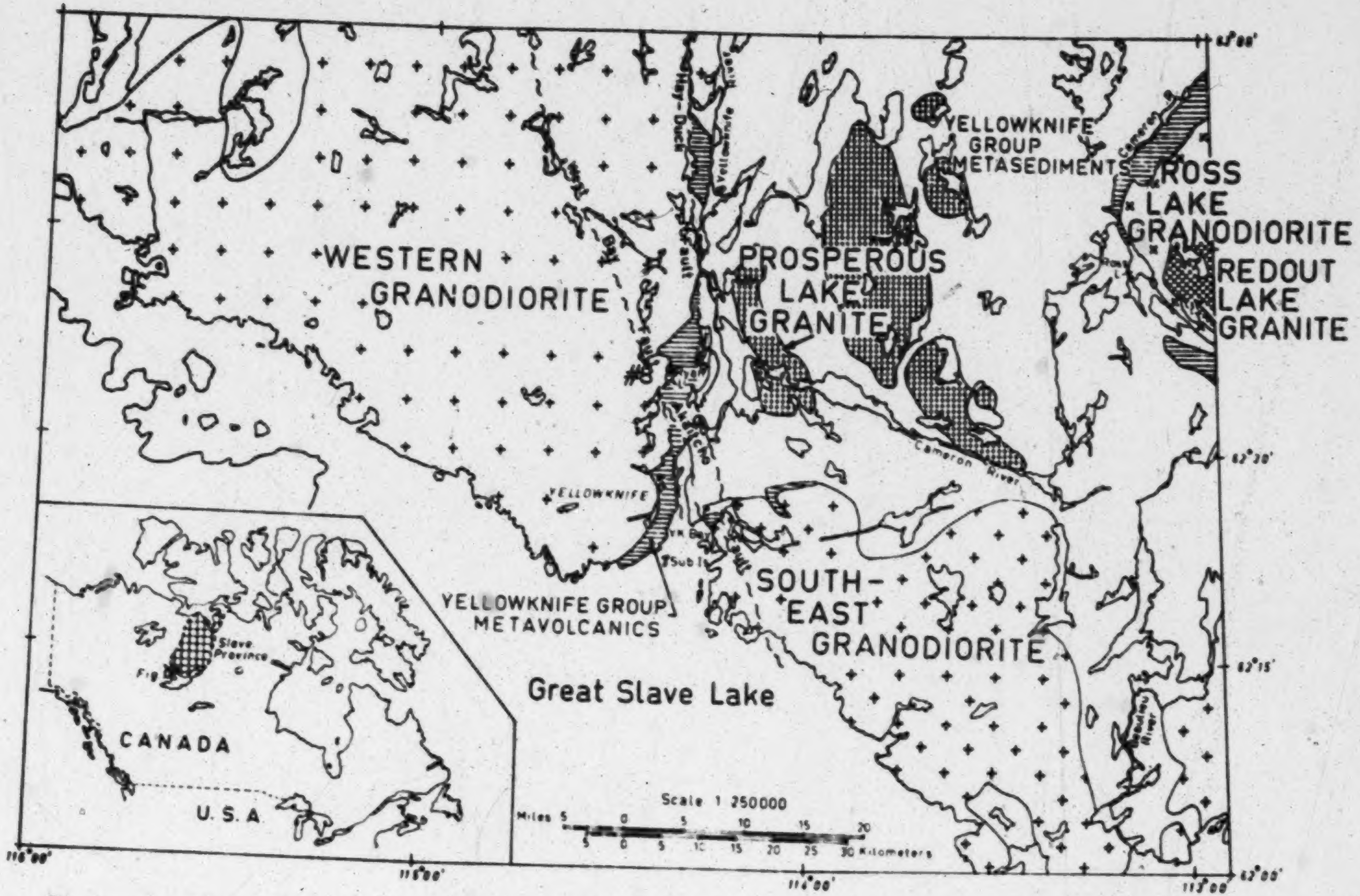

Figure 1. Geological map of the Yellowknife area (after Green and Baadsgaard,1971)

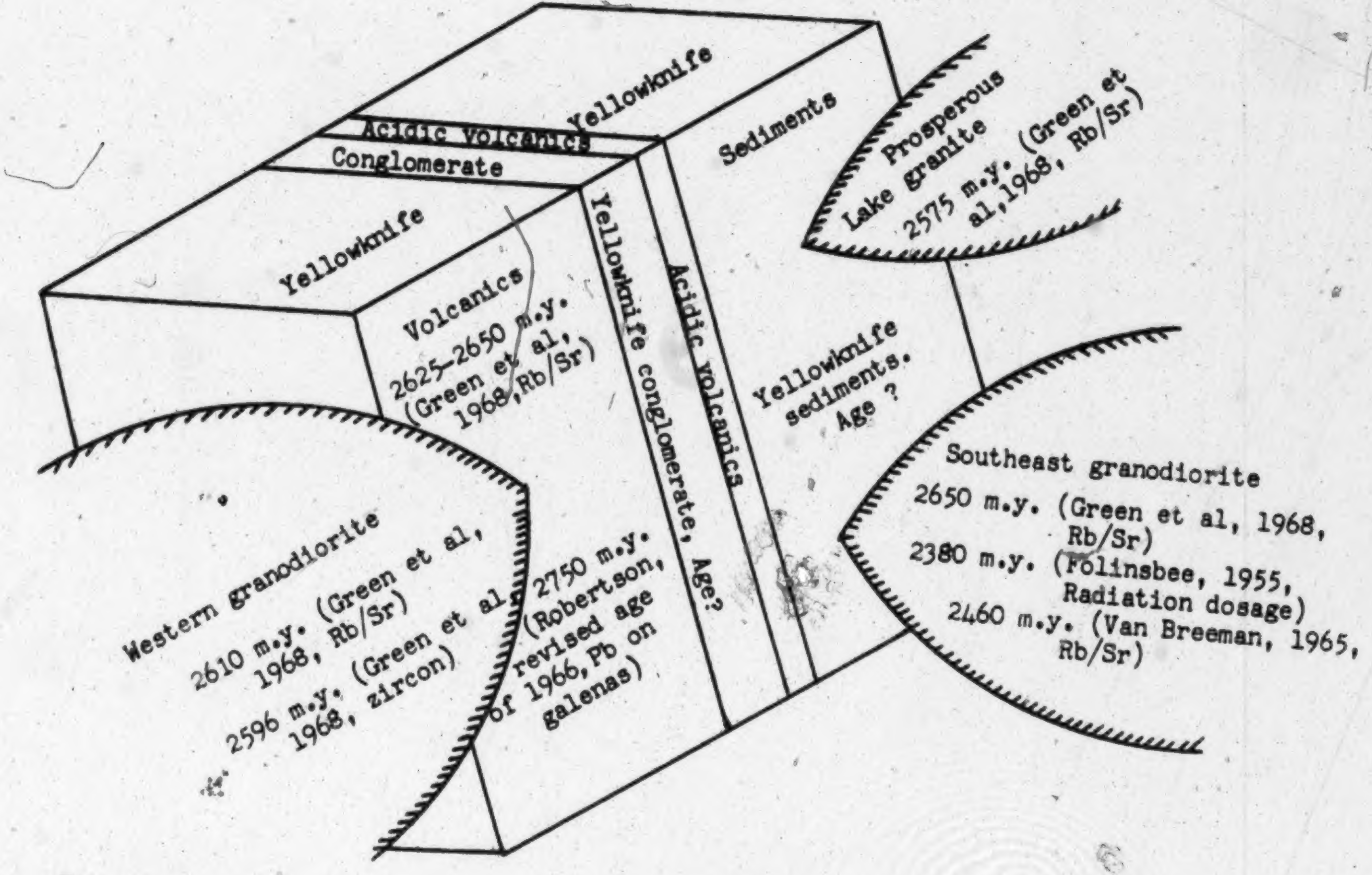

Figure 2. Schematic geological model of the Yellowknife area.

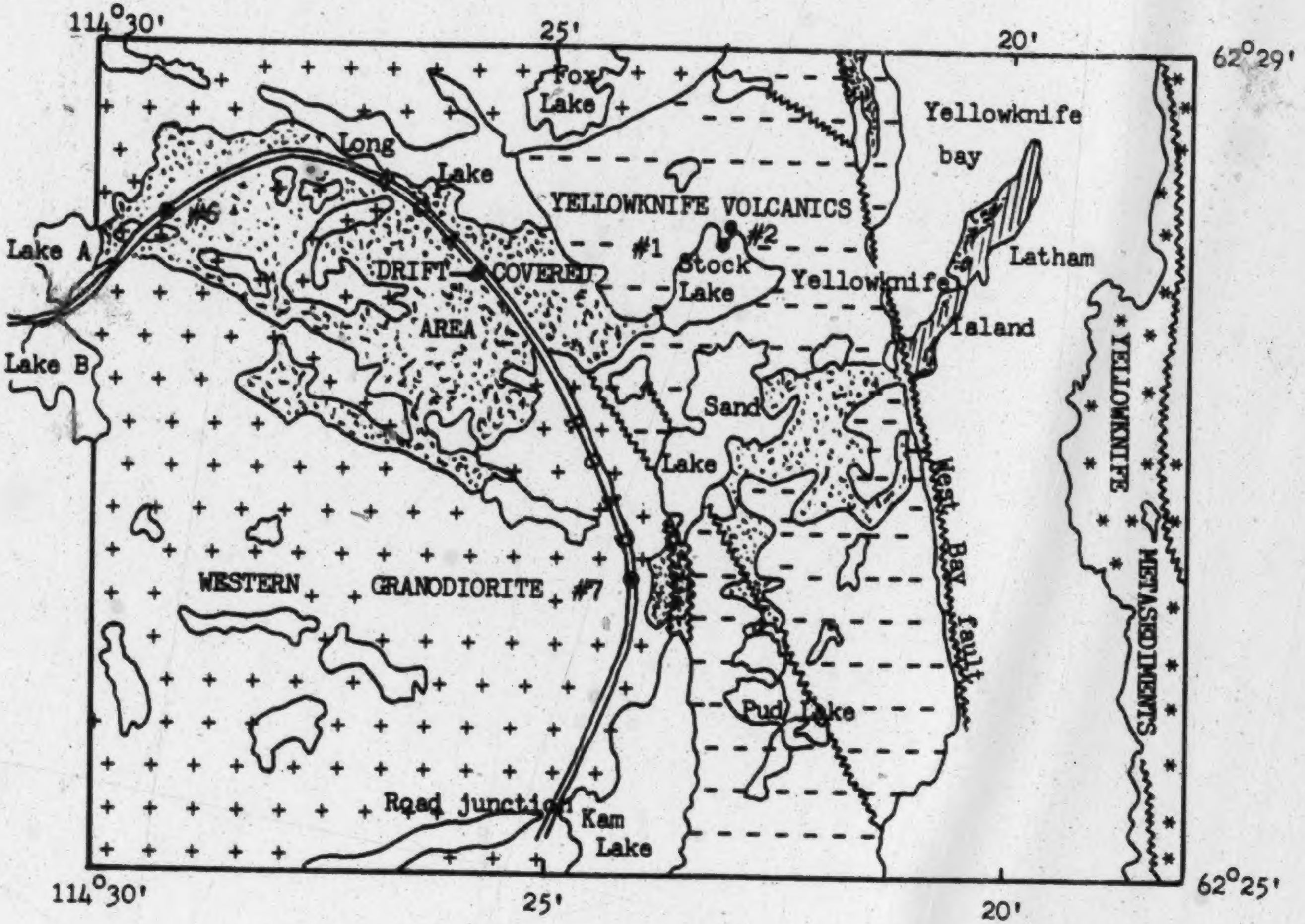

Figure 3. Sample locations

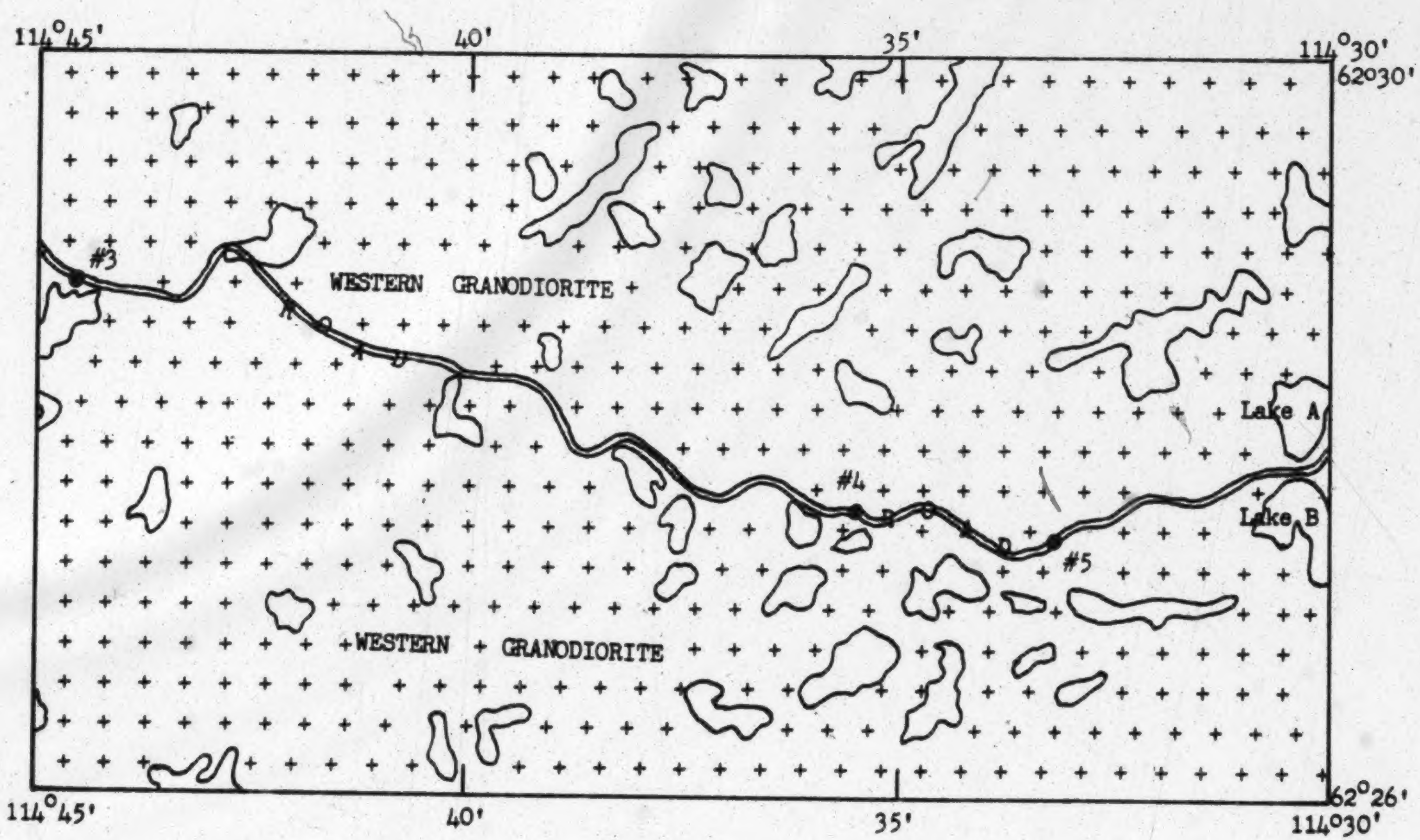

Figure 4. Sample locations

briefly described below;

Sample YKWG #1: Syenite (acidic phase).

Collected from the island in Stock Lake (see map) on the south side of the highway to Yellowknife airport.

Location: 114°23'W, 62°28'N.

Sample YKWG #2: Syenite.

Road cut on the other side of the highway opposite sample YKWG #1.

Location: 114°22.9'W, 62°28.2'N.

Sample YKWG #3: Granodiorite.

9.6 miles on road west of Lake A and Lake B (see map).

Location: 114°30.2'W, 62°27.8'N.

Sample YKWG #4: Granodiorite.

3.1 miles on road west of Lakes A and B.

Location: 114°35.2'W, 62°27.6'N.

Sample YKWG #5: Granodiorite.

1.6 miles on road west of Lakes A and B.

Location: 114°33.0'W, 62°27.4'N.

Sample YKWG #6: Pegmatite.

Collected at 0.9 miles on road east of Lakes A and B.

Location: 114°29.2'W, 62°28.3'N.

Sample YKWG #7: Granodiorite.

From 0.8 miles on road north of the road junction at Kam Lake (see map).

Location: 114°24.1'W, 62°26.4'N.

Sample YKWG #8: Diorite.

From the west shore of Ryan Lake (see map).

Location: 114°21.8'W, 62°35.7'N.

1.3. Radiometric dating

It is well known that the rate of decay of radioactive nuclides remains essentially unchanged regardless of their geological environment . If the amount and rate of decay of the radioactive parent nuclide and the amount of the radiogenic daughter nuclide may be determined, the time taken to accumulate the radiogenic daughter may be determined. There are many naturally-occurring radioactive nuclides each of which is characterized by its decay constant λ, and the daughter nuclides it generates. Only a few are suitable for use as nuclear clocks for radiometric dating (Baadsgaard, 1965). The following decay schemes are commonly used;

$$K^{40} \longrightarrow Ar^{40}$$

$$Rb^{87} \longrightarrow Sr^{87}$$

$$U^{238} \longrightarrow Pb^{206}$$

$$U^{235} \longrightarrow Pb^{207}$$

$$Th^{232} \longrightarrow Pb^{208}.$$

Uranium-lead geochronometry and its application to the problem at hand are described in Chapter V.

An accurate determination of the amount of the radioactive parent as well as the amount and/or the isotopic composition of the accumulated daughter product in the sample is essential. The analytical procedures used for separation of U, Th, and Pb are described in Chapters II and III.

1.4. Mass spectrometry

Mass spectrometry plays an important role in precise measuring of the isotope abundance ratios of an element and the methods of isotope dilution and solid source mass spectrometry make possible the determination of very small amounts of U, Th, and Pb. A description of the mass spectrometric techniques which include data reduction and a discussion of mass discrimination are given in Chapters II and IV.

CHAPTER II

DETERMINATION OF U, Th AND Pb

2.1. Determination of U and Th

Total uranium may be determined by a number of methods which include fluorescence, photometry, colorimetry, polarography and alpha counting for small amounts, while classical gravimetric and titrimetric procedures may be used for samples high in uranium. Thorium may be determined by colorimetry for small amounts or by titrimetric and gravimetric procedures for large amounts (Baadsgaard, 1965). More recently various neutron activation techniques have been applied successfully to rocks containing trace amounts of U and Th (Amiel, 1962; Morgan and Lovering, 1963, 1968; Gale, 1967; Fisher, 1970).

The mass spectrometric method of isotope dilution is used most often for the accurate determination of small amounts of uranium and thorium contained in the sample. U^{235} and Th^{230} are utilized as isotope dilutants or spikes, and U^{235} in a sample is computed from the known ratio of U^{238}/U^{235} and the determined amount of U^{238}. Th^{232} contained in the sample can be calculated from the amount of Th^{230} added and the measured ratio Th^{232}/Th^{230}.

Before mass spectrometric analysis, U and Th are separated from the rock sample. The process involves chemical dissolution of the rock powder (spiked or unspiked) and the use of ion exchange or other methods to recover uranium and thorium from solution. Blanks are always introduced through the chemical reagents used in the separation and an important problem is to ensure complete solution of the U and

Th. Krogh (1972) recently developed a high pressure decomposition technique for the extraction of U and Pb from zircons with very small blanks. Samples are decomposed at 220°C with 48% HF in a self-sealing Teflon capsule confined by a stainless steel jacket; uranium and lead are isolated from the solutions on a Teflon anion exchange column using Dowex 1 resin. Because of the relatively small amount of chemicals required, the blanks are reduced. This high pressure decomposition technique could also be applied to whole rock samples.

2.2. Neutron activation

A new method for U and Th analysis has recently been developed by Gale (1967) and others. This method is based on the detection of delayed neutrons emitted in the decay of fission products of uranium and thorium. Details of the analytical technique have been described by Gale (1967) following some previous studies and applications of this technique by Amiel (1962). The sample is exposed to the intense neutron flux inside a nuclear reactor, and it is the difference in fission cross sectional dependence on neutron energy which make possible the determination of U^{235}, U^{238} and Th^{232}.

It can be seen from Figure 5 that fast neutrons induce fission principally in Th^{232} and U^{238} while slow neutrons produce fission in U^{235}. Since the transuranic elements such as Np^{237}, Pu^{239}, etc. are virtually absent in geological material (Gale, 1967), the detection of delayed neutrons following exposure of a sample to either slow (thermal) or fast neutrons is characteristic of the presence of U^{235} or Th^{232} and/or U^{238}.

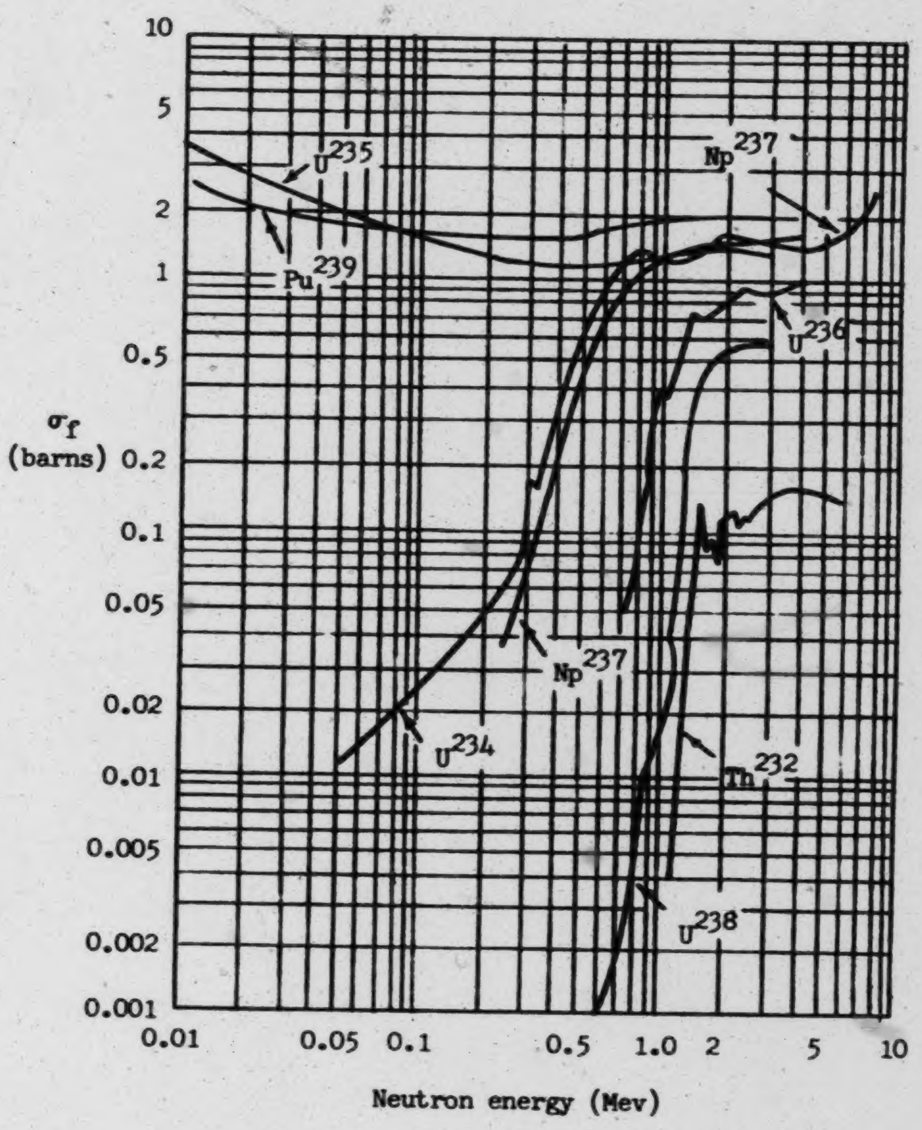

Figure 5. Neutron-induced fission cross-section as a function of energy. (after Gale, 1967)

Two measurements, one in a mixed flux which yields primarily U^{235} fission products and a second with the slow neutrons screened out with a Cd shield are required. The interference of U^{238} on Th^{232} of the second measurement can be corrected from the known ratio of natural uranium and the first measurement. Gale (1967) mentioned a possible interference from the large γ-ray flux emanating from Al^{28} formed in the irradiated sample and noted that the effect is especially serious in feldspar rich samples with high aluminium content. Cumming (personal communication) has shown that this effect may be controlled and that the only serious interference is from the reaction $O^{17}(n,p)N^{17}$, N^{17} decaying to an excited state of O^{17} which then decays by neutron emission, and that this interference is only important at very low U and Th concentrations.

The neutron counts of a sample are compared to those of standards and the amount of U and Th contained in the sample can be calculated. During the course of this work it was possible to compare results from the neutron activation-delayed neutron technique with isotope dilution measurements.

2.3. Comparison of chemical and neutron activation methods for U and Th determinations

When comparing methods some pertinent questions to be asked are; (i). Can the particular method be conveniently carried out in one's laboratory? (ii). How much blank error is involved? (iii). How much time is required?. Based on these questions the advantage of one method over the other may be evaluated. The chemical method is more readily available than the neutron activation technique since the latter requires the use of a nuclear reactor. As there is no need for treatment of the sample, no blank is involved in neutron activation while blanks are always introduced in the chemical method, but with the use of super-pure chemicals and improved decomposition techniques the blank can be reduced, controlled and/or corrected. The time required for a typical single analysis is quite long for the chemical method compared to that required by the neutron activation technique.

Perhaps the biggest advantage of the neutron activation technique over the chemical method is that the activation technique is non-destructive. The sample that had been analysed for uranium and thorium can also be analysed for lead thus eliminating the problem of sample homogeneity. This is very important because large inhomogeneities in the distributions of lead and uranium have been demonstrated to have occurred in meteorites by Marshall (1962) and Goles et al (quoted from Gale, 1967) and could also occur in terrestrial materials.

2.4. Method used for U and Th determinations

Chemical procedures followed in the separations of U and Th are shown by the following flow diagram;

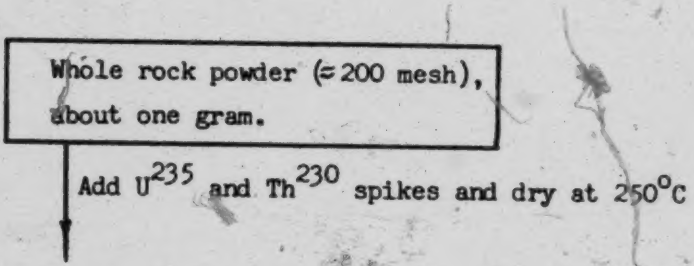

Whole rock powder (≈200 mesh), about one gram.

Add U^{235} and Th^{230} spikes and dry at 250°C

Dried powder
+ spikes

Dissolve in 10 c.c. of HF and 10 c.c. of 8N HNO_3.

Evaporate to dryness and bake.

Residue

Moisten and dissolve in 10 c.c. of 8N HNO_3.

Evaporate to dryness.

Residue

Moisten and dissolve as much as of the residue in 10 c.c. 6N HNO_3 as possible at room temperature.

Transfer into 15 c.c. centrifuge tube and centrifuge.

Pour the supernatant liquid onto the prepared anion exchange column (Dowex 1-X8 resin).

Solution containing U
and Th from exchange column

Evaporate to dryness.

Run on mass spectrometer.

Compute U^{235}, U^{238} and Th^{232} concentrations.

Concentrations of U
and Th calculated

The neutron activation technique was also used (G. L. Cumming, personal communication) for U and Th determination on these samples. A comparison of the data from the two methods is given in Chapter V.

2.5. Extraction of Pb from rock sample

Chemical extraction of rock lead involves a complete dissolution of the rock powder and subsequent recovery of Pb from solutions by anion exchange, dithizone extraction or other methods. Large amounts of pure reagents have to be prepared. Chemical separation of sufficient lead for analysis from rocks which contain trace amounts is difficult. Contamination from chemical reagents and from air borne Pb at those low concentration levels may constitute an appreciable part of the final sample if care is not taken.

Air borne contamination may be eliminated to a large extent in a particle-free laboratory in which positive air pressure with respect to its surrounding is maintained using filtered air. A similar local particle-free enviroment may also be obtained by using laminar flow hoods.

Purification of chemicals from commercial reagent-grade material is customarily done by redistillation. Tilton et al (1955) prepared pure HF by passing hydrogen fluoride gas through a filter of fine Telflon shavings and bubbling the gas into pure water in an ice-cooled platinum vessel. The Pb contamination was reported to be 0.0002 μg/ml. of HF. Tatsumoto (1969) refined Tilton et al's (1955) method by freezing the Telflon filtered hydrogen fluoride gas in a Kel-F tank with liquid nitrogen and then redistilling, refreezing and subsequently introducing the gas into pure water in a Telflon bottle. Pb contamination was reported to be 0.00008 μg/ml. of HF. Techniques for the preparation of highly pure chemical reagents are being constantly sought; Mattinson (1971 and 1972) described a simple two-bottle subboiling still technique for purifications of HF, HCl and HNO_3. Measured lead contamination levels for HF and HCl were reported to be 0.002 ppb to 0.005 ppb, and for HNO_3, 0.02 ppb.

The use of highly pure chemicals combined with the improved decomposition technique, such as the one described by Krogh (1972), the particle-free working enviroment and the high precision of mass spectrometric analyses will no doubt help to improve the precision and reproducibility of the isotope dating methods.

For quantitative determination of Pb, isotope dilution is often used. A 100 per cent dissolution of Pb into the solutions from rock powder is customarily assumed.

2.6. Extraction of Pb by volatilization

The volatilization technique offers distinct advantages over chemical methods; air borne lead contamination during chemical processing is reduced to a minimum and it is not necessary to prepare large amounts of pure reagents. Further, as shown by Cumming et al (1970) fractional removal of lead from a rock sample by volatilization yields lead of varying isotopic composition and the ratios Pb^{207}/Pb^{204} and Pb^{206}/Pb^{204} are linearly related. Its analogue to a mineral isochron is demonstrated in this thesis (see Chapter VII) and thus a mineral isochron may be obtained in a simple fashion utilizing the inhomogeneous distribution of volatilised lead in the rocks without having to actually separate the mineral phases (which is customarily done in the chemical method). (Perhaps a "mineral" isochron of a rock can also be obtained by fractional removal of lead from a rock sample by chemical leaching).

For quantitative analyses of lead, the isotope dilution method is used and total evaporation of lead from the rock powder is necessary. It has been demonstrated by Starik et al (1957) and Marshall and Hess (1960) that the isotopic composition of the volatilised lead is practically the same as that of lead isolated chemically. Black et al (1971) estimated the volatilization yield (at 1250°C for 4 hours under vacuum) on one U.S.G.S. standard sample previously analysed chemically by Tatsumoto and obtained 104% recovery for the volatilization process with respect to the chemical method. It thus becomes apparent that total lead evaporation from rock is obtainable by prolonged heating at high temperature under vacuum.

Purification of volatilised leads can be easily done by the dithizone extraction technique. All the leads studied in this thesis except those from galenas were extracted by volatilization. Details of the extraction procedures and further discussions of this technique are given in Chapter III.

2.7. Mass spectrometric measurement and data reduction

Since the major analytical technique is mass spectrometry and the final data depends on the quality of the mass spectrometer results, it is very desirable that the mass spectrometric technique be developed to the point where precise reproducible data can be obtained on a routine basis. Cumming et al (1971) described an automatic digital mass spectrometer developed in this Department and used by the author. A brief version of a least squares polynomial fitting technique for the data reduction was also given by Cumming et al (1971) and is described in greater detail in this section.

2.7.1. Least squares polynomial fitting

In determining the isotopic composition of an element using a mass spectrometer it is customary to make repeated scans over the mass range of interest and measure the relative abundances of the isotopes often enough to obtain results within useful statistical limits. Errors are easily made because of long-term and/or short-term drift due to changes in resistances, temperature variations and even personnel differences in measuring peak heights (Kanasewich, 1968). The least squares polynomial fitting technique is aimed to minimize these errors.

We make M repeated measurements of a mass spectrum where there are N peaks. An example of three repeated scans of a mass spectrum of four peaks with slightly growing signal is shown in Figure 6a.

Let P_{ij}, where $i = 1,2,3,....$
$j = 1,2,3,....$ be the height of the jth peak of the ith scan in the spectrum. Let λ_j, where $j = 1,2,3,4,...$ be the ratio of the first peak to the jth peak in the scan. We assume λ_j to be constant throughout the measurements.

Let the polynomial representation of the peak as a function of time be

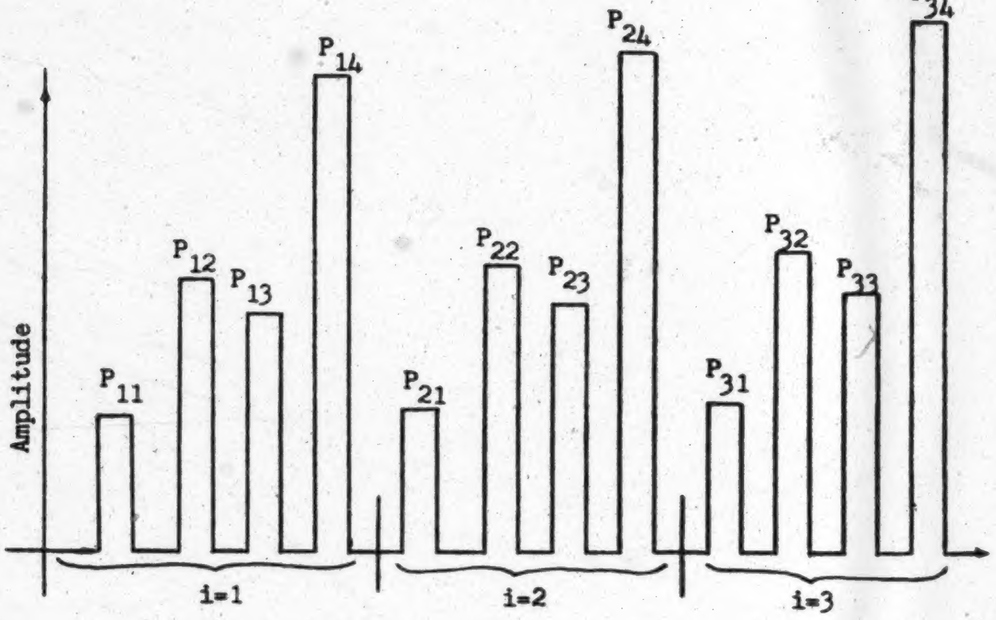

Figure 6a. Time series of a mass spectrum.

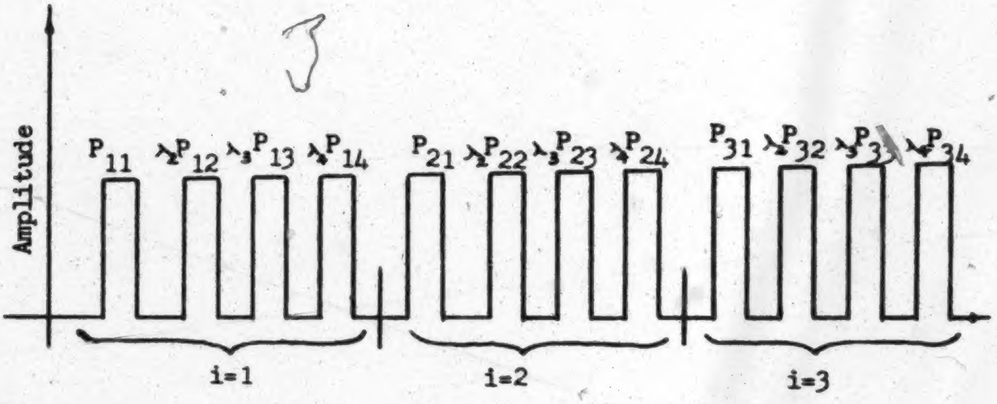

Figure 6b. Time series of a normalized mass spectrum.

$P(t) = b_o + b_1t + b_2t^2 + b_3t^3 + \ldots + b_kt^k$ or simply as

$P(t) = \sum_{k=0}^{k} b_kt^k$, where t is the time when the peak occurs in the spectrum.

Assume that the isotopic ratios are independent of time and let R_j be $R_j = P_j/P_1 = 1/\lambda_j$, the ratio of the jth peak to the first in a scan and normalize the measured peak heights to the height of the first peak in each scan by the parameter λ_j. The time series of the normalized spectrum will then look like that shown in Figure 6b.

The normalized peak heights are not necessarily of equal height due to the growth or decay of signal during the measurements. It is our aim to solve for the normalization parameters λ_j, $j = 1,2,3,\ldots N$ which will normalize the peak heights to fit a single polynomial. Relative isotopic abundances of the isotopes in a mass spectrum with respect to the first peak in this mass spectrum can then be obtained by taking the reciprocals of the normalization parameters.

Letting t_{ij} be the time where P_{ij} occurs in the spectrum then we can express the measured and normalized peak heights as;

$$\left.\begin{aligned}
P_{11} &= b_o + b_1 t_{11} + b_2 t_{11}^2 + \ldots + b_k t_{11}^k \\
\lambda_2 P_{12} &= b_o + b_1 t_{12} + b_2 t_{12}^2 + \ldots + b_k t_{12}^k \\
\lambda_3 P_{13} &= b_o + b_1 t_{13} + b_2 t_{13}^2 + \ldots + b_k t_{13}^k \\
\lambda_4 P_{14} &= b_o + b_1 t_{14} + b_2 t_{14}^2 + \ldots + b_k t_{14}^k \\
\cdots\cdots &\cdots\cdots\cdots\cdots\cdots\cdots\cdots\cdots\cdots\cdots \\
\lambda_n P_{1n} &= b_o + b_1 t_{1n} + b_2 t_{1n}^2 + \ldots + b_k t_{1n}^k
\end{aligned}\right\} \quad \begin{aligned} i &= 1 \\ j &= 1,2,3,4,\ldots n \end{aligned}$$

$$\left.\begin{aligned}
P_{21} &= b_o + b_1 t_{21} + b_2 t_{21}^2 + \ldots + b_k t_{21}^k \\
\lambda_2 P_{22} &= b_o + b_1 t_{22} + b_2 t_{22}^2 + \ldots + b_k t_{22}^k \\
\lambda_3 P_{23} &= b_o + b_1 t_{23} + b_2 t_{23}^2 + \ldots + b_k t_{23}^k \\
\lambda_4 P_{24} &= b_o + b_1 t_{24} + b_2 t_{24}^2 + \ldots + b_k t_{24}^k \\
\cdots\cdots &\cdots\cdots\cdots\cdots\cdots\cdots\cdots\cdots\cdots\cdots \\
\lambda_n P_{2n} &= b_o + b_1 t_{2n} + b_2 t_{2n}^2 + \ldots + b_k t_{2n}^k
\end{aligned}\right\} \quad \begin{aligned} i &= 2 \\ j &= 1,2,3,4,\ldots n \end{aligned}$$

$$\left.\begin{aligned}
P_{31} &= b_o + b_1 t_{31} + b_2 t_{31}^2 + \ldots + b_k t_{31}^k \\
\lambda_2 P_{32} &= b_o + b_1 t_{32} + b_2 t_{32}^2 + \ldots + b_k t_{32}^k \\
\lambda_3 P_{33} &= b_o + b_1 t_{33} + b_2 t_{33}^2 + \ldots + b_k t_{33}^k \\
\lambda_4 P_{34} &= b_o + b_1 t_{34} + b_2 t_{34}^2 + \ldots + b_k t_{34}^k \\
\cdots\cdots &\cdots\cdots\cdots\cdots\cdots\cdots\cdots\cdots\cdots\cdots \\
\lambda_n P_{3n} &= b_o + b_1 t_{3n} + b_2 t_{3n}^2 + \ldots + b_k t_{34}^k
\end{aligned}\right\} \quad \begin{aligned} i &= 3 \\ j &= 1,2,3,4,\ldots n \end{aligned}$$

$$\cdots\cdots\cdots\cdots\cdots\cdots\cdots\cdots\cdots\cdots\cdots\cdots$$

$$\cdots\cdots\cdots\cdots\cdots\cdots\cdots\cdots\cdots\cdots\cdots\cdots$$

$$\left.\begin{aligned}
P_{m1} &= b_o + b_1 t_{m1} + b_2 t_{m1}^2 + \ldots + b_k t_{m1}^k \\
\lambda_2 P_{m2} &= b_o + b_1 t_{m2} + b_2 t_{m2}^2 + \ldots + b_k t_{m2}^k \\
\cdots\cdots &\cdots\cdots\cdots\cdots\cdots\cdots\cdots\cdots\cdots\cdots \\
\lambda_n P_{mn} &= b_o + b_1 t_{mn} + b_2 t_{mn}^2 + \ldots + b_k t_{mn}^k
\end{aligned}\right\} \quad \begin{aligned} i &= m \\ j &= 1,2,3,4,\ldots n \end{aligned}$$

Regrouping the above equations, we have

$$\left.\begin{array}{r} b_o + b_1t_{11} + b_2t_{11}^2 + \dots + b_kt_{11}^k = P_{11} \\ -\lambda_2P_{12} + b_o + b_1t_{12} + b_2t_{12}^2 + \dots + b_kt_{12}^k = 0 \\ -\lambda_3P_{13} + b_o + b_1t_{13} + b_2t_{13}^2 + \dots + b_kt_{13}^k = 0 \\ \cdots\cdots\cdots\cdots\cdots\cdots\cdots\cdots\cdots\cdots\cdots\cdots = 0 \\ -\lambda_nP_{1n} + b_o + b_1t_{1n} + b_2t_{1n}^2 + \dots + b_kt_{1n}^k = 0 \end{array}\right\} \begin{array}{l} i = 1 \\ j = 1,2,3,\dots n \end{array}$$

$$\left.\begin{array}{r} b_o + b_1t_{21} + b_2t_{21}^2 + \dots + b_kt_{21}^k = P_{21} \\ -\lambda_2P_{22} + b_o + b_1t_{22} + b_2t_{22}^2 + \dots + b_kt_{22}^k = 0 \\ -\lambda_3P_{23} + b_o + b_1t_{23} + b_2t_{23}^2 + \dots + b_kt_{23}^k = 0 \\ \cdots\cdots\cdots\cdots\cdots\cdots\cdots\cdots\cdots\cdots\cdots\cdots = 0 \\ -\lambda_nP_{2n} + b_o + b_1t_{2n} + b_2t_{2n}^2 + \dots + b_kt_{2n}^k = 0 \end{array}\right\} \begin{array}{l} i = 2 \\ j = 1,2,3,\dots n \end{array}$$

$$\left.\begin{array}{r} b_o + b_1t_{31} + b_2t_{31}^2 + \dots + b_kt_{31}^k = P_{31} \\ -\lambda_2P_{32} + b_o + b_1t_{32} + b_2t_{32}^2 + \dots + b_kt_{32}^k = 0 \\ -\lambda_3P_{33} + b_o + b_1t_{33} + b_2t_{33}^2 + \dots + b_kt_{33}^k = 0 \\ \cdots\cdots\cdots\cdots\cdots\cdots\cdots\cdots\cdots\cdots\cdots\cdots = 0 \\ -\lambda_nP_{3n} + b_o + b_1t_{3n} + b_2t_{3n}^2 + \dots + b_kt_{3n}^k = 0 \end{array}\right\} \begin{array}{l} i = 3 \\ j = 1,2,3,\dots n \end{array}$$

$$\cdots\cdots\cdots\cdots\cdots\cdots\cdots\cdots\cdots\cdots\cdots\cdots\cdots$$

$$\cdots\cdots\cdots\cdots\cdots\cdots\cdots\cdots\cdots\cdots\cdots\cdots\cdots$$

$$\left.\begin{array}{r} b_o + b_1t_{m1} + b_2t_{m1}^2 + \dots + b_kt_{m1}^k = P_{m1} \\ -\lambda_2P_{m2} + b_o + b_1t_{m2} + b_2t_{m2}^2 + \dots + b_kt_{m2}^k = 0 \\ -\lambda_3P_{m3} + b_o + b_1t_{m3} + b_2t_{m3}^2 + \dots + b_kt_{m3}^k = 0 \\ \cdots\cdots\cdots\cdots\cdots\cdots\cdots\cdots\cdots\cdots\cdots\cdots = 0 \\ -\lambda_nP_{mn} + b_o + b_1t_{mn} + b_2t_{mn}^2 + \dots + b_kt_{mn}^k = 0 \end{array}\right\} \begin{array}{l} i = m \\ j = 1,2,3,\dots n \end{array}$$

Writing in explicit matrix form,

$$
\begin{bmatrix}
0 & 0 & 0 & \cdots\cdots & 1 & t_{11} & t_{11}^{2} & \cdots & t_{11}^{k} \\
-P_{12} & 0 & 0 & \cdots\cdots & 1 & t_{12} & t_{12}^{2} & \cdots & t_{12}^{k} \\
0 & -P_{13} & 0 & \cdots\cdots & 1 & t_{13} & t_{13}^{2} & \cdots & t_{13}^{k} \\
\cdots & \cdots & \cdots & \cdots & \cdots & \cdots & \cdots & \cdots & \cdots \\
0 & 0 & 0 & \cdot\ -P_{1n} & 1 & t_{1n} & t_{1n}^{2} & \cdots & t_{1n}^{k} \\
 & & & & & & & & \\
0 & 0 & 0 & \cdots\cdots & 1 & t_{21} & t_{21}^{2} & \cdots & t_{21}^{k} \\
-P_{22} & 0 & 0 & \cdots\cdots & 1 & t_{22} & t_{22}^{2} & \cdots & t_{22}^{k} \\
0 & -P_{23} & 0 & \cdots\cdots & 1 & t_{23} & t_{23}^{2} & \cdots & t_{23}^{k} \\
\cdots & \cdots & \cdots & \cdots & \cdots & \cdots & \cdots & \cdots & \cdots \\
0 & 0 & 0 & \cdot\ -P_{2n} & 1 & t_{2n} & t_{2n}^{2} & \cdots & t_{2n}^{k} \\
 & & & & & & & & \\
0 & 0 & 0 & \cdots\cdots & 1 & t_{31} & t_{31}^{2} & \cdots & t_{31}^{k} \\
-P_{32} & 0 & 0 & \cdots\cdots & 1 & t_{32} & t_{32}^{2} & \cdots & t_{32}^{k} \\
0 & -P_{33} & 0 & \cdots\cdots & 1 & t_{33} & t_{33}^{2} & \cdots & t_{33}^{k} \\
\cdots & \cdots & \cdots & \cdots & \cdots & \cdots & \cdots & \cdots & \cdots \\
0 & 0 & 0 & \cdot\ -P_{3n} & 1 & t_{3n} & t_{3n}^{2} & \cdots & t_{3n}^{k} \\
\cdots & \cdots & \cdots & \cdots & \cdots & \cdots & \cdots & \cdots & \cdots \\
\cdots & \cdots & \cdots & \cdots & \cdots & \cdots & \cdots & \cdots & \cdots \\
 & & & & & & & & \\
0 & 0 & 0 & \cdots\cdots & 1 & t_{m1} & t_{m1}^{2} & \cdots & t_{m1}^{k} \\
-P_{m2} & 0 & 0 & \cdots\cdots & 1 & t_{m2} & t_{m2}^{2} & \cdots & t_{m2}^{k} \\
0 & -P_{m3} & 0 & \cdots\cdots & 1 & t_{m3} & t_{m3}^{2} & \cdots & t_{m3}^{k} \\
\cdots & \cdots & \cdots & \cdots & \cdots & \cdots & \cdots & \cdots & \cdots \\
0 & 0 & 0 & \cdot\ -P_{mn} & 1 & t_{mn} & t_{mn}^{2} & \cdots & t_{mn}^{k}
\end{bmatrix}
\begin{bmatrix}
\lambda_2 \\ \lambda_3 \\ \lambda_4 \\ \cdot \\ \cdot \\ \lambda_{n-1} \\ \lambda_n \\ b_o \\ b_1 \\ b_2 \\ b_3 \\ b_4 \\ b_5 \\ \cdot \\ \cdot \\ b_{k-1} \\ b_k
\end{bmatrix}
=
\begin{bmatrix}
P_{11} \\ 0 \\ 0 \\ 0 \\ 0 \\ \\ P_{21} \\ 0 \\ 0 \\ 0 \\ 0 \\ \\ P_{31} \\ 0 \\ 0 \\ \cdot \\ \cdot \\ \\ \\ \\ P_{m1} \\ 0 \\ 0 \\ 0 \\ 0
\end{bmatrix}
$$

or simply as

$$Mb = p$$

where M is a $(m\cdot n)$ by $(n+k)$ matrix with $(m\cdot n) > (n+k)$

b is a $(n+k)$ column vector

p is a $(m\cdot n)$ column vector.

The system $Mb=p$ contains more equations than unknowns and in general no solution for b is available. However, we are interested in finding a vector b that is least in error. More precisely, if we take a vector b and calculate $Mb=q$, say, we want the discrepancy between q and p to be as small as possible. The best overall criterion is to minimize the sum of the squares of the discrepancies, which gives a least squares solution for $Mb=p$.

The discrepancies are given in a vector $(q - p)$, and the sum of the squared elements then is given by the square of its norm, or expressed as

$$f=(q-p)^T(q-p).$$

Using $q=Mb$, we can write

$$\begin{aligned} f&=(Mb-p)^T(Mb-p)\\ &=b^TM^TMb-p^TMb-b^TM^Tp+p^Tp\\ &=b^TM^TMb-2b^TM^Tp+p^Tp \end{aligned}$$

where $p^TMb=b^TM^Tp$, since both are simple numbers.

The problem then can be redefined by saying that we want to find a vector b for which f has a minimum. Setting partial derivatives to zero (see Appendix I),

$$\frac{\partial f}{\partial b} = 2M^TMb - 2M^Tp = 0$$

$$\text{Therefore,} \quad M^TMb = M^Tp$$

$$\text{so that} \quad b = (M^TM)^{-1}M^Tp.$$

$(M^TM)^{-1}$ is a symmetric matrix, the determinant of which should be different from zero.

The variance-covariance matrix of b is $(M^TM)^{-1}\sigma^2$, where σ^2 is estimated from

$$\sigma^2 = \frac{1}{N}\sum_{i=1}^{N}(p_i - \bar{p}_i)^2$$

$N = nm - (n + k)$ is the number of degree of freedom, and $\bar{p}_i$ is the normalized smoothed value of p_i. Thus the errors of the ratios and correlation coefficients between ratios may be obtained directly from the variance-covariance matrix. The solutions of those equations are obtained using programs from the IBM scientific subroutine package.

2.7.2. Internal errors and external reproducibility

The size of the errors is controlled by the order of polynomial; although it is possible to use a high order polynomial equation whose graph will pass each of the data points as closely as desired, it is suggested that the polynomials be limited to no more than five terms (depends on number of scans and can be varied). The search for an exact equation presupposes that each of the data points is in itself exact, having no error associated with it. Since it is relatively difficult to deduce the shape of a polynomial equation merely from its coefficients, the development of such an exact equation can produce some rather implausible results. Figure 7 exemplifies such situation.

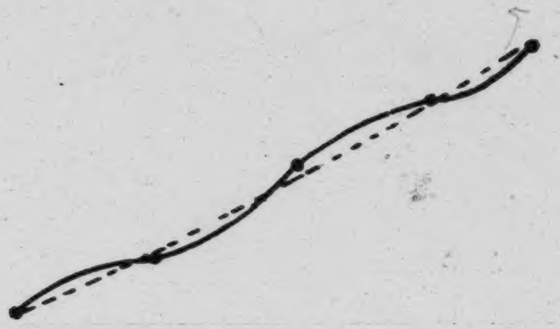

Figure 7. Polynomial fitting of points. (Dashed line: Lower order of polynomial; Solid line: Higher order)

The solid line represents a higher order of polynomial made to fit through all the points. The path is as questionable as the use of linear segments to connect successive values of the points on the graph, especially if the set of data contains one or more points which are grossly in error. A more plausible alternative is the curve shown as a dashed line which has a lower degree of polynomial than the solid line. The internal errors are controlled by the order of the polynomial but the external errors would probably be more realistic with the order of the polynomial limited to a relatively small value. In practice we make 10 to 15 scans over the spectrum yielding 40 to 60 peaks and since there are three unknown terms λ_j, even a relatively high order of polynomial (10 to 15 degree) may be used and still have a large number of degrees of freedom in the least squares solution.

2.7.3. Data recording and reduction

All lead samples were run as PbS on a single tantalum filament and were recorded on magnetic tape as described by Cumming et al (1971) and processed by IBM360 computer as follows;

(1). Each single sweep over the mass spectrum is smoothed by a box-car filter with a running average of a number of points specified by the input to reduce high frequency noise.

(2). To locate the times where the peak heights occur in the spectrum the data is heavily smoothed with a 25 point running average and the times t_{11}, t_{12}, ... t_{1n}, t_{21}, t_{22},... t_{2n}, ... t_{mn} are picked from where the maxima occur (the centers of the smoothed peaks).

(3). The peak heights P_{11}, P_{12}, ... P_{1n}, P_{21}, P_{22}, ... P_{mn} are then obtained by going back to the smoothed data of (1) and take 3 to 5 points average around each of the maxima. The average of 3 to 5 points around each of the maxima is equivalent to a second smoothing with a box-car filter of different length than in (1).

(4). Measured peak heights were corrected for baseline and used for polynomial fitting.

The recorded raw data and the once smoothed, twice smoothed and heavily smoothed data of a scan of mass spectrum of a lead sample are shown in Figure 8.

The computer programs are listed in Appendix II.

2.8. Test runs on standard samples and mass dependent errors

To test the mass spectrometric technique, the author prepared 10 independent "Broken Hill #1" and 9 "NBS Equal Atom #982" standard

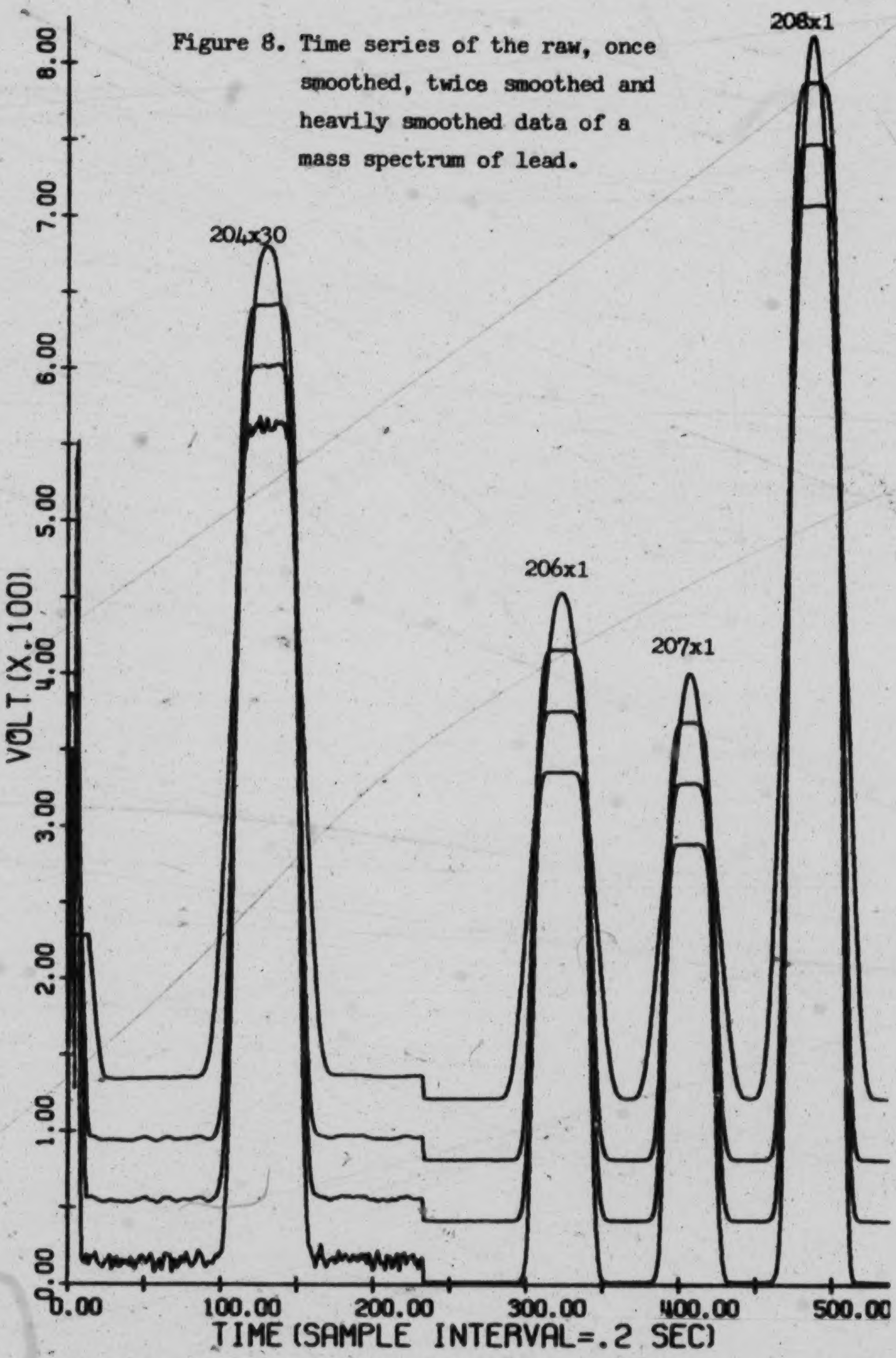

Figure 8. Time series of the raw, once smoothed, twice smoothed and heavily smoothed data of a mass spectrum of lead.

samples. Data were recorded on tape and reduced by the polynomial fitting technique described above. Results are shown in Table 1 and Table 2 with the error shown at one standard deviation.

Examination of the results show external errors of 0.14%, 0.21% and 0.28% for ratios Pb^{206}/Pb^{204}, Pb^{207}/Pb^{204} and Pb^{208}/Pb^{204} respectively which represents 0.07% error for every unit-mass difference in the ratio.

This mass dependent error, known as mass discrimination, is conceded by most investigators to be a major factor which might introduce errors in the final results (Russell and Farquhar, 1960). It has been demonstrated by Cumming et al (1971), Cooper and Richards (1966), Doe et al (1965) and many others that if the mass discrimination errors were eliminated, a very precise mass spectrometric measurement (about 0.05% at one standard deviation or better) could be obtained. In this work an empirical correction factor is applied to all measurements, based on a smoothed mass discrimination factor obtained from the measured values on the NBS Equal Atom #982 standard, so the major mass discrimination effects should be removed from the data (Cumming et al, 1971).

In the early stages of this investigation while the author was developing his mass spectrometric skill, he was bothered by this mass dependent error and decided to pursue this problem a little further. Some studies of this phenomenon are given in Chapter IV.

Table 1. Isotopic ratios of "Broken Hill #1" galena.

	Pb^{206}/Pb^{204}	Pb^{207}/Pb^{204}	Pb^{208}/Pb^{204}
	16.028 .015 *	15.438 .018	35.805 .038
	16.002 .028	15.403 .017	35.702 .054
	16.063 .040	15.471 .042	35.902 .110
	16.056 .030	15.474 .022	35.928 .044
	16.052 .010	15.466 .008	35.902 .019
	16.046 .021	15.473 .022	35.941 .045
	16.010 .021	15.389 .020	35.630 .060
	16.030 .015	15.428 .015	35.786 .035
	16.068 .028	15.486 .026	35.935 .049
	16.019 .013	15.411 .013	35.719 .030
Average:	16.037 ± .022 (.14%)	15.444 ± .033 (.21%)	35.825 ± .107 (.30%)

* Internal estimate of standard deviation.

Table 2. Isotopic ratios of "NBS Equal Atom #982" lead.

	Pb^{206}/Pb^{204}	Pb^{207}/Pb^{204}	Pb^{208}/Pb^{204}
	36.896	17.283	37.074
	.072 *	.026	.037
	36.756	17.195	36.838
	.063	.034	.056
	36.762	17.183	36.842
	.055	.018	.047
	36.807	17.221	36.946
	.047	.025	.068
	36.911	17.254	36.978
	.100	.048	.106
	36.789	17.179	36.793
	.037	.018	.039
	36.819	17.200	36.864
	.041	.020	.043
	36.780	17.179	36.836
	.029	.014	.031
	36.760	17.163	36.754
	.034	.016	.036
Average:	36.809 ± .054	17.206 ± .037	36.881 ± .094
	(.14%)	(.21%)	(.26%)

* Internal estimate of standard deviation.

CHAPTER III

VOLATILIZATION

3.1. Introduction

In this Chapter the volatilization technique used for lead extraction and the loading of the sample onto the filament are described. The volatilization method has been used for trace element separation for some time. Edwards and Urey (1955) separated the alkalies from meteorites by volatilization, Edwards and Hess (1956) carried out preliminary experiments for the same kind of separation of lead from meteorites and Starik et al (1957) investigated in great detail different modes of lead occurrence in pitchblende, monazite, uraninite and a series of granites by volatilization. Marshall and Hess (1960) separated lead from meteorites by volatilization and dithizone purification with small contamination. Many other investigators including Masuda (1964), Hamilton (1965), Sinha (1969), Welke et al (1968), Moorbath et al (1968) and Cumming et al (1970) have employed this technique for lead separation.

Recently, the volatilization technique was used by Silver (1970, 1971), Huey et al (1971) and Doe and Tatsumoto (1972) for separation of lead from lunar samples.

The volatilization procedures used in this thesis for removal of trace lead from rock are similar in principle to that of Marshall and Hess (1960). Powdered rock is volatilized in a graphite crucible inside a furnace under vacuum. Lead, condensed on a water-cooled quartz tube (called a cold finger), is purified by the dithizone extraction method.

3.2. Furnaces

(A). High temperature brick furnace

At the beginning of this investigation a high temperature brick furnace was built. Figure 9 shows a sketch of the furnace and sample assemblage.

The furnace was heated by four silicon carbide elements which surround the outer ceramic liner. A heavy duty transformer was used to control the input current to the temperature regulator which has a quoted accuracy of ±6°C. Due to the large temperature gradient along the furnace, the sample should be placed in the middle of the furnace where maximum temperatures occur. Overall performance of this furnace was unsatisfactory.

(B). Induction furnace

After some of the preliminary work was done using the high temperature brick furnace, an induction furnace became available and produced highly satisfactory results. Figure 10 shows a schematic diagram of the sample assemblage in place in the coil of the induction furnace. The induction coil induces a large current in the graphite crucible containing the rock sample and heats up the sample to the desired temperature without excessive heating of the outer quartz tubing.

The temperature of the crucible is calibrated against the current settings with an optical pyrometer. Although the exact temperature setting is not important in most of this work (see Chapter VI on temperature isochrons), the actual temperature is believed to be close

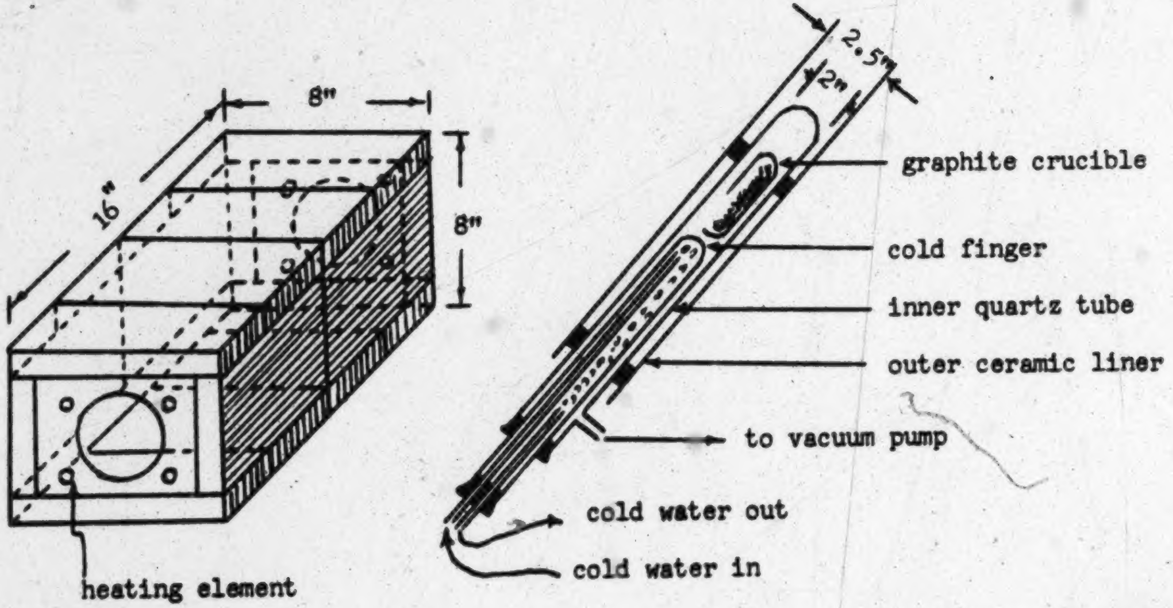

Figure 9. Schematic diagram of the high temperature brick furnace and sample assemblage.

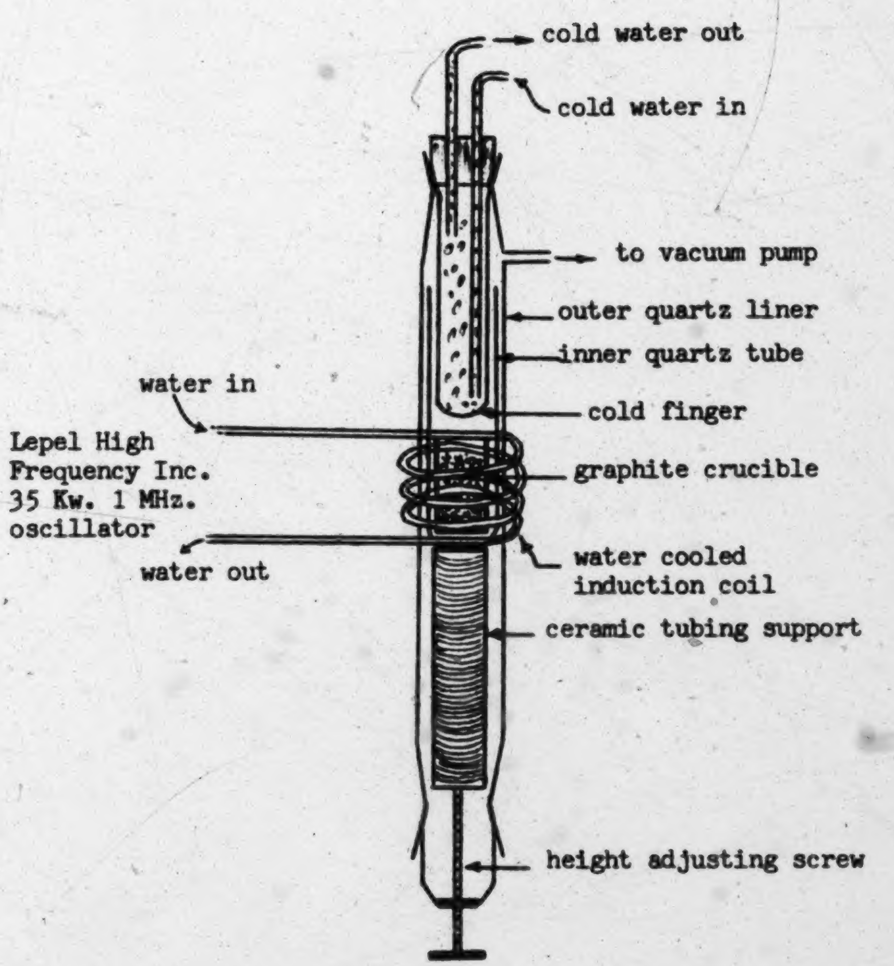

Figure 10. Schematic diagram of the sample assemblage in place in the coil of the induction furnace.

to that indicated by the pyrometer ($\pm 50^{\circ}K$). With an induction furnace the desired temperature can be reached in a few minutes.

With its easy operation and fast heating, the induction furnace is much to be prefered for this work and most of the author's lead samples were obtained using this furnace.

3.3. Analytical procedures

The graphite crucibles, cold fingers, and the inner quartz tubes were cleaned by soaking them in concentrated hot nitric acid for several hours and then rinsed with pure water (several times redistilled). The crucibles were then outgassed in the furnace to about $1400^{\circ}C$ for approximately one hour before being used.

The rock sample was first broken into small fragments and weathered material was discarded. The remaining fragments were crushed to 100-200 mesh, mixed with a small amount of powdered graphite (not essential) and placed in a crucible inside the inner quartz tube. With the cold finger in place slightly above the crucible, the system was then evacuated and current slowly increased. For a powdered sample the evacuation and the preliminary heating must be very gentle otherwise the powdered rock sample will pop up and dirty the walls of the assemblage. For a chipped rock sample the above precaution is not necessary. After the system has been evacuated to 10^{-4} torr, the current can be more rapidly increased to obtain the desired temperature.

Lead and other impurities deposited on the cold finger are dissolved in 5 c.c. of redistilled 3N HNO_3 and purified by the dithizone extraction technique (see Appendix III). All chemical ware was initially cleaned with distilled water and placed in hot nitric acid for several hours or overnight before a final rinsing with pure water and then covered with parafilm ready for use.

Purification of lead has a very important effect on the emission of ions from the lead sample. For best emission results, chemical solutions used for purification of lead should be freshly prepared and the extracted PbS be run as soon as possible.

3.4. Loading PbS on the filament

The loading of the sample on the filament is a critical step in the analytical procedure and the process used is described below.

The tantalum filament (carefully made to ensure that it is tightly and flatly welded on the filament posts) is outgassed at 3.5 amp. for 3 hours or at 3.0 amp. overnight under vacuum (10^{-6} torr or better). The sample is loaded on the filament in the following way;

(1). With a capillary tube (works best if the narrow end is broken off flat) pick up few drops of liquid containing PbS from the centrifuge tube and wet the center of the filament with a small drop of liquid. Excess liquid can be easily drawn up into a spare capillary tube by touching the liquid with the end of the tube.

(2). Pick up some PbS and force it down onto the filament by touching the wetted portion of the filament with the end of the capillary tube. The sample PbS will run down onto the filament. Draw out excess liquid with the spare tube.

(3). Apply a current of up to 1.5 amp. through the filament to evaporate the liquid drop containing PbS. Decrease the current when the drop is about to disappear. Load more sample onto the filament by repeating steps (2) and (3) until desired amount is loaded.

(4). Apply 1.5 amp. of current through the filament and wait until the sample is dried, then gently increase the current to the point at which the ammonia fumes slowly. It is important not to hurry the operation at this point.

(5). After all the ammonia has fumed out, the current is further increased carefully to melt the PbS onto the filament. Let the filament stay at a red-hot temperature for about 5 seconds being careful not to burn out the filament.

3.5. Blanks

Three blank runs were made using Pb^{204} as a spike. They were made with all components set up in operating condition without the sample in the graphite crucible. The furnace was heated to 1400°C for two hours and the deposit on the cold finger was dissolved in 5 c.c. of $3N\ HNO_3$. A known amount of Pb^{204} spike of known composition was added to the solution and the lead was extracted using the dithizone technique with the same amount of chemicals as normally used in processing a regular sample. Results of the blank tests are listed in Table 3.

It can be seen from Table 3 that the blanks are approximately $0.2\mu g$, most of the Pb contamination probably coming from the reagents used. The sample size for most of the runs varied from over $50\mu g$ to

Table 3. Blank tests made on combined volatilization and dithizone purification of lead.

Test run No.	Pb^{204} spike added (μg)	Total sig. recorded	Total impu. recorded	Original impurity	Net blanks %, μg
Test #1	18.318	6840 mv.	90 mv.	18.47 mv.	1.04%, .191 μg
Test #2	16.569	7747 mv.	117 mv.	20.82 mv.	1.24%, .210 μg
Test #3	18.815	6470 mv.	86.5 mv.	17.47 mv.	1.06%, .193 μg

to about 20 μg estimated from the amount of dithizone used for the extraction. No blank corrections were made for ratios obtained in this thesis as it was felt no significant change in the interpretation of the results would arise due to the fact that the isotope ratios observed lie along lines which pass very near to the composition of modern lead and it is believed that the blank composition is essentially modern. Thus no significant change in the slope of the line through the various isotope ratios will be produced.

Separation of lead by volatilization using the induction furnace followed by dithizone extraction is a rapid way of extracting trace amounts of lead from rocks or other material. Lead can be extracted and ready for mass spectrometric analysis within a few hours. If sampling is not important, the rock sample can be heated as chips instead of powder which allows the evacuation and the heating to be done much more rapidly. The rock chips with thickness of about (1/4)" usually were completely melted within 15 minutes at a temperature of 1300°C.

All the leads studied in this thesis except those from galenas are obtained by volatilization followed by dithizone extraction.

CHAPTER IV

MASS DISCRIMINATION IN A MASS SPECTROMETER

4.1. Introduction

The basic function of the mass spectrometer is to produce ions from a sample, then separate them according to their mass to charge ratio. All practical mass spectrometers used to determine lead isotope abundances are fundamentally similar (Russell and Farquhar, 1960). They differ only in the methods employed in producing ions, in the method of measuring and recording the electron current which neutralizes the ion beams, and in the electronic circuits which are used to produce and control the various potentials and magnetic field by which analysis of the samples is accomplished.

Most investigators concede that in any mass spectrometer there are a number of sources of mass fractionation which might introduce errors into the final results (Russell and Farquhar, 1960). In a gas-source mass spectrometer, isotopic fractionation is due to molecular flow from the source ionizing region to the main volume of the instrument. This effect should be constant and according to Whittles (1964) for samples in the mass range of lead tetramethyl it amounts to about 0.2 % per unit-mass (quoted from Stacey et al, 1969). For a solid-source mass spectrometer, various sources of isotopic fractionation have been suggested. Cooper and Richards (1966) found that the beam-building processes can often have a significant effect on the measured ratios (i.e. fractionation occurs during evaporation). Inghram and Hayden (1954) investigated the response of electron multipliers to ion mass and ion velocities and according to them the response is proportional to the square-root of mass. Doe et al (1965) concluded that mass dependent variations in the isotope ratios due to different materials of the source filament were observed and additional mass dependent variations exist which may be due to nonuniform sample purity, particularly the presence of alkalies. On the other hand Cooper and Richards (1966) failed to find any significant effect from different chemical procedures on the observed ratios. In their paper on triple-filament lead isotope measurements, Stacey, Delevaux and Ulrych (1969) found that the exact values of the ratios recorded in any one analysis seem to be dependent on the type of filament material used and indirectly on the exact relative alignment of the filaments (triple-filament) themselves.

Readers are reminded that the mass discrimination error discussed in this thesis refers to the mass dependent errors between runs on a sample. No noticeable mass discrimination between sets of data taken within a run was ever observed by the author in this investigation. Doe et al (1965) reported that no measureable changes in ratios were noted in several runs for which two or three sets of data were taken at hourly intervals. Stacey et al (1969) stated that provided analyses are made under identical conditions using the same filament material, the long-term reproducibility (i.e., over a period of months) is not appreciably worse than the day to day reproducibility. Cooper and Richards (1966) also observed that no appreciable mass discrimination occurred during the data taking period . Catanzaro et al (1968) noted that a small amount of isotope fractionation generally occurs during an analysis. According to them the Pb^{208}/Pb^{206} ratio generally increased by about 0.03% during the data taking period of 24 minutes. This author believes the fractionation observed by Catanzaro et al might have resulted from a slight change in filament conditions which in turn altered the path of the ion beam resulting in a change in the observed ratios.

4.2. Measuring error and fractionation due to the positioning of the filament in the mass spectrometer

In order to obtain estimates of the measuring error, a sample was run continuously for six hours obtaining 200 scans of the lead mass spectrum. The set of 200 scans was subdivided into 20 groups of 10 scans each and ratios were calculated using 5th order of polynomial fitting as described in Chapter II. Results are shown in Table 4.

It can be seen that the scatter is quite small, about 0.06% at one standard deviation and virtually constant for each of the three ratios Pb^{206}/Pb^{204}, Pb^{207}/Pb^{204} and Pb^{208}/Pb^{204}. There is no observable difference between the ratios from the first group and those from the last; that is, no measureable fractionation has taken place for this particular sample during the six hour period within the above mentioned limits.

The above sample was removed from the mass spectrometer and then replaced several days later. At this time it was again found that the ratios obtained were constant for many hours, but the ratios were higher than the previous long-term run. Results of this run are listed in Table 5. This suggests that the positioning of the filament is very critical. To further test this possibility the above mentioned sample was left under vacuum in the mass spectrometer overnight and then the filament reheated and the ratios remeasured the next day. It was found that the ratios were the same as those shown in Table 5. Again no time dependent fractionation was observed. Results of this measurement are shown in Table 6. Thus the only remaining variable factor seems to be the filament position.

Within a run, the position of the filament is fixed provided the filament does not alter its shape during the run. In this case the measuring error is independent of the isotopic mass as demonstrated by the data shown in Tables 4, 5 and 6. Between runs the filament positions might not be the same and this seems to introduce mass dependent errors in the measured ratios as shown by the data of Tables 1 and 2.

It is known that gas-source mass spectrometry has better reproducibility. This is understandable because there is no sample filament involved and the relative position of the source to collector is always the same between different runs, which is in fact similar to the situation for a set of data obtained within a run of a single filament solid-source mass spectrometer.

4.3. Focusing effects on the isotopic ratios

To see if focusing has any effect on the isotopic ratios, the

Table 4. Ratios of a sample continously run for 6 hours

(Broken Hill #1 galena)

	Pb^{206}/Pb^{204}	Pb^{207}/Pb^{204}	Pb^{208}/Pb^{204}
	16.066	15.459	35.844
	16.069	15.480	35.914
	16.070	15.473	35.918
	16.060	15.464	35.895
	16.061	15.473	35.926
	16.050	15.462	35.894
	16.045	15.450	35.876
	16.074	15.474	35.914
	16.074	15.467	35.883
	16.056	15.467	35.896
	16.059	15.460	35.878
	16.048	15.454	35.888
	16.060	15.462	35.836
	16.056	15.460	35.881
	16.071	15.464	35.869
	16.062	15.474	35.902
	16.074	15.475	35.902
	16.053	15.457	35.906
	16.073	15.469	35.896
	16.063	15.467	35.900
Average:	16.062 ± .009 (.056%)	15.466 ± .008 (.045%)	35.890 ± .022 (.061%)

Table 5. Ratios of Broken Hill galena (same sample as that used in Table 4).

	Pb^{206}/Pb^{204}	Pb^{207}/Pb^{204}	Pb^{208}/Pb^{204}
	16.139	15.555	36.122
	16.085	15.507	36.016
	16.115	15.528	36.086
	16.100	15.514	36.023
	16.085	15.512	36.042
	16.117	15.541	36.102
	16.134	15.547	36.080
	16.103	15.520	36.049
	16.118	15.534	36.068
	16.087	15.514	36.030
	16.121	15.541	36.084
Average:	16.109 ± .018 (.11%)	15.528 ± .016 (.11%)	36.064 ± .033 (.09%)

Table 6. Ratios of Broken Hill #1 galena (same sample loading and running condition as that of Table 5)

	Pb^{206}/Pb^{204}	Pb^{207}/Pb^{204}	Pb^{208}/Pb^{204}
	16.126	15.540	36.112
	16.119	15.529	36.071
	16.090	15.504	36.013
	16.090	15.503	35.991
	16.119	15.528	36.073
	16.104	15.530	36.057
	16.087	15.510	36.044
	16.109	15.524	36.052
	16.112	15.525	36.058
	16.102	15.520	36.028
	16.089	15.513	36.015
	16.101	15.526	36.070
	16.116	15.526	36.038
	16.104	15.522	36.024
	16.111	15.517	36.020
	16.122	15.537	36.077
	16.108	15.526	36.077
	16.126	15.542	36.087
	16.101	15.522	36.059
	16.113	15.529	36.047
	16.098	15.519	36.053
	16.105	15.506	35.991
Average:	16.107 ± .011 (.062%)	15.523 ± .010 (.062%)	36.048 ± .030 (.09%)

author ran one Pb^{204} spiked sample continuously for six hours obtaining 200 scans which consist of 20 sets of 10 scans each. Among the 20 sets of data, focusing adjustments were made on Pb^{208}, Pb^{207}, Pb^{206} and Pb^{204} for each 5 sets of data respectively. The sample was spiked with Pb^{204} to increase the Pb^{204} signal so that the Pb^{204} measurement errors are comparable to the errors on the other isotopes. Results of this test are shown in Table 7 and shows that the ratio Pb^{208}/Pb^{204} observed when the beam was focused on Pb^{208} is the highest when compared to the same ratios when the beam was focused on other isotopes. A similar result was also noted for Pb^{207} focusing. The results also show that when the beam was focused on Pb^{204}, the ratios Pb^{208}/Pb^{204}, Pb^{207}/Pb^{204} and Pb^{206}/Pb^{204} are lower when compared to the same ratios observed when the beam were focused on other isotopes.

Mass spectrometric analyses using a triple-filament (Stacey et al, 1969) and double spiking technique (Compston and Oversby, 1969) are aimed at improving the reproducibility of mass spectrometer measurements. The triple filament with a large load of sample and lower filament current may have the effect of making the path of the beam more constant than single filament measurements and consquently yield better reproducibility.

In the double spiking technique, the mass discrimination effects are corrected by making an additional run of the sample mixed with a spike of known composition but in the author's opinion both runs should be made by focusing on the same isotope since this type of discrimination may be non-linear being affected by the beam focusing as shown above.

4.4. Conclusions on the mass discrimination experiment

Based on limited results and discussions in this Chapter, the following conclusions are made;

(1). The mass discrimination error is the basic limitation on the overall reproducibility of a mass spectrometer.

(2). The mass discrimination error is related to filament position in the mass spectrometer and better reproducibility could be obtained if a means of making the sample position constant could be found.

(3). No noticeable fractionation during the course of a six hour run was observed above a limit of about 0.06% (S.D.). Thus during the course of a normal run lasting one or two hours, any fractionation would be negligible.

Table 7. Fractionation test of different focusing made on different isotope

Focus on:	Pb^{206}/Pb^{204}	Pb^{207}/Pb^{204}	Pb^{208}/Pb^{204}	Pb^{207}/Pb^{206}	Pb^{208}/Pb^{206}
	1.3060	1.2228	2.9156	0.9363	2.2326
	1.3060	1.2229	2.9159	0.9364	2.2327
(Pb^{208})	1.3062	1.2233	2.9173	0.9365	2.2333
	1.3064	1.2233	2.9180	0.9364	2.2335
	1.3059	1.2233	2.9175	0.9368	2.2341
Total:	6.5305	6.1156	14.5843	4.6824	11.1662
	1.3061	1.2228	2.9151	0.9362	2.2319
	1.3059	1.2228	2.9150	0.9364	2.2322
(Pb^{207})	1.3069	1.2239	2.9178	0.9365	2.2326
	1.3066	1.2234	2.9178	0.9364	2.2332
	1.3065	1.2234	2.9169	0.9363	2.2325
Total:	6.5320	6.1163	14.5826	4.6818	11.1624

Table 7 cont'd

Focus on:	Pb^{206}/Pb^{204}	Pb^{207}/Pb^{204}	Pb^{208}/Pb^{204}	Pb^{207}/Pb^{206}	Pb^{208}/Pb^{206}
	1.3060	1.2226	2.9151	0.9362	2.2322
	1.3064	1.2231	2.9166	0.9363	2.2327
(Pb^{206})	1.3060	1.2230	2.9161	0.9364	2.2328
	1.3061	1.2229	2.9171	0.9363	2.2334
	1.3066	1.2235	2.9179	0.9364	2.2331
Total:	6.5311	6.1151	14.5828	4.6816	11.1642
	1.3047	1.2219	2.9127	0.9365	2.2324
	1.3054	1.2223	2.9144	0.9364	2.2326
(Pb^{204})	1.3061	1.2229	2.9163	0.9363	2.2329
	1.3063	1.2230	2.9169	0.9363	2.2330
	1.3065	1.2232	2.9166	0.9362	2.2324
Total:	6.5290	6.1133	14.5769	4.6817	11.1633

CHAPTER V

WHOLE ROCK DATA AND U/Pb AGES

5.1. Whole rock Pb, U and Th determinations

All the whole rock leads except that of YKWG #8 were extracted by heating about 10 grams of sample in the induction furnace. The temperature was raised slowly to 1400°C and maintained at that temperature for approximately 30 minutes. Appreciable amounts of lead are observed as soon as the temperature exceeds about 900°C and hence it is felt that it is not necessary to maintain the temperature for more than 30 minutes at 1400°C in order to obtain complete recovery of the lead.

Lead collected on the cold finger was dissolved in 10 c.c. of 3N HNO_3 and split into two portions of 5c.c. each, one for lead-isotope composition measurement and one for isotope-dilution determination of lead content. Purification of lead was done by the dithizone extraction technique as described in Appendix III.

For sample YKWG #8, two separate heatings one with plain rock powder for lead composition and one with Pb^{204} spiked powder for lead concentration were made.

Replicate volatilization of the sample YKWG #6 was made to give an indication of the furnace reproducibility.

U and Th determinations were made following the chemical procedures described in Chapter II. Neutron activation analyses were also made for U and Th determinations (by Dr. Cumming).

Tables 8 and 9 show the analytical data for Pb, U and Th determinations. Both the observed and spiked lead isotope ratios are given.

Table 8. Whole rock isotopic ratios

Sample:	Pb ratios, unspiked					Pb ratios, 204 spiked			
	206/204	207/204	208/204	207/206	208/206	206/204	207/204	207/206	208/206
YKWG #1	18.324 .027 *	15.627 .024	36.158 .055	.8536 .0013	1.9770 .0030	1.0896 .0010	0.9303 .0009	.8546 .0008	1.9841 .0019
YKWG #2	18.473 .020	15.817 .017	39.331 .044	.8570 .0009	2.1331 .0023	0.4383 .0009	0.3737 .0008	.8533 .0017	2.1248 .0043
YKWG #3	21.445 .069	16.153 .053	36.395 .120	.7539 .0023	1.7003 .0055	0.8618 .0007	0.6467 .0006	.7511 .0006	1.6894 .0015
YKWG #4	16.504 .102	15.293 .100	40.264 .265	.9230 .0052	2.4396 .0155	0.5548 .0002	0.5171 .0002	.9220 .0004	2.4289 .0008
YKWG #5	17.763 .038	15.450 .034	38.052 .080	.8701 .0018	2.1420 .0046	0.8471 .0005	0.7385 .0005	.8693 .0005	2.1504 .0014
YKWG #6	41.086 .119	19.770 .058	46.774 .141	.4815 .0014	1.1406 .0033	2.6851 .0014	1.2914 .0007	.4814 .0003	1.1379 .0006
	40.802 .136	19.550 .066	45.876 .157	.4796 .0016	1.1264 .0037	1.2640 .0005	0.6085 .0003	.4819 .0002	1.1324 .0005
YKWG #7	19.919 .048	15.968 .039	36.496 .090	.8024 .0019	1.8356 .0044	0.6859 .0048	0.5459 .0039	.7966 .0055	1.8252 .0128
YKWG #8	18.654 .103	15.748 .088	40.291 .228	.8450 .0046	2.1640 .0119	1.1436 .0008	0.9627 .0007	.8425 .0006	2.1527 .0015

* Internal estimate of standard deviation.

Table 9. Pb and U, Th concentrations and U-Pb ages

Sample:	Total Pb (ppm)	Total U (ppm)	Total Th (ppm)	Radiogenic Pb (ppm)		U-Pb ages (m.y.)		Observed μ
				Pb^{206}	Pb^{207}	206/238	207/235	
YKWG #1	10.365	——	——	.6535	.1279	——	——	——
YKWG #2	5.034	2.100	9.41	.3081	.0666	1024	1856	31.4
YKWG #3	7.499	3.189	15.98	.7568	.1338	1585	2102	31.7
YKWG #4	5.560	0.734	5.86	.1948	.0434	1749	2416	9.7
YKWG #5	7.215	1.200	5.80	.3855	.0724	2065	2435	11.9
YKWG #6	14.269	——	——	3.5504	.6426	——	——	——
YKWG #7	5.581	1.493	3.76	.4605	.0846	1993	2376	19.8
YKWG #8	8.686	2.110	14.33	.5321	.0988	1673	2201	17.4

Note: Common lead correction (generally very large) is calculated from the lead-lead isochron age, isochron μ and the primordial lead compositions of a_o=9.346, b_o=10.218. Age of the earth t_o is taken to be 4578 m.y.

$\lambda_U{}^{235}$=0.9722x10^{-9}/yr. $\lambda_U{}^{238}$=0.1537x10^{-9}/yr. $\lambda_{Th}{}^{232}$= 0.0499x10^{-9}/yr.

Ratios were reduced to conform to NBS Equal Atom standard given by Stacey et al (1969).

Table 10 shows a comparison of U and Th concentration determinations by the isotope dilution measurements and neutron activation analyses on the same rock samples. The agreement is not good and the reasons for the disagreement are not known. The isotope dilution measurements have been used in this work for all the samples except YKWG #6, when the isotope dilution measurement was not available.

5.2. Uranium-lead radiometric method (after Kanasewich, 1968)

There are four stable isotopes of lead, Pb^{204}, Pb^{206}, Pb^{207} and Pb^{208}. Pb^{204} has not been generated by any radioactive decay while Pb^{206}, Pb^{207} and Pb^{208} are being added as they are the end products of U^{238}, U^{235} and Th^{232} decays. Therefore the relative abundances of Pb^{206}, Pb^{207} and Pb^{208} with respect to Pb^{204} will increase as time progresses.

Let the present be t=0 and count time positively into the past, and let N_o be the number of radioactive atoms at the present time. Then the number of the atom in the past at time t is $N=N_o e^{\lambda t}$, where λ is the decay constant.

With respect to Pb^{204}, let

a_o, b_o and c_o be the ratios of Pb^{206}/Pb^{204}, Pb^{207} and Pb^{208}/Pb^{204} respectively at $t=t_o$ (taken to be the age of the earth)

λ, λ' and λ'' be the decay constants of U^{238}, U^{235} and

Table 10. Concentrations of U and Th

Sample:	U(ppm) I. D.*	U(ppm) D.N.@	Th(ppm) I.D.*	Th(ppm) D.N.@
YKWG #1	—	7.62 .14	—	20.0 1.6
YKWG #2	2.10	2.08 .04	9.41	9.36 .70
YKWG #3	3.19	4.34 .03	15.98	9.89 .11
YKWG #4	0.734	0.62 .01	5.86	5.43 .02
YKWG #5	1.20	1.33 .02	5.80	8.93 .41
YKWG #6	—	13.51 .15	—	40.9 .3
YKWG #7	1.49	2.63 .01	3.76	5.82 .24
YKWG #8	2.11	2.33 .01	14.33	12.45 1.19

* Isotope dilution measurement by the author.

@ Delayed neutron measurement by Dr. Cumming (personal communication). The values shown are the means of two measurements. The errors are standard deviation of the mean.

Th^{232} respectively,

$\mu(t)$ and $w(t)$ be the ratios of the number of atoms of U^{238} and Th^{232} with respect to Pb^{204} at the present time, and

x, y, z, be the ratios of Pb^{206}/Pb^{204}, Pb^{207}/Pb^{204} and Pb^{208}/Pb^{204} at time t.

Then the evolution of lead since the earth was formed can be expressed as

$$x = a_o + \int_t^{t_o} \lambda[\mu(t)e^{\lambda t}]dt \qquad \text{------------}(4)$$

$$y = b_o + (1/137.8)\int_t^{t_o} \lambda'[\mu(t)e^{\lambda' t}]dt \qquad \text{------------}(5)$$

$$z = c_o + \int_t^{t_o} \lambda''[w(t)e^{\lambda'' t}]dt \qquad \text{------------}(6)$$

The parameters $\mu(t)$ and $w(t)$ may vary from point to point in the earth but metamorphic or orogenic events are episodic locally and brief in comparison to the half-lives of uranium and thorium, so they can be treated as constant for discrete intervals of time and approximate solutions to the above equations (4), (5), and (6) can be written as

$$x_n = a_o + \mu_1(e^{\lambda t_o} - e^{\lambda t_1}) + \mu_2(e^{\lambda t_1} - e^{\lambda t_2}) + \ldots\ldots$$
$$+\ldots\ldots+ \mu_n(e^{\lambda t_{n-1}} - e^{\lambda t_n}) \qquad \text{--------}(7)$$

$$y_n = b_o + (1/137.8)[\ \mu_1(e^{\lambda' t_o} - e^{\lambda' t_1}) + \mu_2(e^{\lambda' t_1} - e^{\lambda' t_2}) + \cdots + \cdots + \mu_n(e^{\lambda' t_{n-1}} - e^{\lambda' t_n})\ ] \text{ ——(8)}$$

$$z_n = c_o + w_1(e^{\lambda'' t_o} - e^{\lambda'' t_1}) + w_2(e^{\lambda'' t_1} - e^{\lambda'' t_2}) + \cdots + \cdots + w_n(e^{\lambda'' t_{n-1}} - e^{\lambda'' t_n}) \text{ ——(9)}$$

where n is the number of stages where the uranium and thorium in the system has been altered since the earth was formed at t_o.

(A). For a single stage lead

$$x_1 = a_o + \mu_1(e^{\lambda t_o} - e^{\lambda t_1}) \text{ ———— (10)}$$

$$y_1 = b_o + (1/137.8)[\mu_1(e^{\lambda' t_o} - e^{\lambda' t_1}) \text{ ———— (11)}$$

$$z_1 = c_o + w_1(e^{\lambda'' t_o} - e^{\lambda'' t_1}) \text{ ———— (12)}$$

The above equations may be used to solve for t_1, the time when the system became closed.

$$\frac{y_1 - b_o}{x_1 - a_o} = R = \frac{(e^{\lambda' t_o} - e^{\lambda' t_1})}{137.8(e^{\lambda t_o} - e^{\lambda t_1})} \text{ ———— (13)}$$

This equation defines a straight line with slope R and passes through the points (a_o, b_o).and (x_1, y_1). All leads which have evolved from the same initial ratios (Primordial lead) through different environments which became closed systems at the same time t_1 will fit on the same straight line called an isochron.

(B). For two stage lead

At time t_1 the leads were differentiated from their source and contemporaneously, uranium and thorium were also incorporated into the same enviroment. At time t_2 a geological event occurred in this area. Some of the initial lead formed from t_o to t_1 and the radiogenic lead formed between time t_1 and t_2 may become mixed. Leads which evolved from the initial ratio (x_1, y_1) through different enviroments but entered closed systems at the same time t_2 will fit on a straight line defined by

$$\frac{y_2 - y_1}{x_2 - x_1} = \frac{(e^{\lambda' t_1} - e^{\lambda' t_2})}{137.8(e^{t_1} - e^{t_2})} \qquad \text{——————} (14)$$

called an anomalous lead line.

The two stage model assumes that the incorporations of lead, uranium and thorium into the crust occurred contemporaneously during an early period of tectonic activity at time t_1. A schematic diagram illustrating the development of lead and a lead-lead isochron diagram of the two stage model are shown in Figure 11.

(C). Three stage lead evolution

For three stage lead, we have

$$\begin{aligned} x_3 = a_o &+ \mu_1(e^{\lambda t_o} - e^{\lambda t_1}) + \mu_2(e^{\lambda t_1} - e^{\lambda t_2}) \\ &+ \mu_3(e^{\lambda t_2} - e^{\lambda t_3}) \qquad \text{——————} (15) \end{aligned}$$

$$\begin{aligned} y_3 = b_o &+ (1/137.8)[\, \mu_1(e^{\lambda' t_o} - e^{\lambda' t_1}) + \mu_2(e^{\lambda' t_1} - e^{\lambda' t_2}) \\ &+ \mu_3(e^{\lambda' t_2} - e^{\lambda' t_2})] \qquad \text{——————} (16) \end{aligned}$$

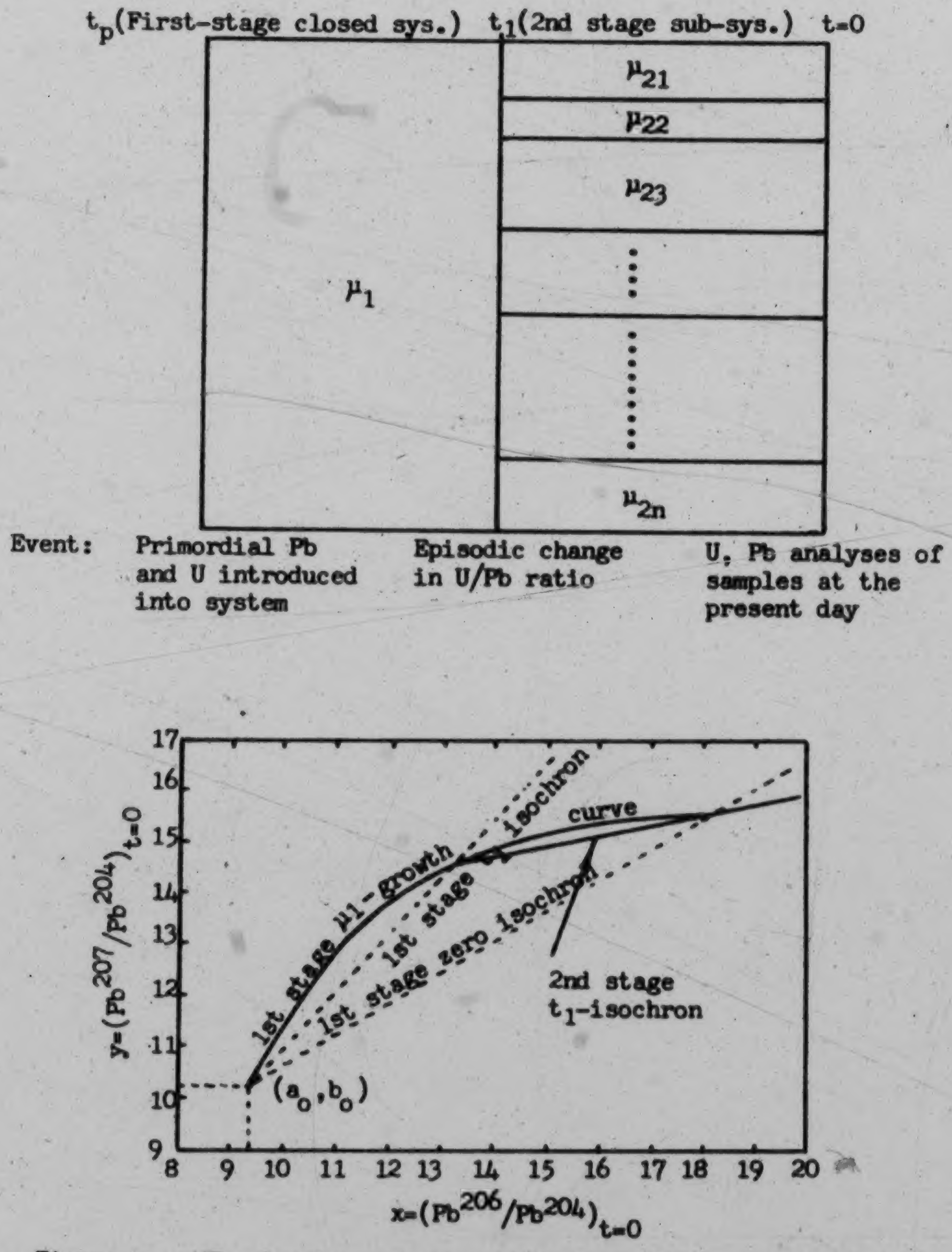

Figure 11. The development of lead in a two stage system and the lead-lead diagram (after Gale and Mussett, 1973).

$$z_3 = c_0 + w_1(e^{\lambda'' t_0} - e^{\lambda'' t_1}) + w_2(e^{\lambda'' t_1} - e^{\lambda'' t_2})$$
$$+ w_3(e^{\lambda'' t_2} - e^{\lambda'' t_3}) \quad \text{———}(17)$$

If the uranium and thorium concentration varies from place to place, the isotopic ratios will scatter about an anomalous lead line with the slope determined by times t_1 and t_3.

Only under two special cases when μ_1/μ_{2i} and μ_{2i}/μ_{3j} for each of the subsystems are constants (see Figure 12) will a rectilinear plot of Pb^{206}/Pb^{204} versus Pb^{207}/Pb^{204} be obtained (Gale and Mussett, 1973). In general it is impossible to obtain a unique solution of t_0, t_1, t_2, μ_1 and μ_2 for three stage lead from the isotope data alone.

For the two special cases, Gale and Mussett (1973) have shown that for the case $f_{1i}=\mu_1/\mu_{2i}$=constant, an isochron equation

$$\frac{y_3 - y_1''}{x_3 - x_1''} = \frac{(e^{\lambda' t_2} - e^{\lambda' t_3})}{137.8(e^{\lambda t_2} - e^{\lambda t_3})} \quad \text{———}(18)$$

where $x_1'' = a_0 + \mu_1(e^{\lambda t_0} - e^{\lambda t_1}) + (\mu_1/f_1)(e^{\lambda t_1} - e^{\lambda t_2})$

$$y_1'' = b_0 + (1/137.8)[\,\mu_1(e^{\lambda' t_0} - e^{\lambda' t_1}) + (\mu_1/f_1)(e^{\lambda' t_1} - e^{\lambda' t_2})]$$

is obtained. These isochrons define a family of parallel lines with meaningless intercepts with the growth curve. The slope of the isochron depends on t_2 and t_3 but not on t_1. When t_3 is assigned, t_2 is calculated from the slope. As f_1 approches 1, the model reduces to a two stage model. Figure 12 shows the schematic diagram illustrating the development of this particular model lead and the associated isochron diagram.

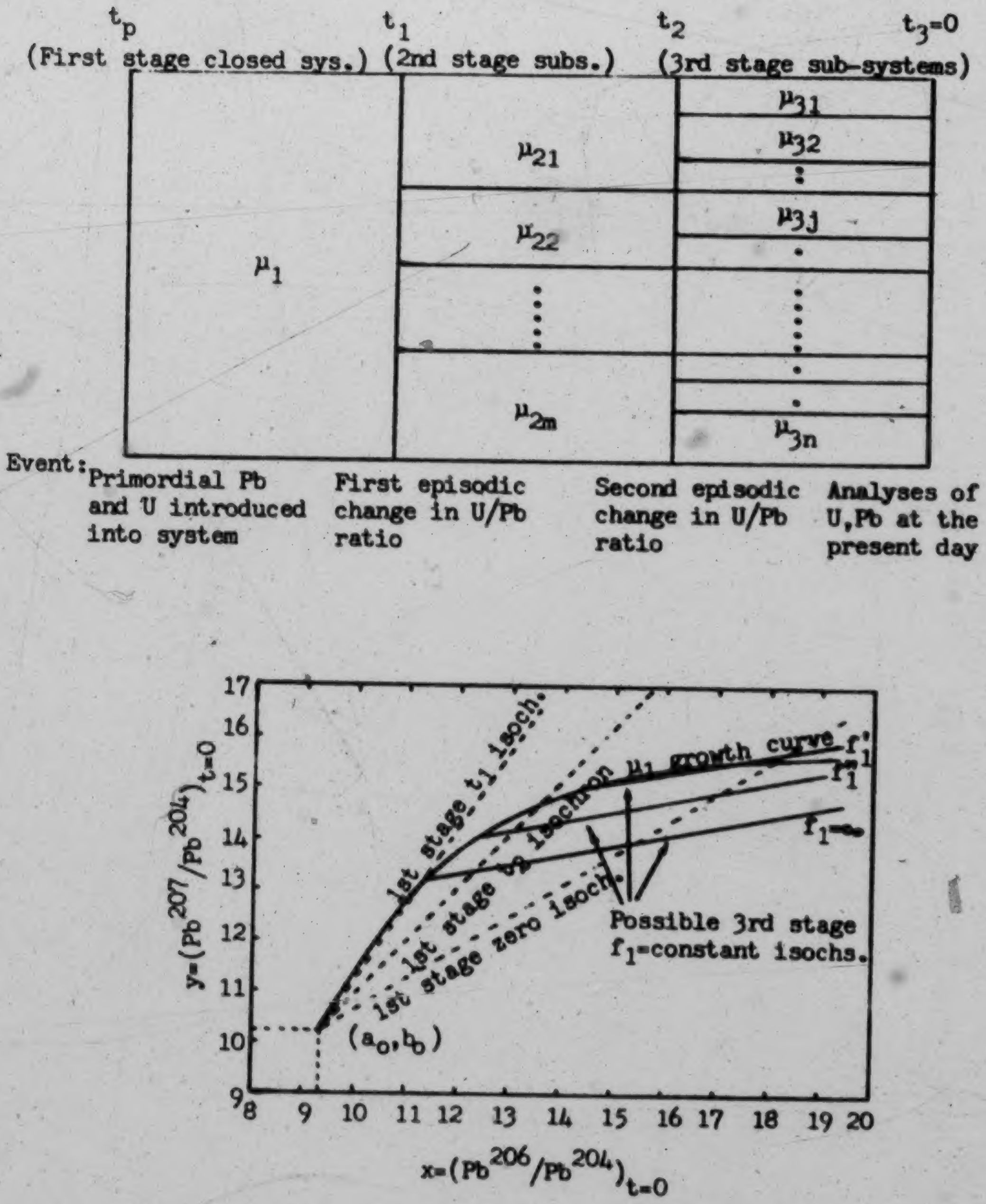
t_p
(First stage closed sys.)
t_1
(2nd stage subs.)
t_2
(3rd stage sub-systems)
$t_3=0$
μ_1
μ_{21}
μ_{22}
μ_{2m}
μ_{31}
μ_{32}
μ_{3j}
μ_{3n}
Event:
Primordial Pb and U introduced into system
First episodic change in U/Pb ratio
Second episodic change in U/Pb ratio
Analyses of U,Pb at the present day
$y=(Pb^{207}/Pb^{204})_{t=0}$
$x=(Pb^{206}/Pb^{204})_{t=0}$
17
16
15
14
13
12
11
10
9
8
9
10
11
12
13
14
15
16
17
18
19
20
1st stage t_1 isoch.
isoch on μ_1 growth curve
1st stage t_2
1st stage zero isoch.
f'_1
f_1
$f_1=\infty$
(a_0,b_0)
Possible 3rd stage f_1=constant isochs.

Figure 12. The development of lead in a three stage system and the lead-lead diagram for lead that has evolved according to a three stage f_1=constant history.
(atfer Gale and Mussett, 1973)

For the case $f_{2j}=\mu_{2i}/\mu_{3j}$=constant, the isochron equation is given by

$$\frac{y_3 - y_1'}{x_3 - x_1'} = \left(\frac{1}{137.8}\right)\left[\frac{f_2(e^{\lambda' t_1} - e^{\lambda' t_2}) + (e^{\lambda' t_2} - e^{\lambda' t_3})}{f_2(e^{\lambda t_1} - e^{\lambda t_2}) + (e^{\lambda t_2} - e^{\lambda t_3})}\right] \text{—(19)}$$

where

$$x_1' = a_o + \mu_1(e^{\lambda t_o} - e^{\lambda t_1})$$

$$y_1' = b_o + (\mu_1/137.8)(e^{\lambda' t_o} - e^{\lambda' t_1})$$

In this case the possible isochrons have different slopes (dependent on the value of f_2, but all pass through the point (x_1', y_1') which is the point of intersection of the single stage μ_1 growth curve with the single stage t_1 isochron. The lead-lead diagram of this particular case of lead evolution is shown in Figure 13.

(D). Uranium-lead and thorium-lead ages

Determination of uranium-lead and thorium-lead ages of a rock depends on a determination of the total amount of radiogenic lead produced by the decay of the parent U or Th subsequent to an initial state of the rock assuming it to be a closed system thereafter. Three independent ages are obtai[illegible]d from the following three equations

$$t_{206} = \frac{1}{\lambda}\log_e\left(1 + \frac{Pb^{206} - (Pb^{206})_{t=t_1}}{(U^{238})_{t=0}}\right) \text{————(20)}$$

$$t_{207} = \frac{1}{\lambda'}\log_e\left(1 + \frac{Pb^{207} - (Pb^{207})_{t=t_1}}{(U^{235})_{t=0}}\right) \text{————(21)}$$

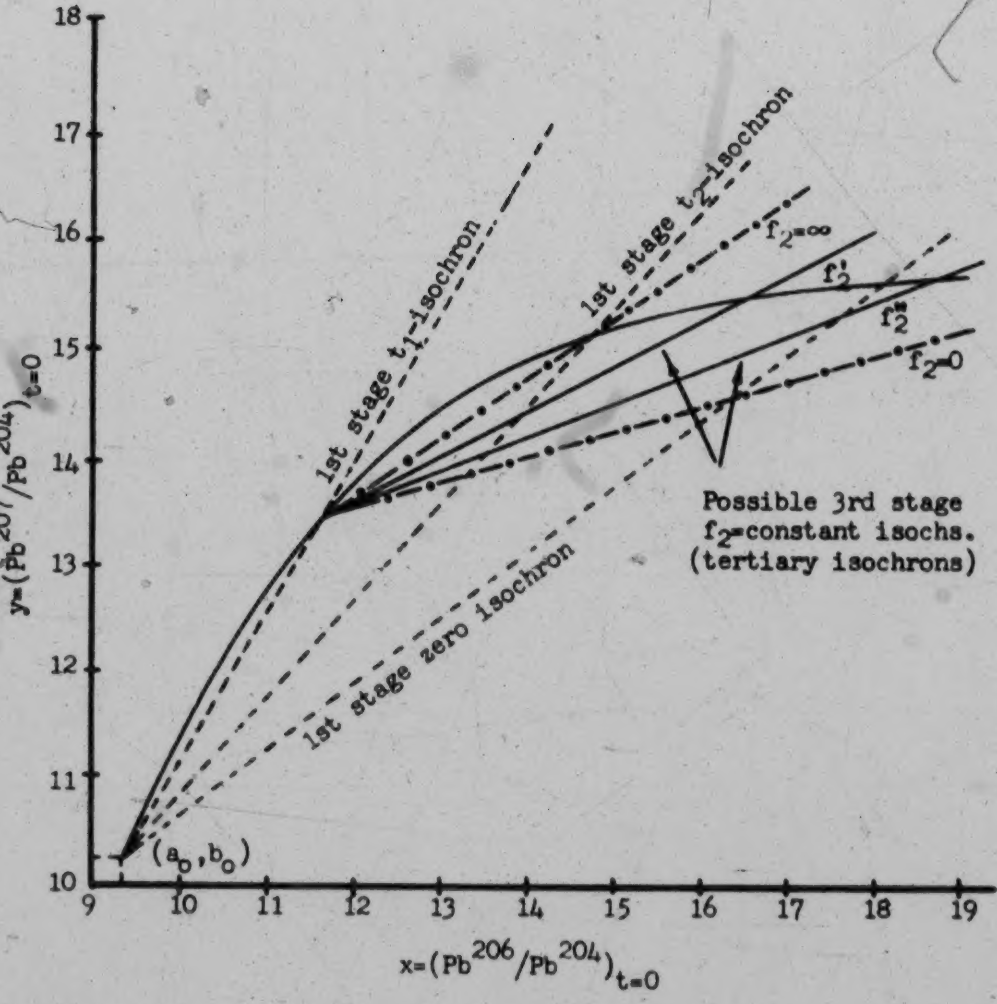

Figure 13. Lead-lead diagram for lead that has evolved according to a three stage f_2=constant history. The region of the diagram accessible to the tertiary isochrons is limited in both the $f_2=\infty$ and $f_2=0$ directions.
(after Gale and Mussett, 1973)

$$t_{208} = \frac{1}{\lambda} \log_e\left(1 + \frac{Pb^{208} - (Pb^{208})_{t=t_1}}{(Th^{232})_{t=0}} \right) \quad \text{———}(22)$$

where Pb^{206} is the amount of lead 206 present in the rock at the time of analysis and $(Pb^{206})_{t=t_1}$ is the amount incorporated into the rock when the system became closed. For a two stage evolution of lead the plot of Pb^{206}/U^{238} versus Pb^{207}/U^{235} is a straight line which intersects the concordia curve at two points (Wetherill, 1956; Ulrych, 1967) as shown in Figure 14. The lower intercept yields t_1, the time when the system became closed and the upper intercept yields an independent age of the earth. In general individual Pb^{206}/U^{238} and Pb^{207}/U^{235} ages are usually discordant due to the loss of lead and/or loss or gain of uranium. Wetherill (1956) showed that if Pb loss occurs in a single episode after the original formation of the U-bearing mineral, then a concordia plot of Pb^{207}/U^{235} versus Pb^{206}/U^{238} for cogenetic samples of varying Pb loss will yield a straight line which intersects the concordia curve at the time of the original mineral formation and the time of the subsequent episodic lead loss (Baadsgaard, 1965).

According to Tilton (1960) Pb may diffuse slowly from a mineral over its lifetime, rather than being lost at one or more discrete intervals. A plot of this model of Pb-loss on a concordia diagram gives a straight line over most of the concordia plot, but the line curves to the origin at low values of Pb^{206}/U^{238} and Pb^{207}/U^{235} with the upper intercept being the time when the system became closed.

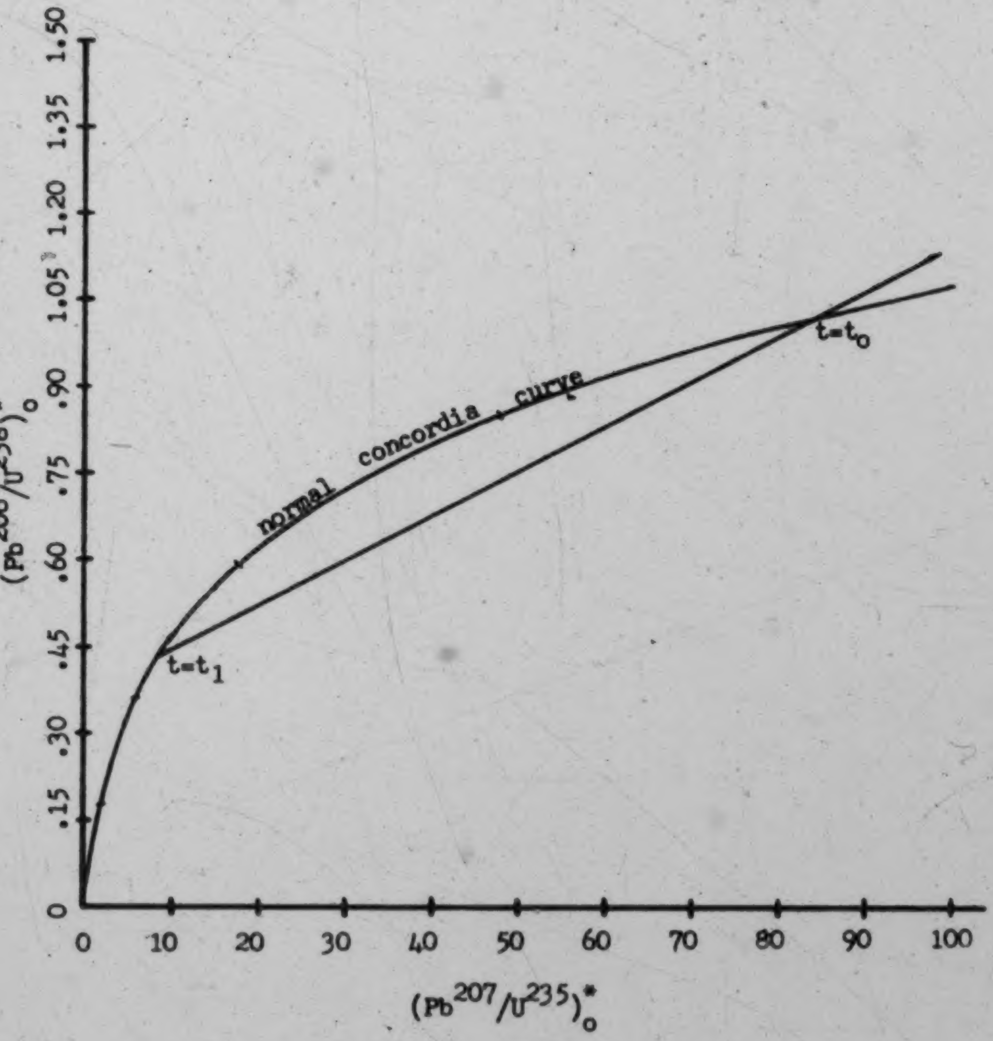

Figure 14. Modified concordia plot for a two-stage evolution of lead. (after Gale and Mussett, 1973)

For the two special cases of three-stage lead, f_1=constant and f_2=constant, Gale and Mussett (1973) showed that the modified concordia plots are families of straight lines as shown in Figures 15a and 15b. In the case of f_1=constant, all the lines pass through the same lower intercept with the concordia curve at t_2 but in the case of f_2=constant, all the lines are parallel with meaningless upper and lower intercepts, and the slope of the line yields t_1 if t_o, the age of the earth, is assumed.

5.3. Whole rock lead-lead and uranium-lead ages

Figure 16 shows the plot of Pb^{206}/Pb^{204} versus Pb^{207}/Pb^{204} for the whole rock lead isotope data of Table 8. The best straight line was calculated following the method of Cumming et al (1972) using equal weighting factors for all ratios. The slope of this line as given by equation (14) is

$$R = 0.1808 \pm .0094 \text{ (one standard deviation).}$$

The two-stage lead model age at which the system had an initial uniform lead composition is determined to be 2700 ± 75 m.y. (S.D.). This age is slightly higher than the Rb/Sr whole rock isochron age of 2610 ± 58 m.y. (Green et al, 1968) for the same intrusive rock. The μ value for the growth curve which intersects the above line at t_1=2700 m.y. and t_2=0 is calculated to be 8.8 ± .10 (95% C.L.) similar to the value for the comformable leads obtained by Cooper et al (1969).

The individual Pb^{206}/U^{238} and Pb^{207}/U^{235} ages are discordant (see Table 9) and follow a general discordant trend of lead loss with the Pb^{207}/Pb^{206} isochron age being higher than the Pb^{207}/U^{235} age

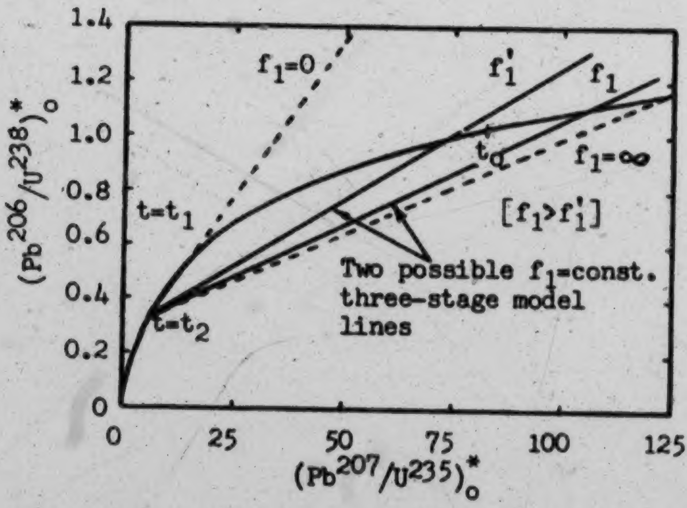

Figure 15a. Modified concordia diagram for lead that has evolved according to three-stage f_1=const. history. (after Gale and Mussett, 1973)

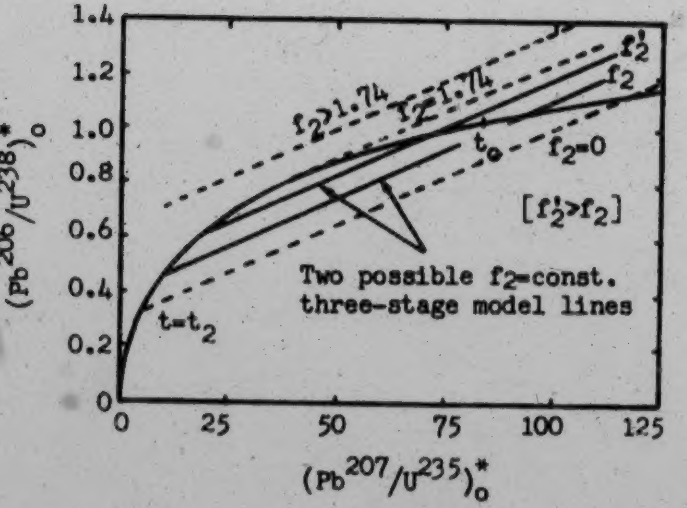

Figure 15b. Modified concordia diagram for lead that has evolved according to a three-stage f_2-constant history. The accessible region of the diagram is limited only in the f_2=0 direction. (after Gale and Mussett, 1973)

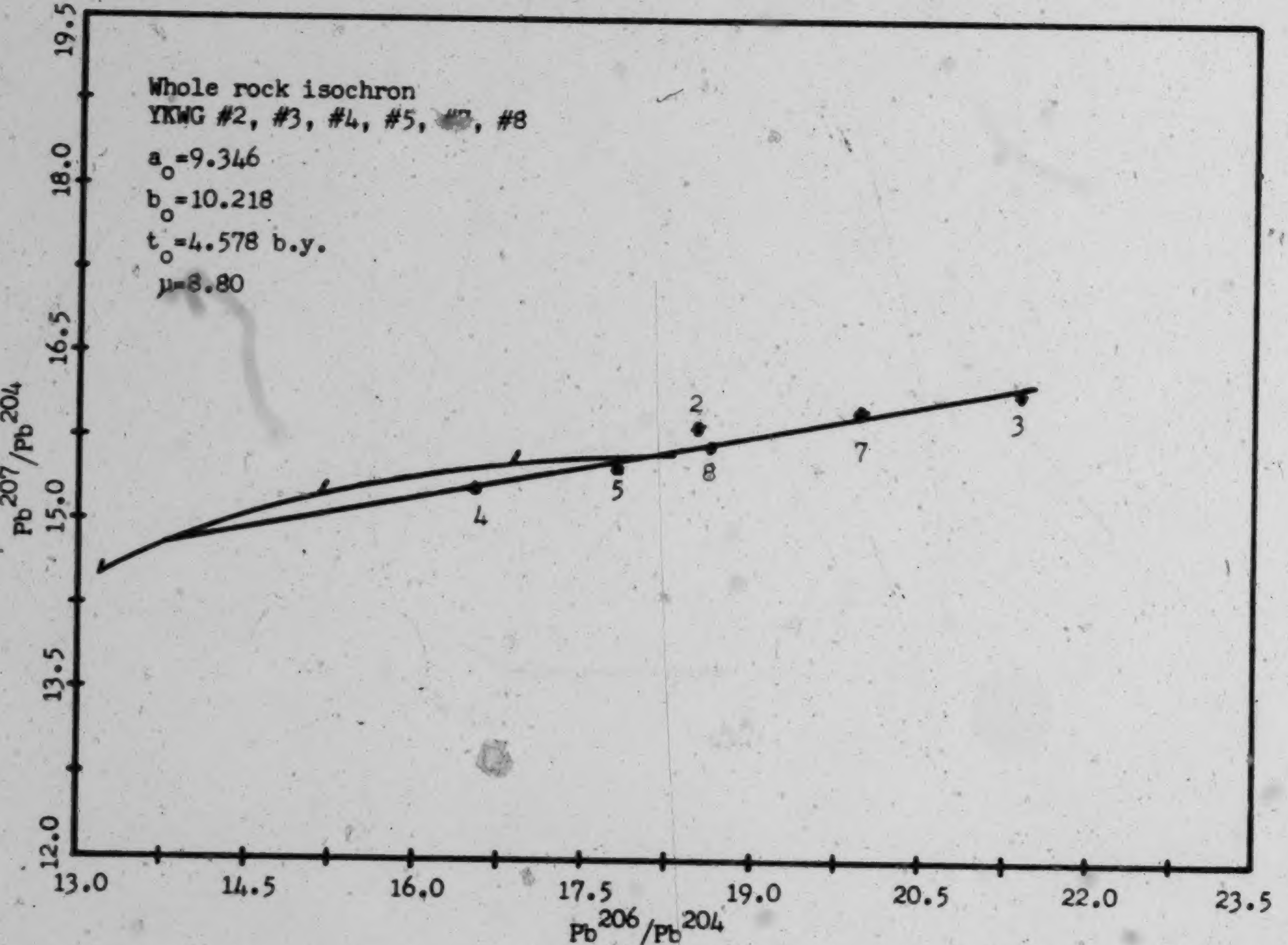
Whole rock isochron
YKWG #2, #3, #4, #5, #7, #8
a_o=9.346
b_o=10.218
t_o=4.578 b.y.
μ=8.80
Pb^{207}/Pb^{204}
19.5
18.0
16.5
15.0
13.5
12.0
13.0
14.5
16.0
17.5
19.0
20.5
22.0
23.5
Pb^{206}/Pb^{204}
2
3
4
5
7
8

Figure 16

which in turn is higher than the Pb^{206}/U^{238} age. These discordant ages may indicate that the samples have lost a fraction of their lead content before or during their analysis in the laboratory. The effect of this loss is to lower the Pb^{206}/U^{238} age proportionately more than Pb^{207}/U^{235} age, but since the Pb^{207}/Pb^{206} age is based entirely on the relative proportions of two isotopes, their ratio, and hence the age calculated from that ratio will be relatively insensitive to loss of lead (Russell and Farquhar, 1960).

The modified concordia plot of the form

$$(Pb^{206}/U^{238})^*_o=[(Pb^{206}/Pb^{204})_o - a_o](Pb^{204}/U^{238})_o$$

versus

$(Pb^{207}/U^{235})^*_o=[(Pb^{207}/Pb^{204})_o - b_o](Pb^{204}/U^{235})_o$ is shown in Figure 17.

A linear trend is observed although the data show considerable scatter, and no simple model can account completely for the data. We may however fit a straight line to the data points (omitting sample point YKWG #2) and this line intersects the normal concordia curve at 1540 m.y. and 5000 m.y. These intercept ages cannot be interpreted on the assumption of an approximation to a two stage model and the upper intercept age of 5000 m.y. makes it impossible to apply the single episodic lead-loss theory proposed by Wetherill (1956) or the continous loss of lead by diffusion described by Tilton (1960).

Because of the lack of a consistent pattern in ages obtained from different approaches, that is the lead-lead isochron diagram, the U-Pb age equations and the concordia diagram, it is clear that a simple

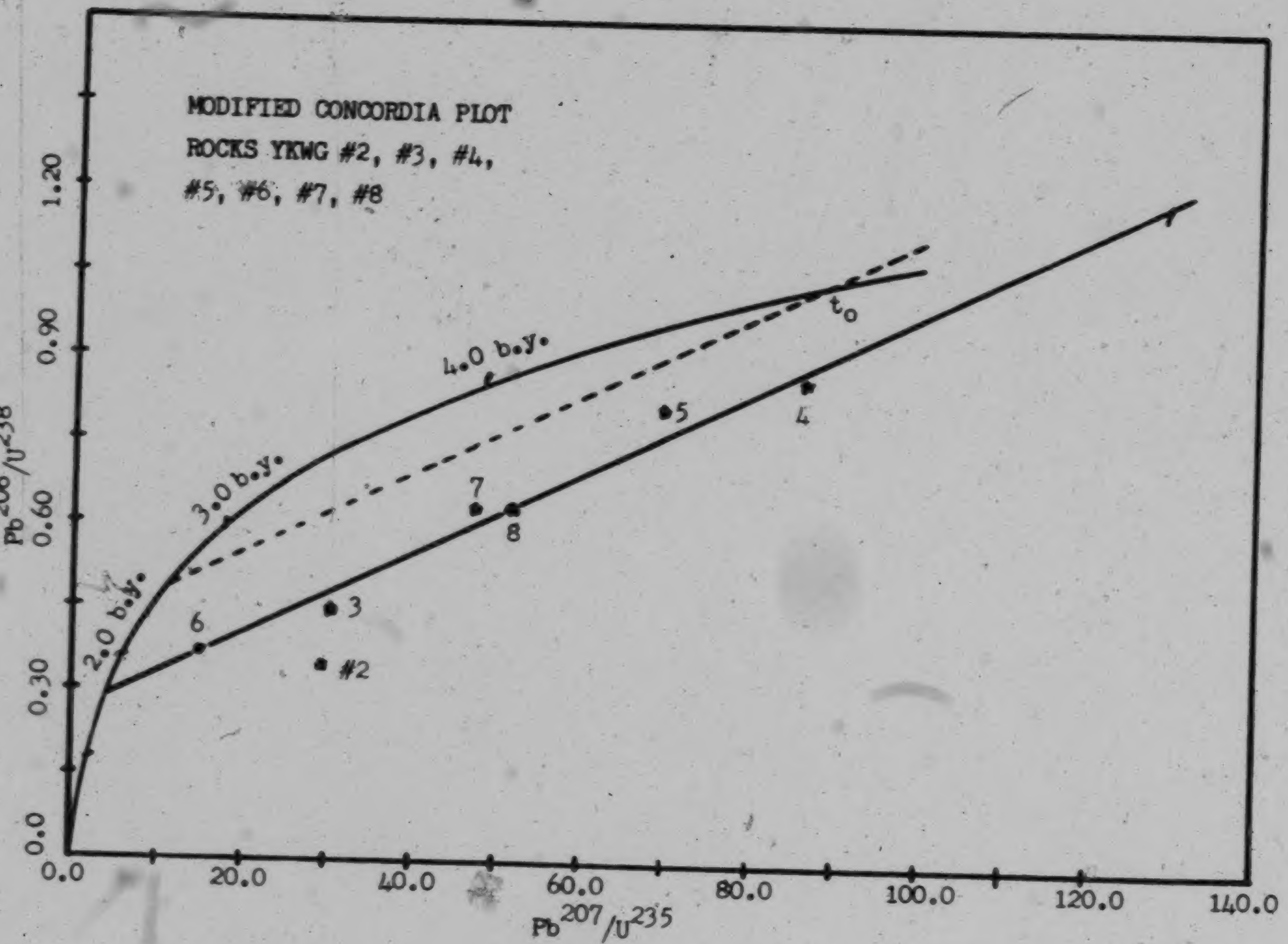
MODIFIED CONCORDIA PLOT
ROCKS YKWG #2, #3, #4,
#5, #6, #7, #8
Pb^{206}/U^{238}
0.0
0.30
0.60
0.90
1.20
Pb^{207}/U^{235}
0.0
20.0
40.0
60.0
80.0
100.0
120.0
140.0
2.0 b.y.
3.0 b.y.
4.0 b.y.
t_o
#2
3
4
5
6
7
8

Figure 17

two-stage model is not adequate to describe the lead evolution in this area even as a first approximation although the lead-lead isochron age of 2700 m.y. ± 85 m.y. agrees within the statistical limits of the Rb/Sr age of 2610 m.y. ± 58 m.y. obtained by Green et al (1968). It was then decided to perform some studies of fractional removal of lead from each of the eight sample rocks by volatilization. Cumming et al (1970) have shown that incremental heating of a rock sample yields lead of varying isotopic composition depending on the heating temperature and the data fit on a single straight line analogous to a mineral isochron. It was hoped that this inhomogeneous distribution of lead in rocks would help to clarify the age differences obtained by the different methods. The results of this volatilization studies are given in Chapter VI.

5.4. Possible three or higher-stage system

An examination of the concordia plot of Figure 17 shows that the best straight line which fits the six data points is parallel to one which has an upper intercept-age of 4578 m.y. (the age of the earth) and a lower intercept-age of 2450 ± 450 m.y. (S.D.) with the normal concordia curve. If a three-stage f_2-constant lead evolution history were assumed as first approximation to the data, the lower intercept-age calculated from the slope of the best fitting straight line and the age of the earth is t_1, the time when the system was subjected to the first change in U/Pb ratios. There is no simple way of finding t_2 from the modified concordia diagram.

It is not clear whether a three-stage f_2-constant lead evolution model can be used to represent the observed data, since the straight line of the modified concordia diagram, which has a lower intercept-age of 1540 m.y. ± 200 m.y., lies considerably below that of $f_2=1$ (see Figure 17) and according to Gale and Mussett (1973) the accessible region is limited by the line which represen[illegible]0 and has a lower intercept-age of t_2. Therefore if the three-stage f_2=constant model is used, the time t_2 when the system was subjected to a second event which resulted in the changes of U/Pb ratios of the system must be less than the above lower intercept-age of 1540 m.y. ± 200 m.y.. The only data from the Yellowknife area which may fall within these limits is the poorly defined Rb/Sr isochron on dyke set III (Gates and Hurley, 1973).

5.5. Second whole rock ratios

As mentioned in section 5.1 the lead samples were extracted by heating rock powder at 1400°C for 30 minutes. For the purpose of experimentation, the author reheated three samples two of these in the form of chips instead of powder (samples YKWG #3 and #5) and one with powder to check the reproducibility. All the samples were heated at 1400°C for 3 hours. The use of rock chips allows faster vacuum evacuation and faster increase of heating temperature. All chips (up to ¼" thick) were completely melted within 15 minutes when the temperature rose above 1300°C. Table 11 shows the ratios of the three reheated samples along with the corresponding ratios from Table 8.

It can be seen that ratios from the two separate heatings made on powdered sample from YKWG #8 are the same. The differences in ratios

Table 11. Comparison of whole rock Pb ratios between the first heating of Table 8 and the second heating, 1973

	Pb^{206}/Pb^{204}		Pb^{207}/Pb^{204}		Pb^{208}/Pb^{204}	
Sample:	1973	Table 8	1973	Table 8	1973	Table 8
YKWG #3	16.336*	21.445	15.284*	16.153	36.407*	36.395
	.017●	.069	.016	.053	.037	.120
YKWG #5	18.108*	17.763	15.612*	15.450	39.112*	38.052
	.024	.038	.021	.034	.052	.080
YKWG #8	18.657	18.654	15.726	15.748	40.843	40.291
	.032	.103	.027	.088	.072	.228

* Sample was heated as rock chips.

● Internal estimate of standard deviation for samples YKWG #3 and #5 are believed to be mainly due to sampling problems arising from the fact that the first heating was made with rock powder while the second heating was made with chips.

The lead-lead isochron diagram of the three data points is shown in Figure 18. A sharply defined straight line with slope of

$$R = 0.188 \pm .008 \text{ (S.D.)}$$

is obtained. The slope-age is calculated to be 2760 m.y. ± 85 m.y. which agrees within the statistical limits with the age 2700 m.y. ± 85 m.y. obtained previously.

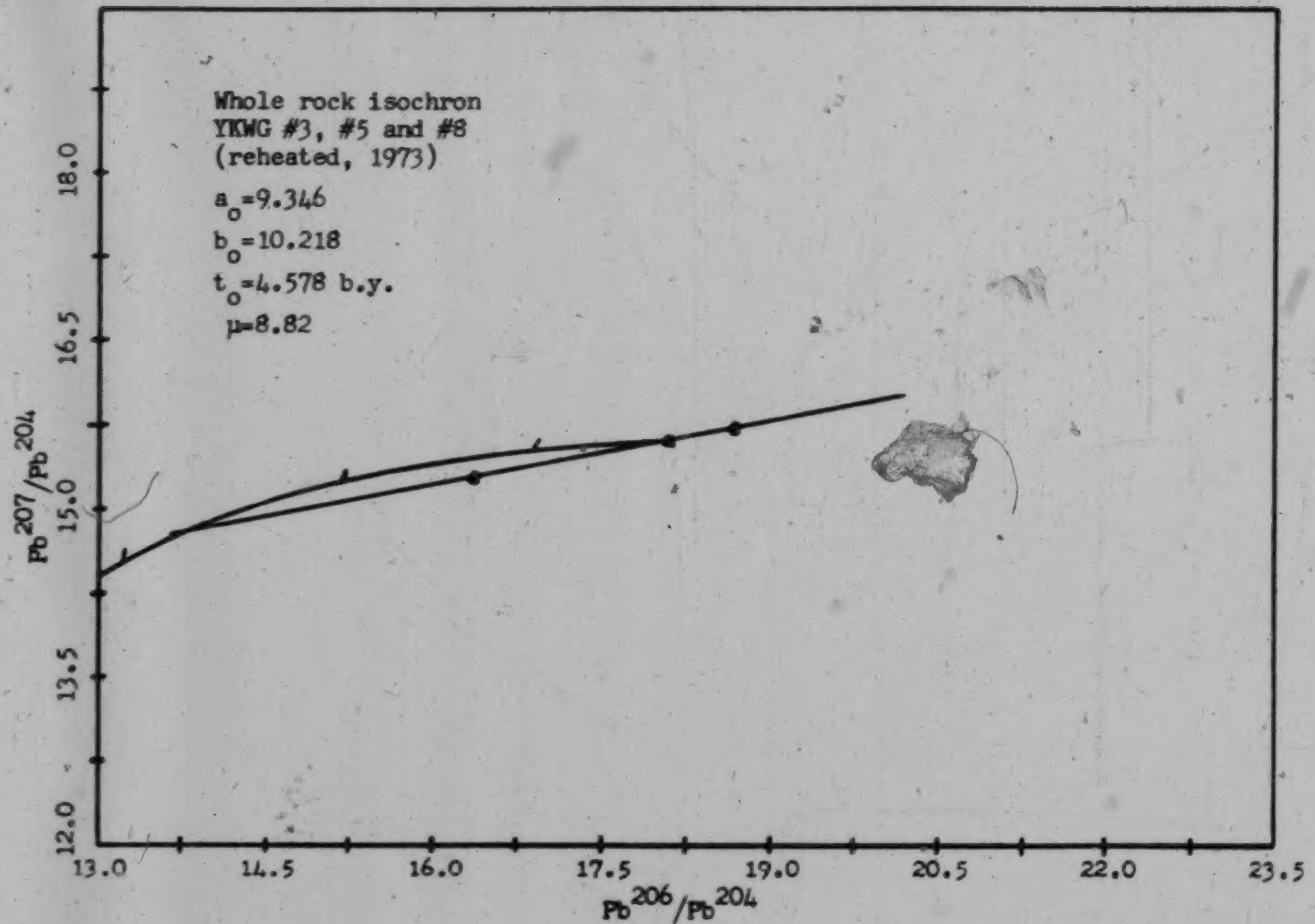
Whole rock isochron
YKWG #3, #5 and #8
(reheated, 1973)
a_o=9.346
b_o=10.218
t_o=4.578 b.y.
μ=8.82
Pb^{207}/Pb^{204}
12.0
13.5
15.0
16.5
18.0
13.0
14.5
16.0
17.5
19.0
20.5
22.0
23.5
Pb^{206}/Pb^{204}

Figure 18

CHAPTER VI

ISOTOPIC COMPOSITION OF FRACTIONALLY VOLATILIZED LEAD AND THE TEMPERATURE ISOCHRON

6.1. Introduction

The existence of different modes (forms) of lead occurrence in natural environments was indicated by Tilton (1956) who obtained a displacement in the isotopic composition of lead by acid leaching of certain minerals. Starik et al (1957) conducted extensive volatilization experiments with pitchblende, monazite, uraninite and a series of granites and made the following conclusions.

"(1). Lead is present in minerals as well as in rocks in different forms.

(2). Different forms of lead sublimate with different speeds when the parent minerals or rocks are heated. This results in a displacement of the isotopic composition of the isolated lead.

(3). Sublimation in vacuum of lead from pitchblende (from Joachimsthal) is toward an impoverishment of common lead in proportion to an increase in temperature and duration of heating. When sublimated in hydrogen the shift in the isotopic composition is toward an enrichment in radiogenic isotopes, and this change proceeds much more smoothly.

(4). The displacement in isotopic composition of uraninite is in the direction of enrichment in extraneous lead, namely, masses 204 and 208. In monazite, on the other hand, the shift is toward an impoverishment of extraneous lead.

(5). When a sample of ancient Karelian granite was sublimated in a stream of hydrogen and the Caledonian granite of Terek Ala-Tau in vacuum,first fractions were enriched in radiogenic isotopes. Apparently, radiogenic lead occurs in granites to a large extent disseminated in the metallic state.

(6). Under natural conditions impoverichment and enrichment of any isotope of lead regardless of its mode of occurrence may take place at relatively moderate temperature (about 600°C).

(7). Investigation of modes of lead occurrence by sublimation methods may aid in the solution of problems relating to the age and genesis of some rocks and minerals."

As pointed out by Starik et al (1957), the different origin of lead, determined by a number of factors, in turn determines the various modes of lead occurrence. The modes of occurrence of primary lead were determined by physico-chemical conditions of the primeval material that make up the earth. As a result of natural radioactive decay of uranium and thorium, radiogenic lead is being continously generated and its mode of occurrence should be quite distinct. Because of processes of remelting, granitization, weathering, etc., original and radiogenic leads may occur together in many different ratios. Identification of the lead types should determine the mode of occurrence of common lead. The chemical compounds in which common lead participates are varied. Radiogenic lead, on the other hand, accumulating in a rock or mineral which has already formed, evidently remains either in the native state or in the form of oxides. Its position in the crystal lattice of a mineral depends upon the crystallochemical peculiarities of the given mineral. Its mode of occurrence depends on the position in the mineral of parent elements related to its original formation and those radioactive elements related to secondary mineralization. However, a certain portion of Pb^{206} in a uranium mineral would be in a position different from the bulk of radiogenic lead even if there had been no secondary mineralization, because a part of U^{234} does not enter the crystal lattice (Starik et al, 1957). The same may be said of some other intermediate decay products of uranium and actino-uranium. This explains the "fragile structures" of radiogenic lead occurrence (Starik et al, 1957).

Generally speaking, processes of leaching, emanation, diffusion, volatilization, recrystallization and isotopic exchange may bring about changes in the isotopic composition of lead in nature and intermixing of different forms of lead.

The Volatilization technique has been used for some time as a means of extracting lead from minerals and rocks (e.g., Edwards and Hess, 1956; Marshall and Hess, 1960; Masuda, 1964; Hamilton, 1965; Cooper and Richards, 1966; Welke et al, 1968; Cooper and Green, 1969; Sinha, 1969; Cumming et al, 1970; Black et al, 1971; Silver, 1970 and 1971; Huey et al, 1971; Doe and Tatsumoto, 1972), but up to the present time there have been few investigations that dealt with the problem of modes of lead occurrence. Different modes of lead occurrence were indirectly indicated by Sinha (1969) who measured isotopic compositions of lead in three fractions of potassium feldspars (the bulk material, the first volatile fraction, and the residual volatile fraction) from granitic rocks and pegmatites and found that lead was more radiogenic in the first volatile fraction and less radiogenic in the residual volatile fraction compared to the bulk sample, indicating that radiogenic lead is not uniformly distributed in feldspar crystals. Sinha interpretated the relative ease with which the radiogenic lead can be volatilized as a suggestion that radiogenic lead is concentrated along grain boundaries and/or in distorted lattice sites in feldspar crystals.

Cooper and Green (1969) made the following evaluation of the volatilization separation of lead;

> " If the efficiency of lead volatilization is less than 100%, it remains possible that the data obtained are not representative of the whole rock lead because the extraction process has preferentially favoured the lead in some minerals relative to others. Such partial lead extractions should yield a linear distribution of points on the Pb^{206}/Pb^{204} versus Pb^{207}/Pb^{204} diagram, with slope dependent on the age of crystallization of the rock sample. The line developed would extrapolate

back to the initial lead isotopic ratios of the parent material."

Cumming et al (1970) independently observed and exploited the inhomogeneous distribution of lead isotopic composition and showed that the range of isotopic data on a plot of Pb^{206}/Pb^{204} versus Pb^{207}/Pb^{204} fit on a simple straight line from which some information regarding the history of the rock may be obtained.

Volatilised lead from some of the Apollo 12 and 14 soils reported by Doe and Tatsumoto (1972) showed that the ratios become more radiogenic as temperature increases in the range 600°C to 1000°C which is contrary to the results observed by Cumming et al (1970) and Black et al (1971) for terrestrial rocks, but the linear relationship between the ratios Pb^{206}/Pb^{204} and Pb^{207}/Pb^{204} is evident, except for one data point extracted at temperature 1350°C.

6.2. Temperature isochron

The isotopic compositions of leads removed from the eight sample rocks at various different temperatures are shown in Table 12. The leads of each rock sample were obtained by volatilizing approximately 20 grams of rock powder mixed with a little pure graphite powder at each of the various indicated temperatures for 3 hours in the high temperature brick furnace (see Chapter III).

It can be seen that the volatilized leads have different isotopic composition depending on the heating temperature and in general lead extracted at lower temperature is more radiogenic than that extracted at higher temperatures. There is also evidence that when the heating temperature rises above a certain critical value, which

Table 12. Pb ratios of fractionally volatilized lead

Sample:	Volatilization temperature (°C)	Pb^{206}/Pb^{204}	Pb^{207}/Pb^{204}	Pb^{208}/Pb^{204}
YKWG #1	750 - 850	27.503 .044*	16.536 .026	40.256 .064
	850 - 950	24.222 .033	16.202 .022	38.702 .053
	950 - 1050	16.412 .021	15.232 .020	34.635 .045
	1050 - 1150	14.832 .013	15.135 .013	34.137 .030
	Whole rock (1400°C)	18.324 .027	15.627 .024	36.158 .055
YKWG #2	850 - 950	20.593 .094	16.149 .074	41.998 .198
		20.441 .014	15.980 .011	41.593 .029
	950 - 1050	18.015 .015	15.535 .013	38.023 .031
	1050 - 1150	16.537 .017	15.282 .016	36.630 .038
	Whole rock (1400°C)	18.473 .020	15.817 .017	39.331 .044

* Internal estimate of standard deviation.

Table 12 cont'd

Sample:	Volatilization temperature(^{o}C)	Pb^{206}/Pb^{204}	Pb^{207}/Pb^{204}	Pb^{208}/Pb^{204}
YKWG #3	750 - 850	21.165	16.037	37.203
		.020*	.015	.036
	850 - 950	17.636	15.428	35.277
		.016	.014	.032
	950 - 1050	15.509	15.060	34.118
		.015	.014	.033
	1050 - 1150	14.773	14.978	33.889
		.010	.011	.024
	Whole rock (1400°C)	21.446	16.153	36.395
		.070	.053	.119
YKWG #4	750 - 850	20.110	16.950	51.789
		.868	.732	2.254
	850 - 950	17.377	15.390	44.984
		.026	.023	.069
	950 - 1050	16.498	15.246	39.780
		.029	.027	.072
	1050 - 1150	16.868	15.325	36.127
		.027	.025	.061
	Whole rock (1400°C)	16.504	15.293	40.265
		.102	.100	.265

* Internal estimate of standard deviation.

Table 12 cont'd

Sample:	Volatilization temperature(°C)	Pb^{206}/Pb^{204}	Pb^{207}/Pb^{204}	Pb^{208}/Pb^{204}
YKWG #5	750 - 850	19.599	15.808	41.716
		.045*	.037	.099
		19.521	15.758	41.640
		.047	.038	.104
	850 - 950	18.514	15.568	39.927
		.025	.021	.055
	950 - 1050	16.503	15.255	36.376
		.029	.027	.066
	1050 - 1150	16.039	15.187	34.769
		.012	.011	.025
	Whole rock (1400°C)	17.763	15.450	38.052
		.040	.035	.069
YKWG #6	750 - 850	60.878	23.088	57.614
		.051	.020	.049
	950 - 1050	28.049	17.370	40.736
		.047	.029	.069
	1050 - 1150	20.891	16.062	36.724
		.029	.023	.052
	over 1150	16.983	15.489	34.986
		.024	.022	.052
	Whole rock (1400°C)	40.802	19.550	45.876
		.140	.066	.157

* Internal estimate of standard deviation.

Table 12 cont'd

Sample:	Volatilization temperature(°C)	Pb^{206}/Pb^{204}	Pb^{207}/Pb^{204}	Pb^{208}/Pb^{204}
YKWG #6 (Reheat)	750 - 850	67.177	24.245	58.422
		.218*	.079	.193
	850 - 950	49.782	21.184	50.116
		.099	.043	.102
		49.843	21.241	50.239
		.042	.018	.043
	950 - 1000	42.155	19.853	46.528
		.023	.011	.026
		42.192	19.867	46.546
		.065	.031	.072
	1000 - 1150	22.756	16.459	37.546
		.039	.028	.065
		22.798	16.485	37.607
		.007	.005	.012
YKWG #7	750 - 850	27.294	16.941	39.325
		.036	.023	.053
	850 - 950	21.725	16.100	37.044
		.012	.009	.021
	950 - 1050	18.070	15.538	35.491
		.017	.015	.034
	1050 - 1150	16.877	15.314	34.966
		.011	.010	.023
	Over 1150	15.520	15.107	34.162
		.024	.023	.053
	Whole rock (1400°C)	19.919	15.968	36.496
		.048	.039	.090

Table 12 cont'd

Sample:	Volatilization temperature(°C)	Pb^{206}/Pb^{204}	Pb^{207}/Pb^{204}	Pb^{208}/Pb^{204}
YKWG #8	750 - 850	21.363 .026 *	16.127 .020	51.006 .062
		21.396 .031	16.136 .024	51.036 .076
	850 - 950	17.388 .043	15.338 .038	38.871 .100
	950 - 1050	16.632 .046	15.297 .043	——
		16.667 .034	15.407 .032	——
		16.743 .037	15.468 .035	——
	1050 - 1150	23.751 .119	16.615 .084	——
	Whole rock (1400°C)	18.654 .103	15.748 .088	40.291 .228

* Internal estimate of standard deviation.

probably depends on the mineralogy of the individual sample rock, the volatilised lead becomes more radiogenic again at the higher temperatures. The different ratios observed for different extracting temperatures indicate possible differences in the modes of lead occurrence.

The fact that the lowest temperatures yield the most radiogenic lead suggests that lead generated by the interstitial material which often contains appreciable amounts of uranium and thorium (Austin and Slawson, 1961) breaks down first and subsequent heatings yield lead from the more refractory minerals. It is known that the uranium-bearing mineral zircon is very refractory and contains highly radiogenic leads. For rocks which contain abundant zircon, we would expect to see the isotopic composition of volatilised lead become more radiogenic as the temperature exceeds that above which the zircon starts to break down. This phenomenon is evidented in samples YKWG #4 and #8.

It is clear that lead is very inhomogeneous in the rock as a whole and that, unless extraction is quantitative, the volatilised lead is unlikely to be isotopically representative of the whole rock sample. This inhomogeneity was also reported by Doe and Tatsumoto (1972) for lunar samples. Similar results were also observed by Sinha (1969) and Starik et al (1957) even in a single mineral fraction of the rock. Cumming et al (1970) cautioned that the volatilization method must be used with care when total lead composition is required. Black et al (1971) made several analyses of whole rock lead composition both by volatilization and by chemical dissolution. Among the six rocks they analysed, three rocks were reported to yield consistent isotopic composition by both methods. However in one rock which was said to be more radiogenic, they reported a gross analytical disagreement of about 6% between the the two methods with the volatilised lead being more radiogenic than the dissolution lead. They suggested the incomplete lead recovery by volatilization as a reason for the discrepancy.

As mentioned previously, the refractory minerals such as zircon contain very radiogenic lead and therefore the isotopic composition of the volatilised lead for a complete recovery should be more radiogenic than that of slightly incomplete recovery. It is difficult to judge whether or not the chemical dissolution method gives a complete lead recovery, as Black et al reported in the same paper that the volatilization method yields 104% of lead compared to the chemical dissolution method reported by Tatsumoto (1969) which was made on U.S.G.S. standard basalt BCR-1.

These data appear to indicate that the volatilization technique can yield complete recovery as long as a temperature of 1300°C or higher is attained.

The plots of Pb^{206}/Pb^{204} versus Pb^{207}/Pb^{204} for leads volatilised at different temperatures for the eight sample rocks are shown in Figures 19 to 26. Data of each rock fit reasonably well on a single straight line (called a temperature isochron here) as expected by Cooper and Green (1969) and Cumming et al (1970). The slopes of the best-fit lines through the data points were calculated by the method of Cumming et al (1972) which includes the effects of correlated

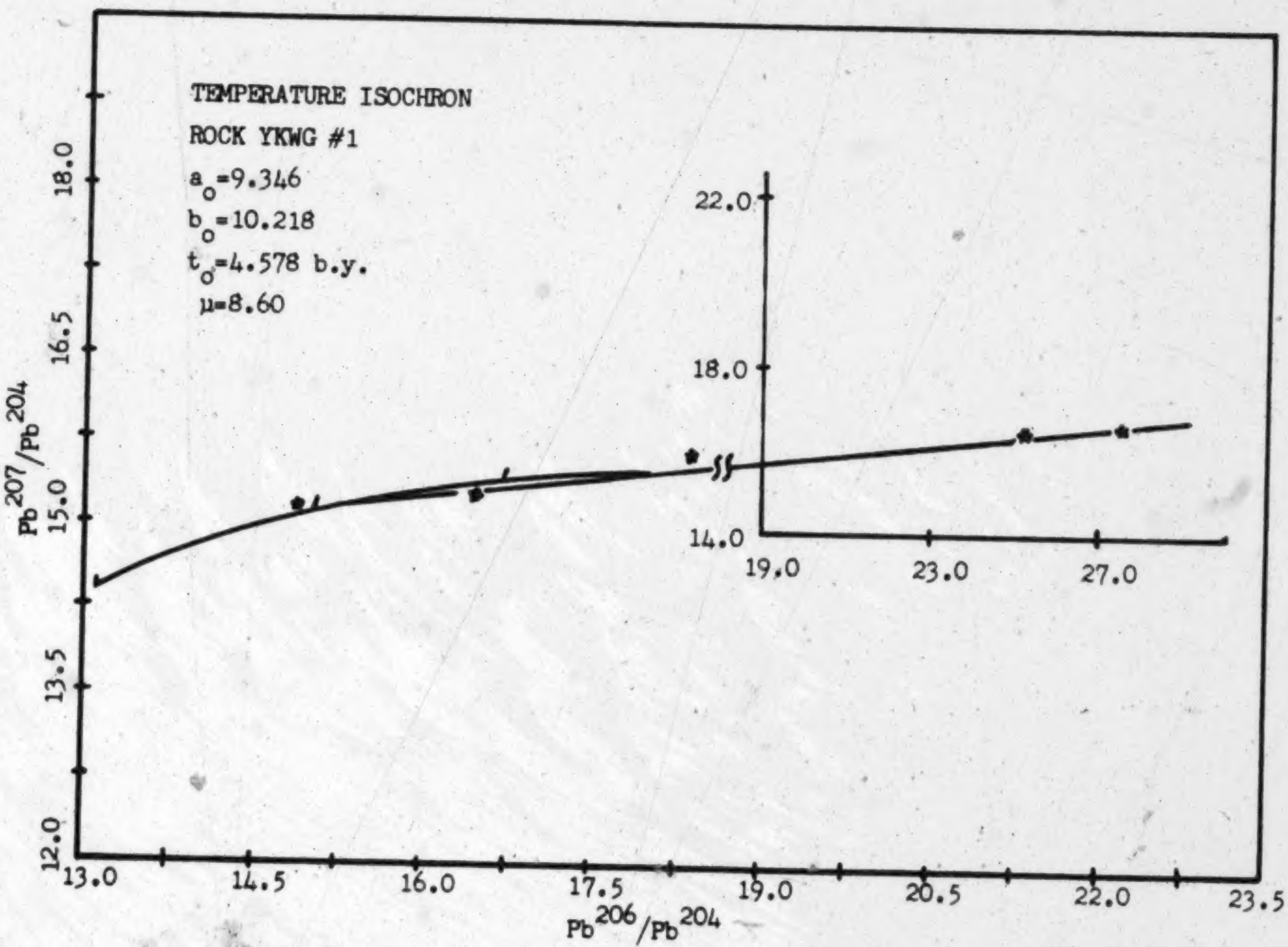
TEMPERATURE ISOCHRON
ROCK YKWG #1
a_o=9.346
b_o=10.218
t_o=4.578 b.y.
μ=8.60
Pb^{207}/Pb^{204}
12.0
13.5
15.0
16.5
18.0
Pb^{206}/Pb^{204}
13.0
14.5
16.0
17.5
19.0
20.5
22.0
23.5
22.0
18.0
14.0
19.0
23.0
27.0

Figure 19

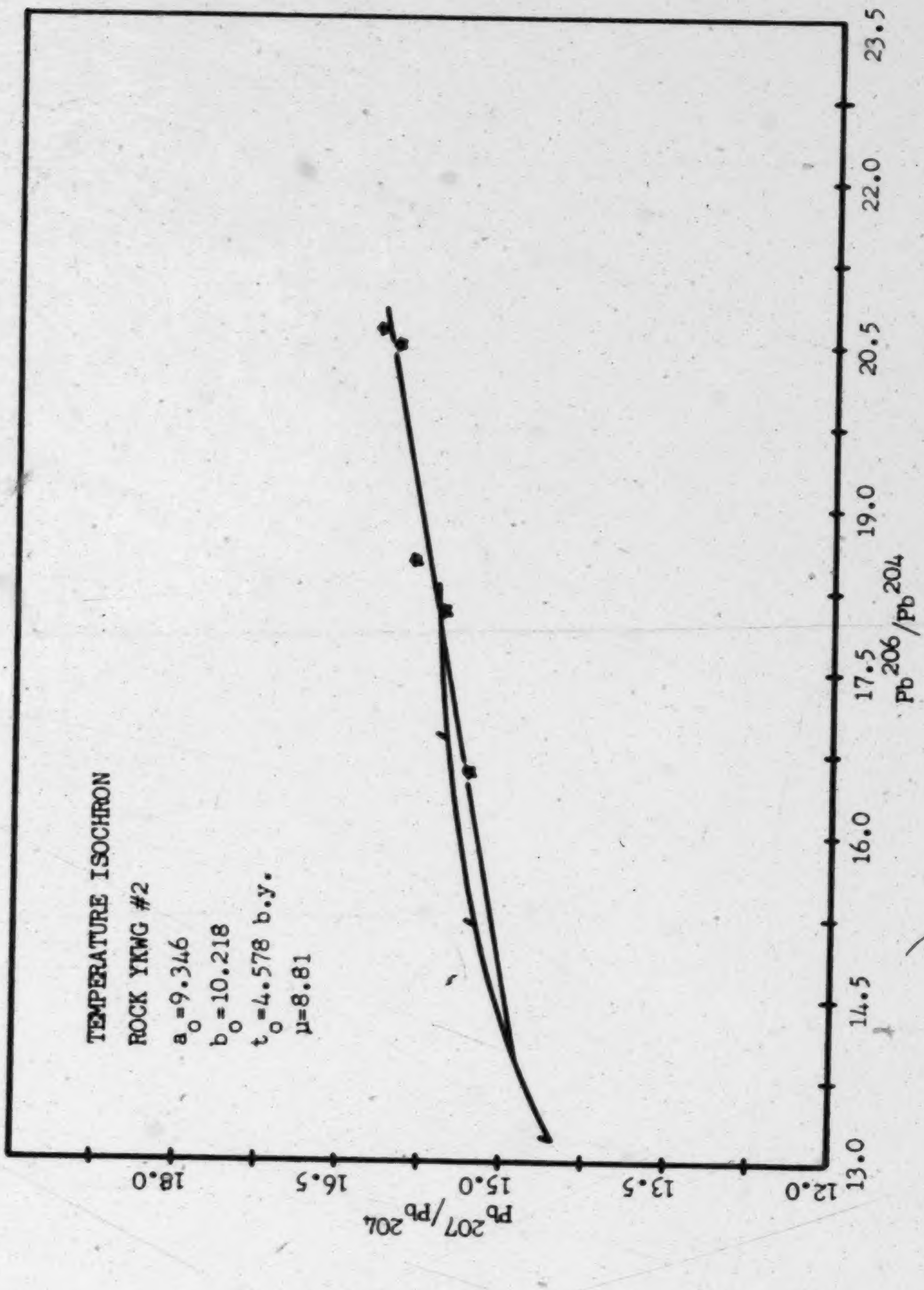
TEMPERATURE ISOCHRON
ROCK YKWG #2
a_o=9.346
b_o=10.218
t_o=4.578 b.y.
μ=8.81
Pb^{207}/Pb^{204}
12.0
13.5
15.0
16.5
18.0
13.0
14.5
16.0
17.5
19.0
20.5
22.0
23.5
Pb^{206}/Pb^{204}

Figure 20

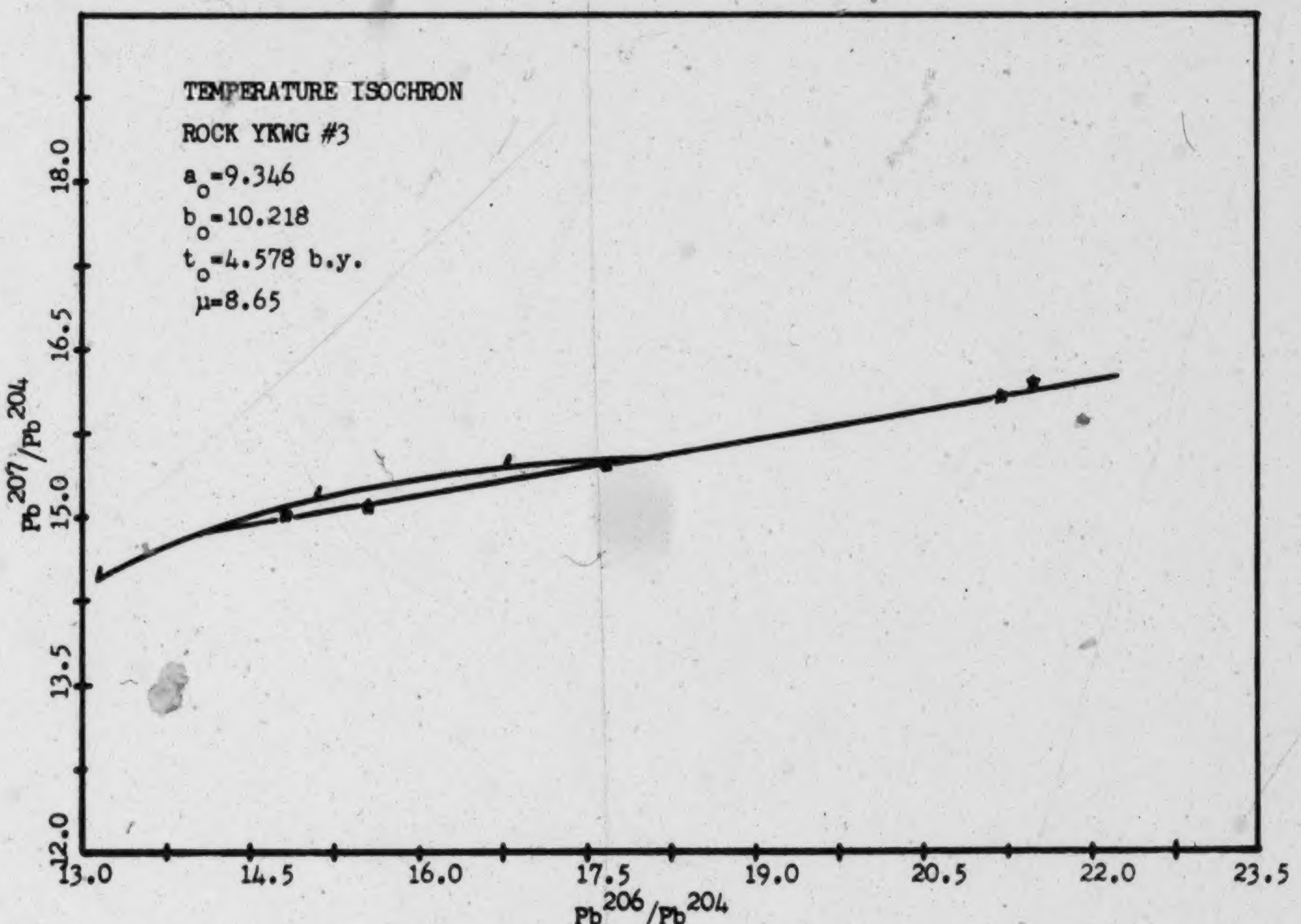
TEMPERATURE ISOCHRON
ROCK YKWG #3
a_o=9.346
b_o=10.218
t_o=4.578 b.y.
μ=8.65
Pb^{207}/Pb^{204}
12.0
13.5
15.0
16.5
18.0
13.0
14.5
16.0
17.5
19.0
20.5
22.0
23.5
Pb^{206}/Pb^{204}

Figure 21

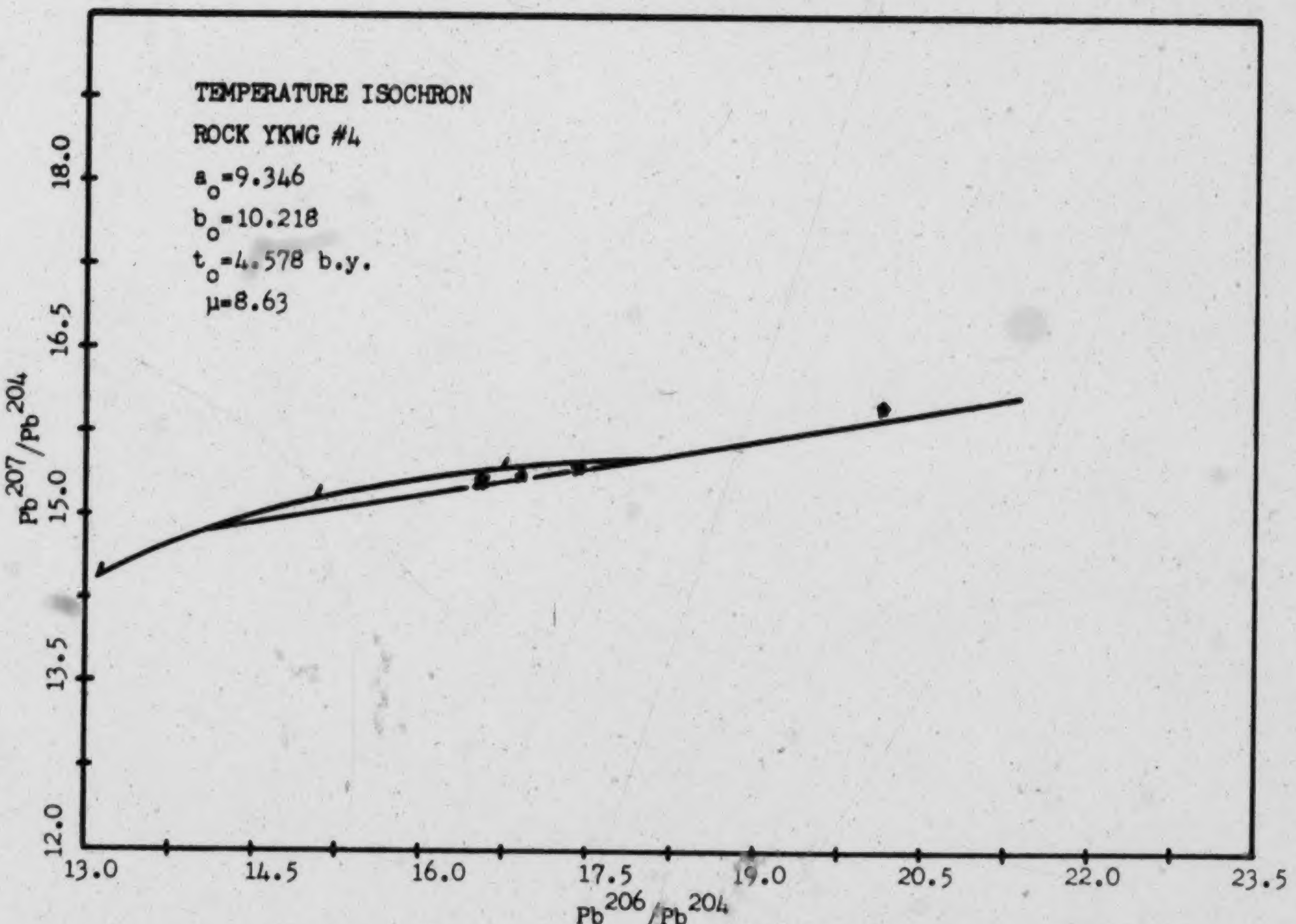
TEMPERATURE ISOCHRON
ROCK YKWG #4
a_o=9.346
b_o=10.218
t_o=4.578 b.y.
μ=8.63
18.0
16.5
15.0
13.5
12.0
Pb^{207}/Pb^{204}
13.0
14.5
16.0
17.5
19.0
20.5
22.0
23.5
Pb^{206}/Pb^{204}

Figure 22

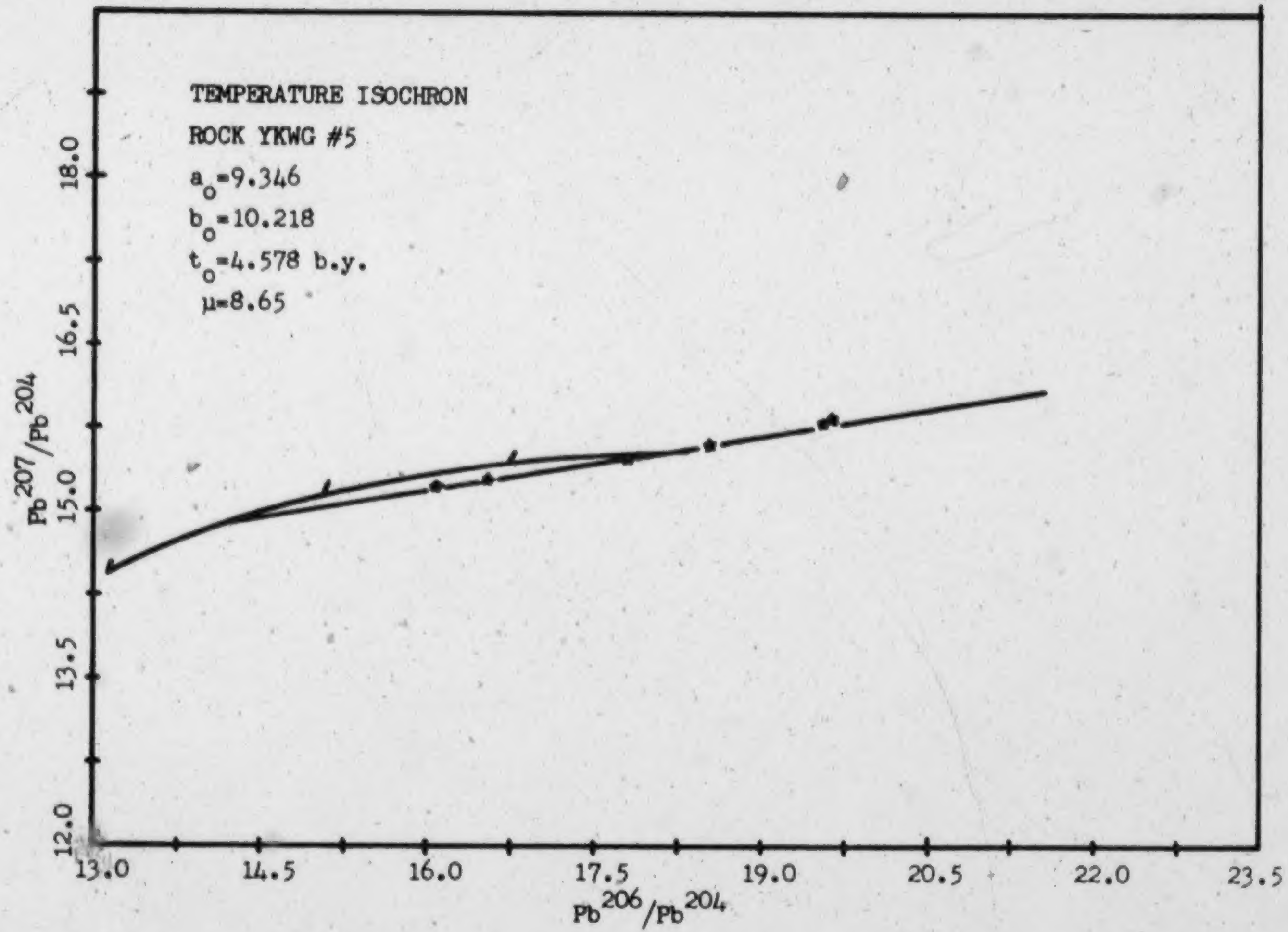
TEMPERATURE ISOCHRON
ROCK YKWG #5
a_o=9.346
b_o=10.218
t_o=4.578 b.y.
μ=8.65
Pb^{207}/Pb^{204}
18.0
16.5
15.0
13.5
12.0
13.0
14.5
16.0
17.5
19.0
20.5
22.0
23.5
Pb^{206}/Pb^{204}

Figure 23

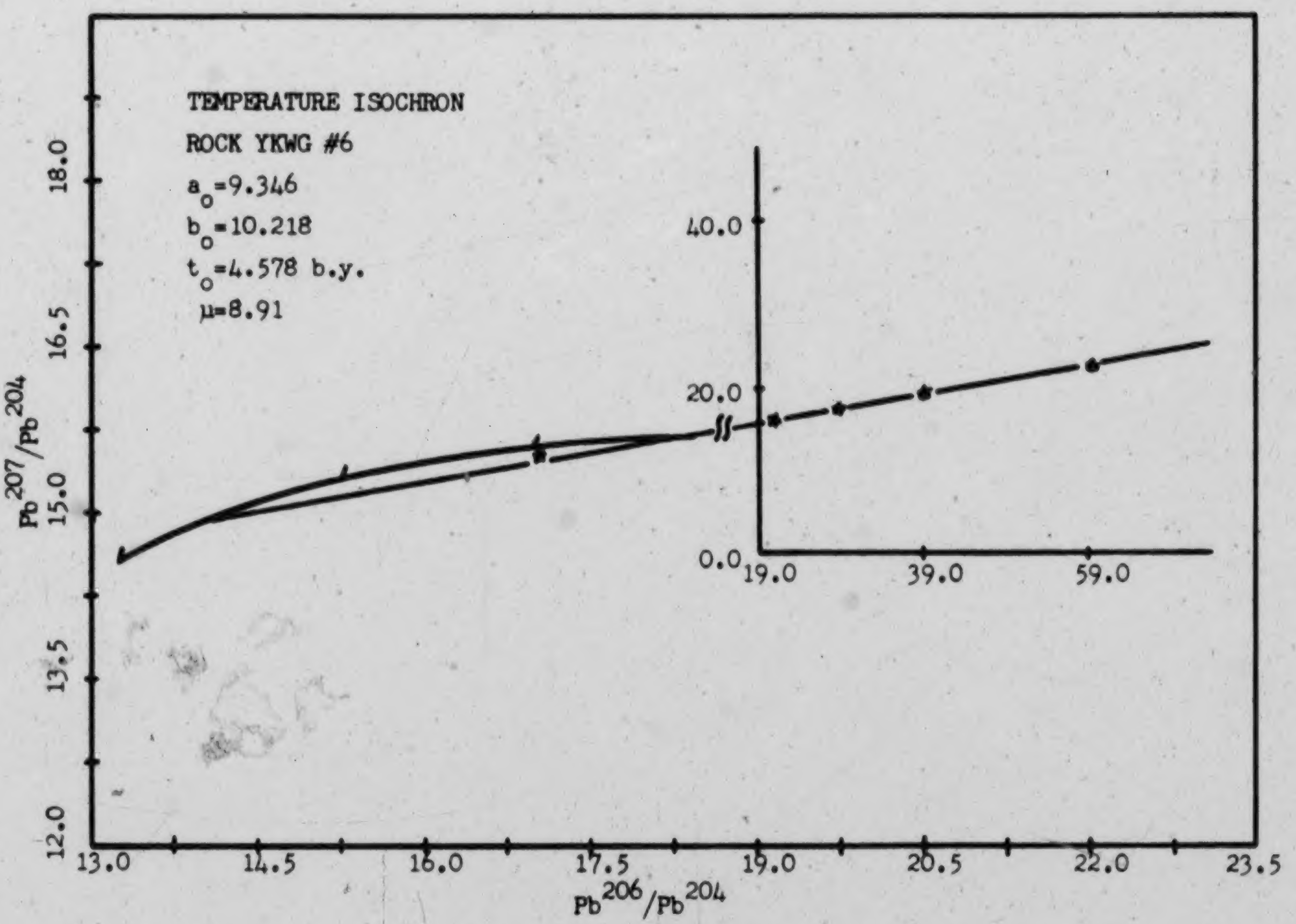
TEMPERATURE ISOCHRON
ROCK YKWG #6
a_o=9.346
b_o=10.218
t_o=4.578 b.y.
μ=8.91
Pb^{207}/Pb^{204}
12.0
13.5
15.0
16.5
18.0
Pb^{206}/Pb^{204}
13.0
14.5
16.0
17.5
19.0
20.5
22.0
23.5
0.0
20.0
40.0
19.0
39.0
59.0

Figure 24

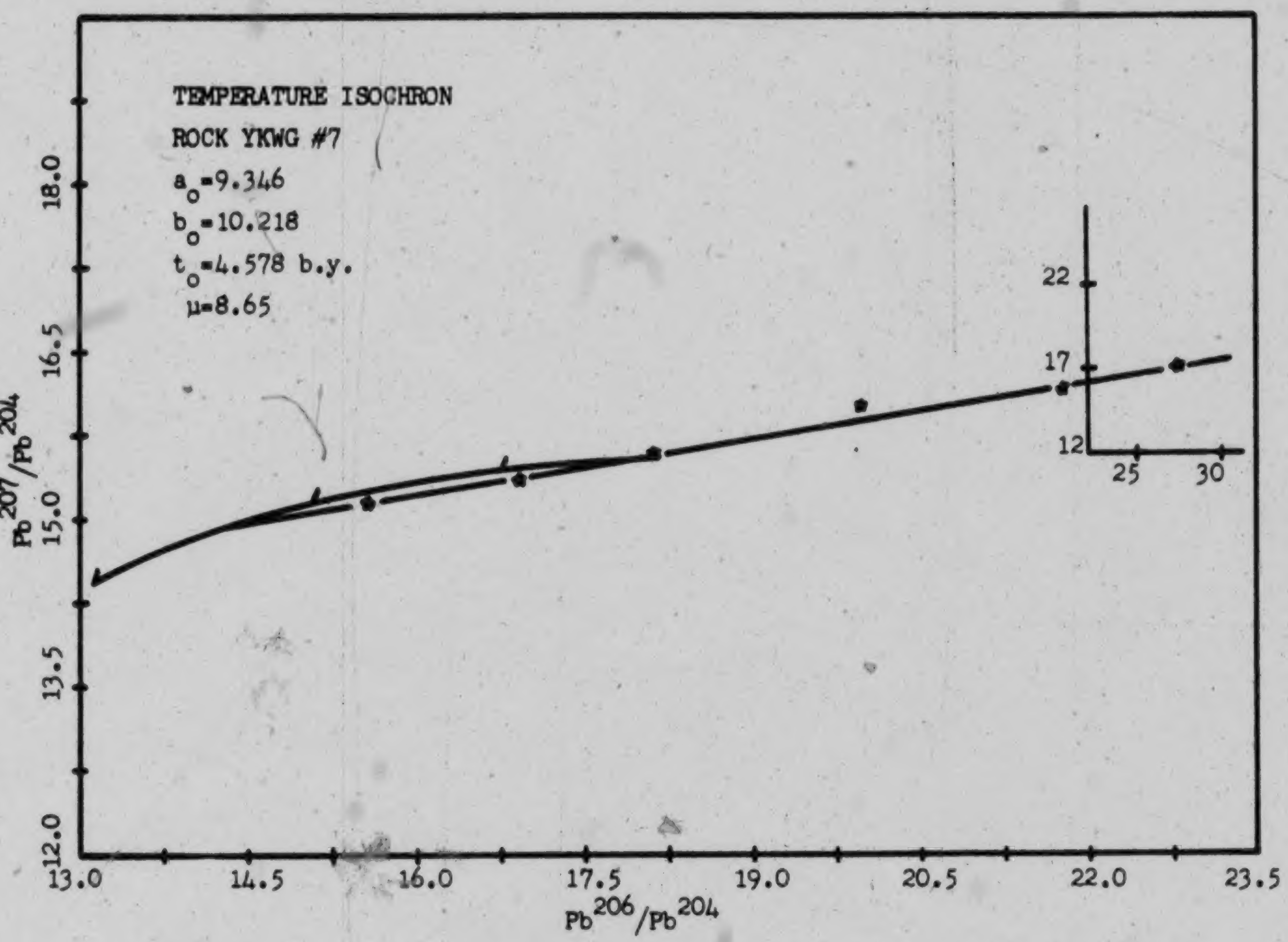
TEMPERATURE ISOCHRON
ROCK YKWG #7
a_o=9.346
b_o=10.218
t_o=4.578 b.y.
μ=8.65
Pb^{207}/Pb^{204}
12.0
13.5
15.0
16.5
18.0
13.0
14.5
16.0
17.5
19.0
20.5
22.0
23.5
Pb^{206}/Pb^{204}
22
17
12
25
30

Figure 25

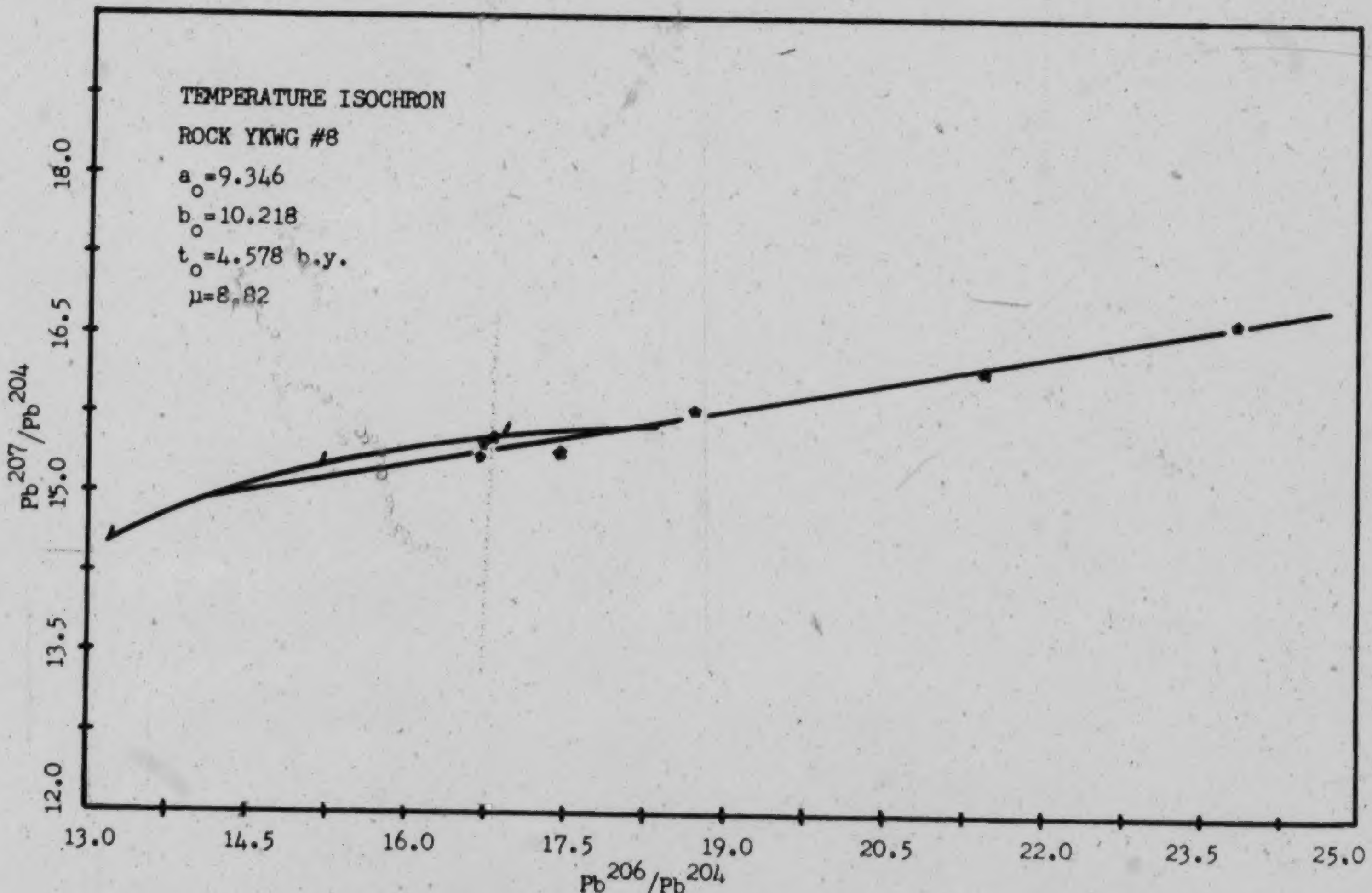
TEMPERATURE ISOCHRON
ROCK YKWG #8
a_o=9.346
b_o=10.218
t_o=4.578 b.y.
μ=8.82
Pb^{207}/Pb^{204}
12.0
13.5
15.0
16.5
18.0
13.0
14.5
16.0
17.5
19.0
20.5
22.0
23.5
25.0
Pb^{206}/Pb^{204}

Figure 26

errors in the two variables. For most of the analyses the sum of the squared residuals exceeds the number of degrees of freedom indicating that the data do not fit the line within the experimental error assigned to the data. The discrepancy may indicate that there is some lack of closed system behaviour for the rock or that the precision of the analyses has been over estimated. As a first approximation the data are treated as if they fit the calculated line and the error estimates of the slope have been increased by the ratio (Σ residuals/degrees of freedom)$^{\frac{1}{2}}$. This procedure has the effect of combining the measuring error with possible geological variation but at the present stage of this work it is believed that this procedure leads to the most satisfactory interpretation of the data.

The linear relationship of ratios derives from the fact that if the rock as a whole contained initial amounts of lead which were homogeneous in composition, then the lead contained in different mineral phases would changes isotopically with time according to their respective U/Pb ratios and at any particular temperature we measure some linear combination of contributions from the various minerals. Thus if the system remains closed, the slope of the straight line may be interpreted in terms of the time since the formation of the system.

6.3. Two stage model temperature isochron ages

The slope-ages and calculated values of μ based on a two-stage lead evolution model are shown in Table 13. An inspection of the data shows that samples YKWG #3, #4, #7 and #8 have ages of about 2550 m.y. The sample YKWG #6 which is a pegmatite dike should, according to the

Table 13. Slope ages of the temperature isochrons

Sample:	µ value (95% C.L.)	Slope (S.D.)	Age in m.y. (S.D.)
YKWG #1 (Syenite, acidic)	8.60 ±.02	.113 ±.005	1880 ±75
YKWG #2 (Syenite)	8.81 ±.02	.176 ±.036	2650 ±300
YKWG #3 (Granodiorite)	8.65 ±.02	.168 ±.004	2575 ±40
YKWG #4 (Granodiorite)	8.63 ±.04	.165 ±.030	2550 ±270
YKWG #5 (Granodiorite)	8.65 ±.02	.163 ±.005	2525 ±50
YKWG #6 (Pegmatite)	8.91 ±.03	.174 ±.001	2635 ±15
	8.97 ±.02	.175 ±.001	2645 ±15
YKWG #7 (Granodiorite)	8.65 ±.01	.158 ±.004	2474 ±45
YKWG #8 (Diorite)	8.82 ±.02	.163 ±.009	2530 ±90

geological relationships, be younger than its host rock. The older age suggested by the lead isotope ratios, may for the time being be explained on the basis of B type anomalous lead as defined by Houtermans. Possibly some addition of radiogenic lead from the surrounding rocks to the pegmatite might have occurred during the formation of the dyke. The age of YKWG #1 (1880 m.y. ± 75 m.y.) is identical within experimental error with the data of Gates and Hurley (1973) for the high Rb samples of dyke set I. In fact a recalculation of the age of these data, using 5 samples containing the highest Rb/Sr ratios, yield an age of 1870 m.y. ± 50 m.y. in excellent agreement with the data given here. There seems to be no reason to ignore these interesting data on the diabase dykes.

6.4. Mineral and whole rock isochrons

When all ratios except those of YKWG #1 are used for the straight line fitting (Figure 27), a line, called "all-temperature" isochron here, with slope 0.175 ± .002 is obtained and the slope-age is 2650 m.y. ± 20 m.y. intermediate between the whole rock and heating results. If the temperature isochrons are to be interpreted as the equivalent of mineral isochrons then one would expect this relationship and no particular significance may be attached to the slope obtained.

The difference in ages between the whole rock isochron and the average of the individual temperature isochrons may be significant and the time interval compares well with the period of tectonic activity deduced by Green and Baadsgaard (1971).

The comparison of the whole rock lead isochron with mineral or heating temperature isochrons is analogous to the

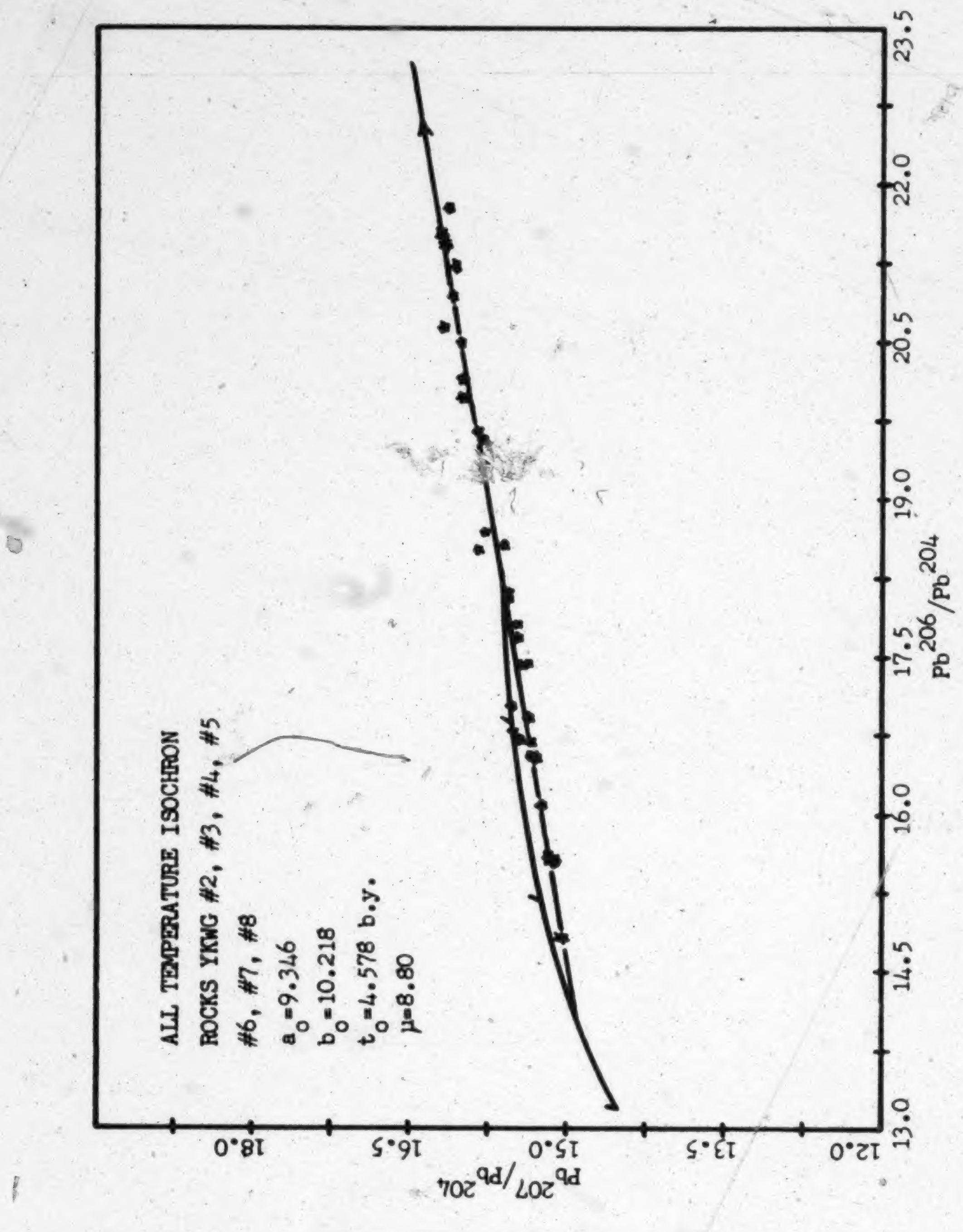
ALL TEMPERATURE ISOCHRON
ROCKS YKWG #2, #3, #4, #5
#6, #7, #8
a_o=9.346
b_o=10.218
t_o=4.578 b.y.
μ=8.80
Pb^{207}/Pb^{204}
12.0
13.5
15.0
16.5
18.0
13.0
14.5
16.0
17.5
19.0
20.5
22.0
23.5
Pb^{206}/Pb^{204}

Figure 27

similar situation (Ulrych and Reynolds, 1966) in Rb/Sr systematics which are well known (for example, see Baadsgaard 1965). Let the subscript o denote the time at which a rock or mineral first became a closed system and p denote the present time. Combining the known relations

$$(Rb^{87})_o = (Rb^{87})_p e^{\lambda t}$$

and $$(Rb^{87})_o - (Rb^{87})_p = (Sr^{87})^*_p \quad \text{(radiogenic only)}$$

we obtain $$(Rb^{87})_p(e^{\lambda t} - 1) = (Sr^{87})^*_p.$$

Considering the change in the total amount of Sr^{87},

$$(Sr^{87})_p = (Sr^{87})_o - (Sr^{87})^*_p$$

we obtain the equation

$$\left(\frac{Sr^{87}}{Sr^{86}}\right)_p = \left(\frac{Sr^{87}}{Sr^{86}}\right)_o + \left(\frac{Rb^{87}}{Sr^{86}}\right)_p (e^{\lambda t} - 1) \text{ ——— (A)}$$

Equation (A) is the equation of a straight line as shown in Figure 28 for samples which have same initial $(Sr^{87}/Sr^{86})_o$ ratios. When the rock is metamorphosed at time t_m, the Sr in the rock is redistributed and the Rb/Sr in the recrystallized minerals need not be the same as formerly so the slopes of the growth lines may be different after metamorphism. The whole rock growth line is unaffected, because of the fact that the rock is a closed system. The Sr^{87}/Sr^{86} in the recrystallized (or newly-formed) minerals grows again from the Sr^{87}/Sr^{86} values for the whole rock at t_m. Figure 29 shows the whole-rock and mineral

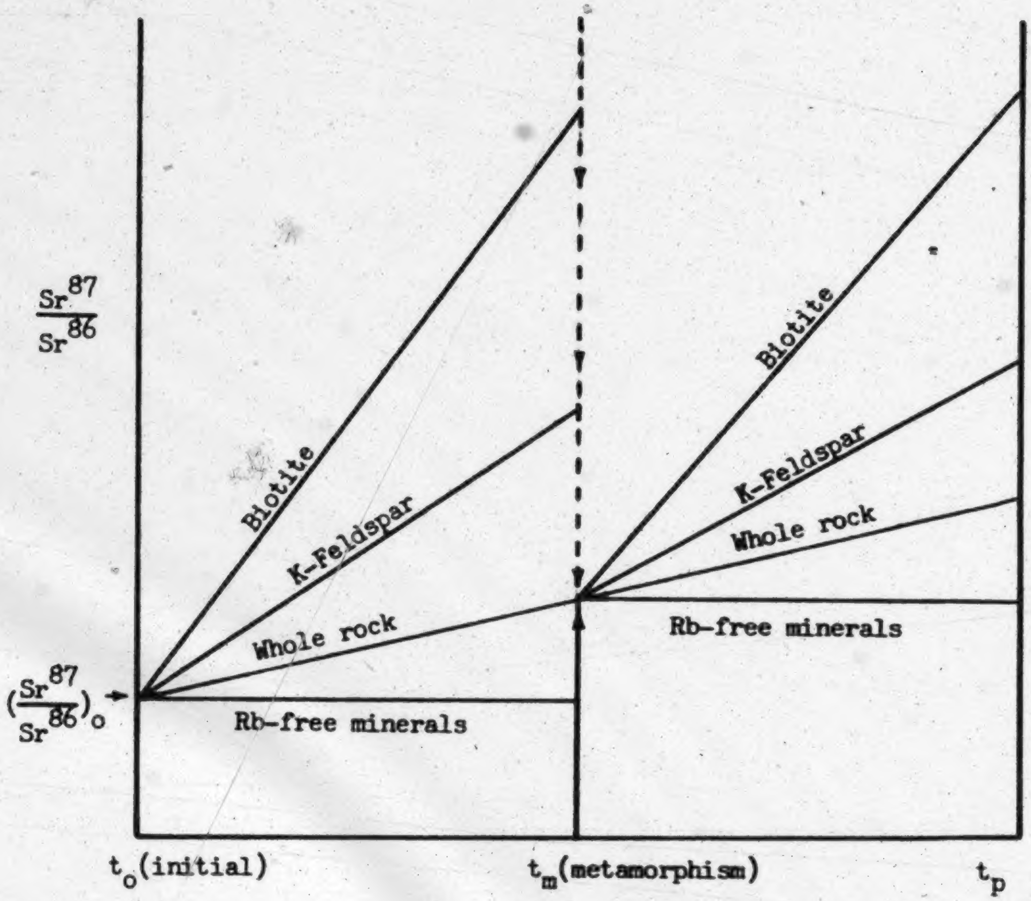

Figure 28. Effect of metamorphism on the change in Sr^{87}/Sr^{86} with time in a rock (closed system) and its constituent minerals (open systems). (after Baadsgaard, 1965)

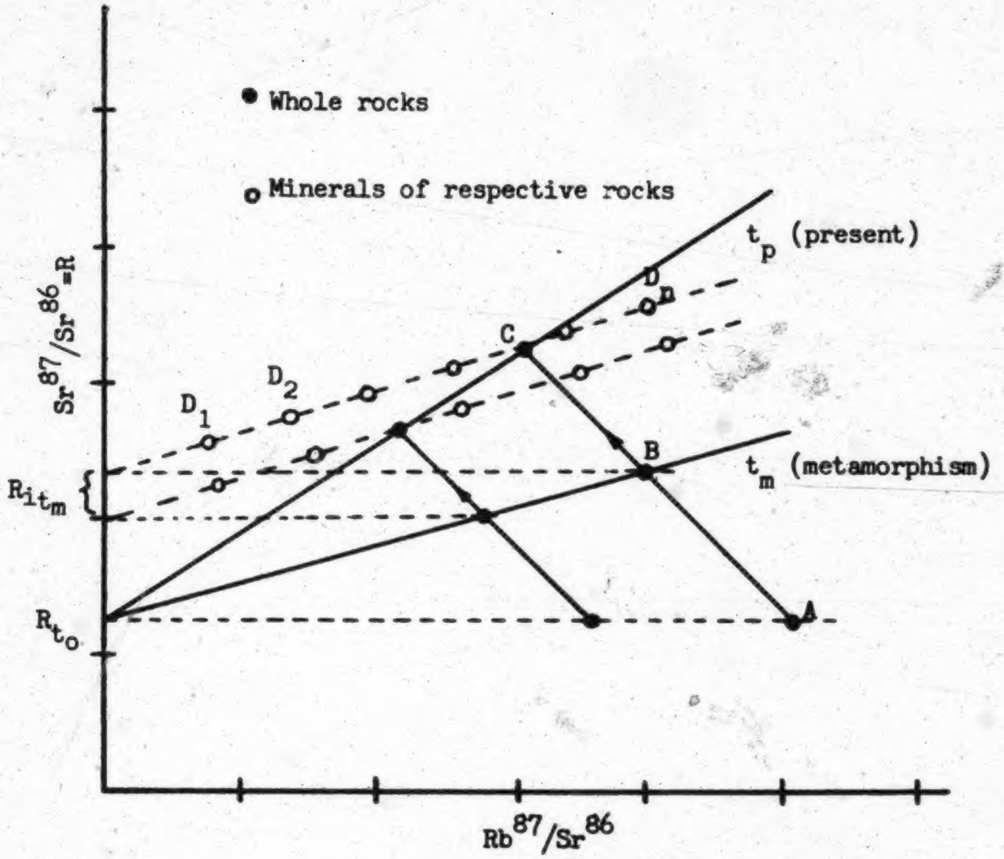

A — whole rock composition at t_o.

B — whole rock composition at $t_m = R_i$ at t_m, the new initial ratio for the minerals at the time t_m.

C — whole rock composition at t_p.

D_{1-n} — mineral composition at t_p after resetting of R at time t_m.

Figure 29. Variation in Sr^{87}/Sr^{86} vs. Rb^{87}/Sr^{86} for whole-rock and the effect on constituent minerals by a metamorphic event at time, t_m.

isochrons for two whole rock phases and the result of a metamorphic event at t_m.

In the case of a U-Pb system, the equation for Pb^{206} may be written as

$$\left(\frac{Pb^{206}}{Pb^{204}}\right)_p = \left(\frac{Pb^{206}}{Pb^{204}}\right)_o + \left(\frac{U^{238}}{Pb^{204}}\right)(e^{\lambda t} -1) \text{ ——————— (B)};$$

equivalent expressions exist for Pb^{207} and Pb^{208}.

A lead-lead diagram showing the whole rock isochron and the mineral isochrons similar to Figure 29 will also occur for lead isotopes and is shown in Figure 30.

The difference in ages between the whole rock isochron and the average individual temperature isochrons may in fact represent two different ages. A whole rock isochron age (2700 m.y. ± 85 m.y.) is the time when the rock crystallized. The mineral isochron age 2550 m.y. ± 50 m.y. is equivalent to the temperature isochron age, the time which signals the end of a metamorphic event when the individual mineral phases are able to retain their radiogenic lead.

6.5. Some implications

From the volatilized lead ratios discussed in this Chapter, some important implications regarding the volatilization technique and its application to geochronology may be derived.

(1). The temperature isochron obtained from the incremental heating of a rock is analogous to the mineral isochron of the rock as claimed

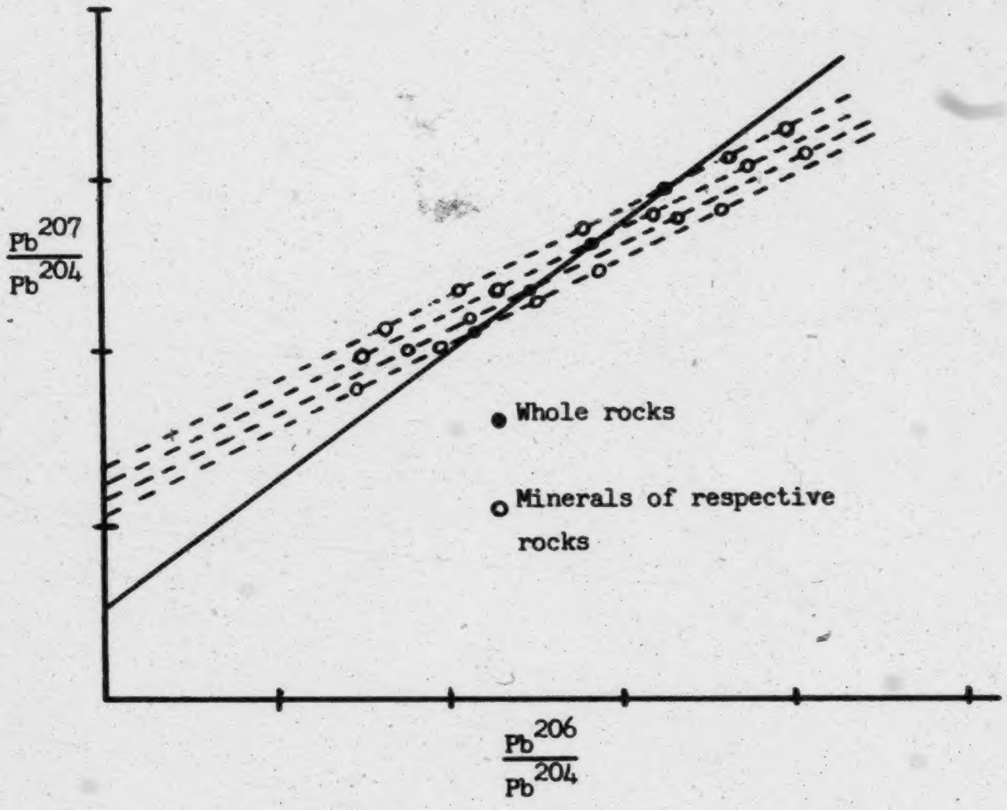

Figure 30. Lead-lead diagram for whole rocks and minerals showing a two-event history.

by Cumming et al (1970).

(2). The all-temperature isochron age obtained from the incremental heating of a number of cogenetic rocks is intermediate between the whole rock isochron and the mineral isochron ages.

(3). Extraction of lead from a number of cogenetic rocks by incremental heating of each rock is a fast and efficient method of finding some information about the history of the rocks.

To test the first suggestion that the temperature isochron is analogous to the mineral isochron, mineral separations were made on three rock samples and lead from each of the mineral phases were extracted by volatilization. Results of the mineral leads are discussed in Chapter VII.

6.6. Temperature isochron of southeast granodiorite

As mentioned in Chapter I, one rock sample from the southeast granodiorite obtained from the Department of Geology was analysed. Table 14 shows the ratios of lead extracted at various different temperatures and the lead-lead diagram is shown in Figure 31 The temperature isochron has a slope of 0.1767 ± .0043(S.D.) which represents a slope-age of 2660 m.y. ± 45 m.y.. Thus if this sample is representative of the material of the southeast granodiorite, it then appears that the mineral age of the southeast granodiorite is similar to that of the western granodiorite. A similar relationship was also observed by Green (1968) using the Rb/Sr decay scheme.

Table 14. Ratios of the volatilized lead of the southeast granodiorite

Volatilization temperature(°C)	Pb^{206}/Pb^{204}	Pb^{207}/Pb^{204}	Pb^{208}/Pb^{204}
900	21.738	16.071	43.177
	.020*	.015	.040
950	20.701	15.871	41.568
	.062	.048	.126
1000	20.627	15.911	41.619
	.023	.018	.047
1050	18.864	15.608	38.443
	.051	.043	.106
1075	18.584	15.493	38.133
	.024	.020	.049
1100	17.287	15.303	36.451
	.026	.024	.057
	17.240	15.300	36.381
	.066	.059	.140

* Internal estimate of standard deviation.

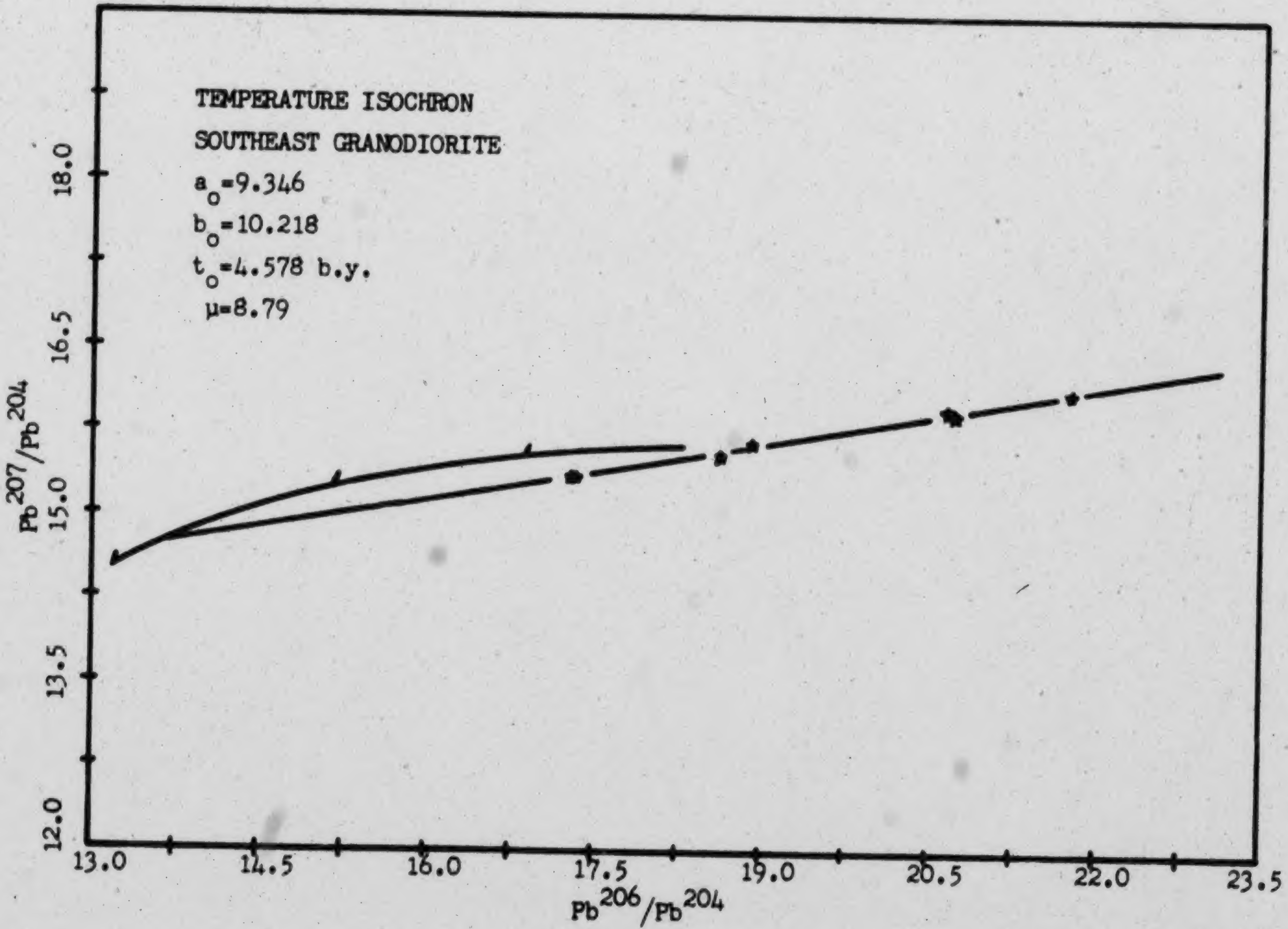
TEMPERATURE ISOCHRON
SOUTHEAST GRANODIORITE
a_o=9.346
b_o=10.218
t_o=4.578 b.y.
μ=8.79
Pb^{207}/Pb^{204}
12.0
13.5
15.0
16.5
18.0
13.0
14.5
16.0
17.5
19.0
20.5
22.0
23.5
Pb^{206}/Pb^{204}

Figure 31

CHAPTER VII

MINERAL LEAD COMPOSITION AND THE MINERAL ISOCHRON

7.1. Introduction and mineral separation

To test the prediction made by Cumming et al (1970) that the temperature isochron is analogous to a mineral isochron, mineral separations were made on three samples; YKWG #1, YKWG #4 and YKWG #5.

Mineral separations were performed with standard heavy liquid techniques involving the use of tetrabromoethane, methylene iodide and Clerici solution. The analytical procedures are described below.

(1). The rock was first broken into small pieces and weathered material discarded. The remaining material was then crushed to about 120 mesh.

(2). A Wilfley table was then used to separate the rock powder into three gross fractions, the light (called gravity up and denoted by W↑), the heavy (called gravity down and denoted by W↓) and the intermediate (called gravity float and denoted by W→).

(3). After drying the powder, the irons (from the crusher) were picked out with a hand magnet. Magnetic separations were then made on the light fraction (for biotite and feldspar) and the heavy fraction (for apatite, zircon, pyrite, ... etc.). Nonmagnetic material (denoted by M↑) was separated from the magnetic fraction (denoted by M↓).

(4). The heavy liquids tetrabromoethane (TBr_4) and methylene iodide (MI_2) were then used for density separation.

Because of the low content of zircon and the small sample of rock available, a final separation of zircon, pyrite, sphene, .. etc. was not possible and the final residual mixture was treated as a mixed-mineral phase for lead extraction.

The combinations for the separations of the four mineral phases used for lead extractions, biotite, potassium feldspar, apatite and the mixture of zircon, pyrite, ...etc. are:

Biotite: W↑ , M↓ , TBr_4↓
Biotite impurity: W↑ , M↓ , TBr_4↑
K feldspar: W↑ , M↑ , dilute TBr_4↑
Apatite: W↓ , M↑ , TBr_4↓ , MI_2↑
Mixture of zircon, pyrite, etc.: W↓ , M↓ , TBr_4↓ , MI_2↓

7.2. Mineral lead composition and the mineral isochron

Table 15 shows the mineral lead composition of the three rock samples. The leads were extracted by induction furnace heating and purified by the dithizone extraction technique. Ratios shown are normalized to N.B.S. Equal Atom lead ratios given by Stacey et al (1969). Each of the minerals was heated in the furnace at 1350°C for about one hour. It can be seen that lead contained in K-feldspar is least radiogenic followed by lead in biotite, apatite and the mixture of zircon, pyrite, etc..

The lead-lead diagrams are shown in Figures 32, 33 and 34. The mineral lead ratios of each sample fit on a straight line with a slope which agrees within the standard deviation to the slope of its respective temperature isochron.

Table 15. Mineral lead ratios

Sample:	Mineral phase	Pb^{206}/Pb^{204}	Pb^{207}/Pb^{204}	Pb^{208}/Pb^{204}
YKWG #1	K-feldspar	14.975 .010*	15.207 .010	34.355 .023
		14.930 .014	15.143 .014	34.259 .034
	Biotite	21.310 .022	15.907 .016	37.444 .039
		21.298 .036	15.870 .027	37.331 .066
	Biotite impurity	18.248 .020	15.517 .020	36.523 .033
	Mixture of zircon, pyrite, etc.	no lead	no lead	no lead
YKWG #4	Biotite	——	——	——
	K-feldspar	14.169 .019	14.818 .020	35.004 .052
		14.265 .015	14.905 .016	35.196 .039
	Apatite	87.981 .145	27.374 .045	90.899 .153
	Mixture of zircon, pyrite, etc.	123.054 .236	34.159 .066	79.521 .156
		122.835 .501	34.109 .140	79.442 .328

* Internal estimate of standard deviation.

Table 15 cont'd

Sample:	Mineral phase	Pb^{206}/Pb^{204}	Pb^{207}/Pb^{204}	Pb^{208}/Pb^{204}
YKWG #5	K-feldspar	15.608	14.970	35.621
		.013*	.012	.029
		15.582	14.964	35.596
		.013	.013	.031
	Biotite	—	—	—
	Apatite	45.710	19.019	47.961
		.370	.157	.406
		45.482	18.984	47.645
		.375	.150	.381
		45.863	19.088	48.415
		.163	.069	.181
	Mixture of zircon, pyrite, etc.	135.467	34.688	63.990
		.279	.072	.134

* Internal estimate of standard deviation.

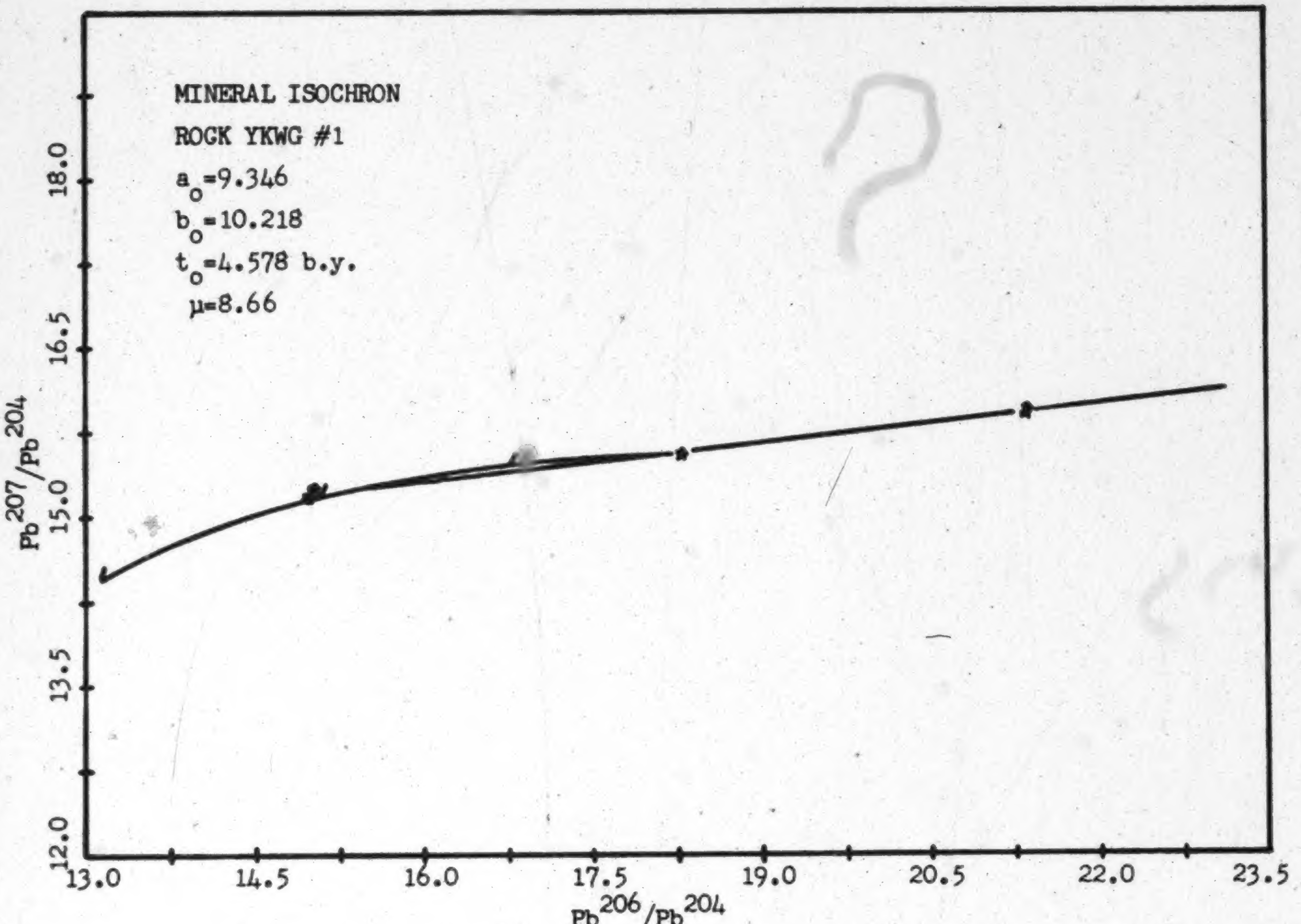
MINERAL ISOCHRON
ROCK YKWG #1
a_o=9.346
b_o=10.218
t_o=4.578 b.y.
μ=8.66
18.0
16.5
15.0
13.5
12.0
13.0
14.5
16.0
17.5
19.0
20.5
22.0
23.5
Pb^{207}/Pb^{204}
Pb^{206}/Pb^{204}

Figure 32

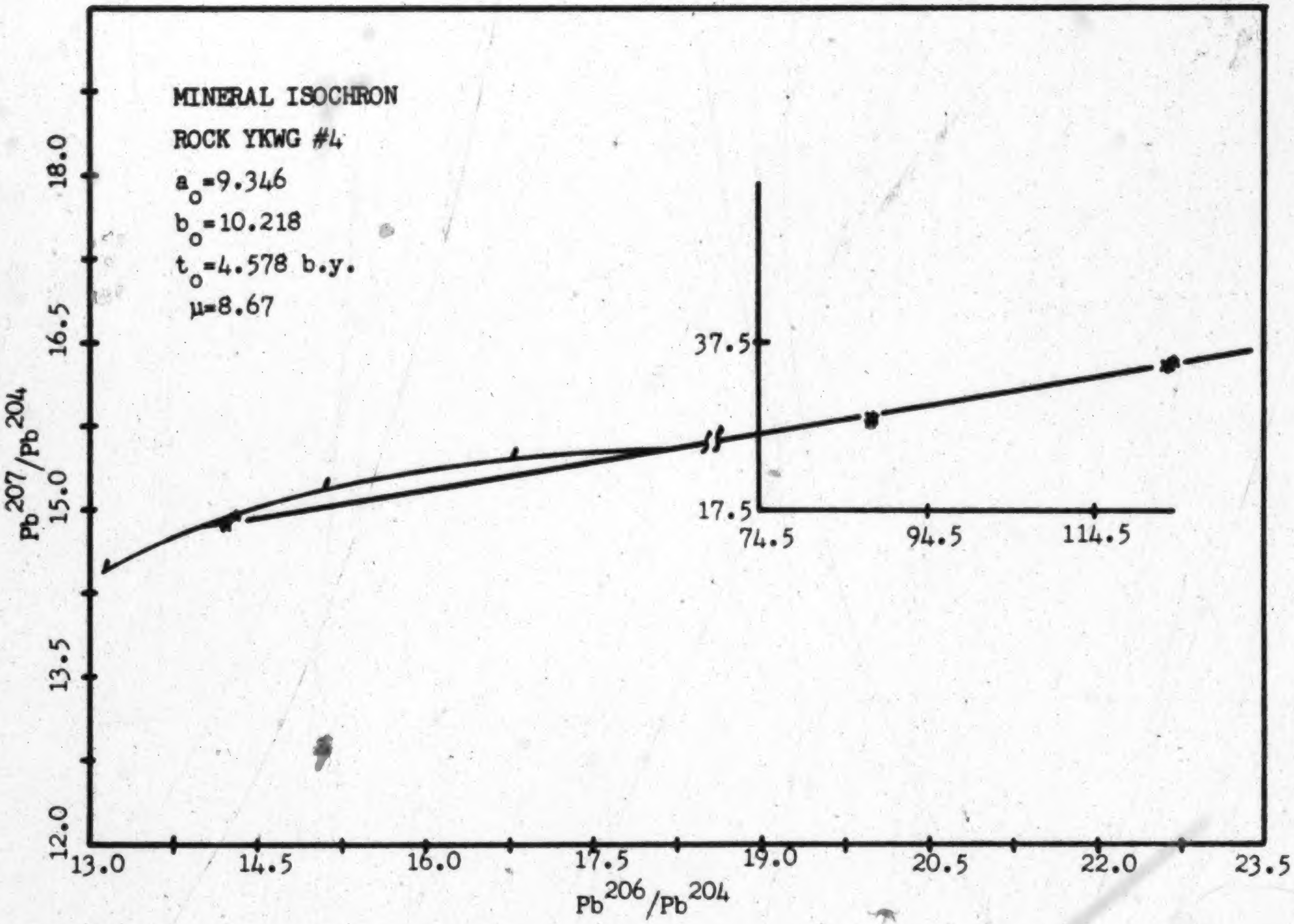
MINERAL ISOCHRON
ROCK YKWG #4
a$_o$=9.346
b$_o$=10.218
t$_o$=4.578 b.y.
μ=8.67
Pb^{207}/Pb^{204}
12.0
13.5
15.0
16.5
18.0
13.0
14.5
16.0
17.5
19.0
20.5
22.0
23.5
Pb^{206}/Pb^{204}
17.5
37.5
74.5
94.5
114.5

Figure 33

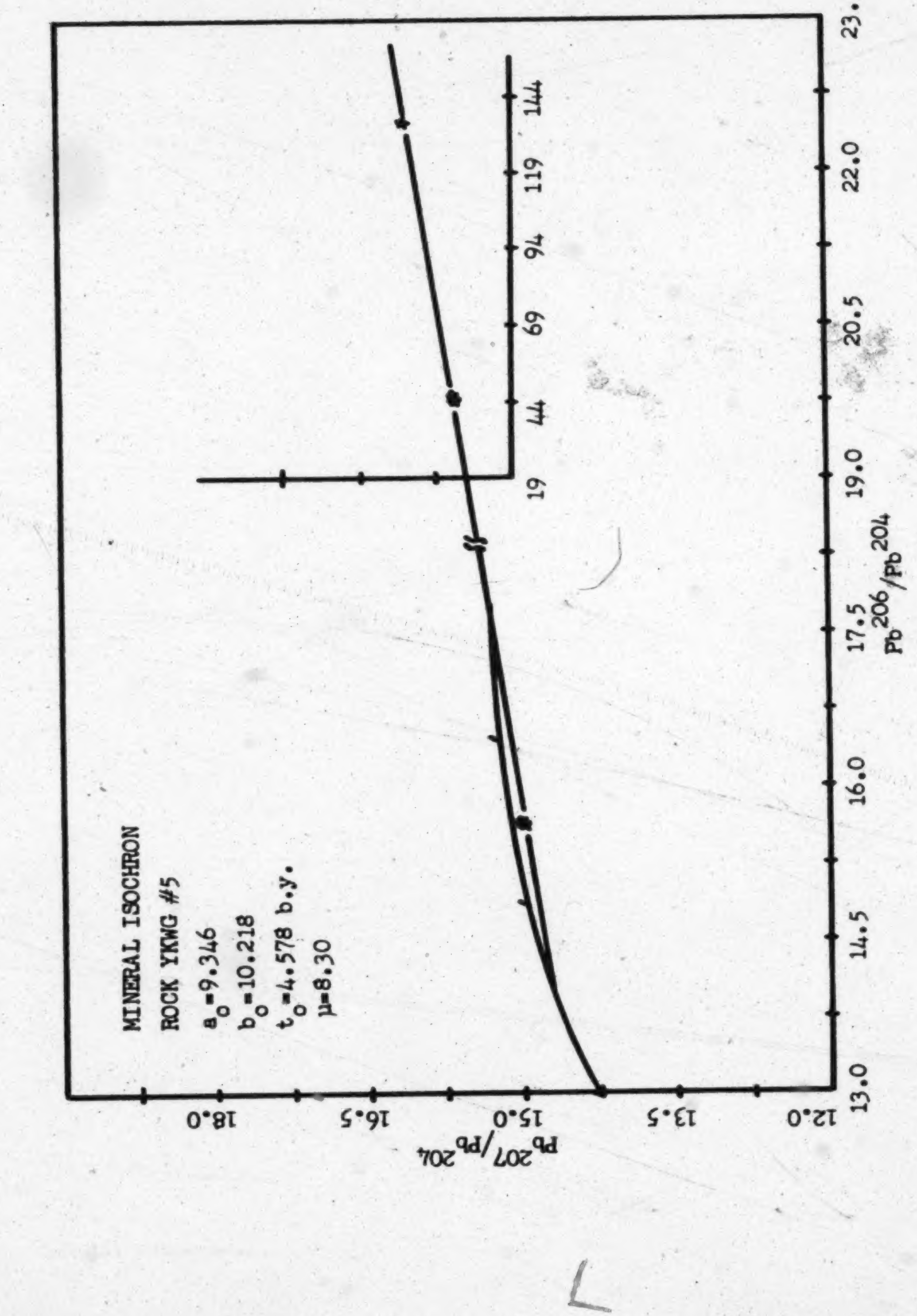
MINERAL ISOCHRON
ROCK YKWG #5
a_o=9.346
b_o=10.218
t_o=4.578 b.y.
μ=8.30
19
44
69
94
119
144
13.0
14.5
16.0
17.5
19.0
20.5
22.0
23.5
Pb^{206}/Pb^{204}
12.0
13.5
15.0
16.5
18.0
Pb^{207}/Pb^{204}

Figure 34

Table 16. Slope-ages and μ values of the mineral isochrons

Sample:	Calculated μ value (95% C.L.)	Slope (S.D.)	Age in m.y. (S.D.)
YKWG #1	8.66 ± .02	0.112 ± .005	1865 ± 85
YKWG #4	8.67 ± .03	0.171 ± .002	2600 ± 35
YKWG #5	8.30 ± .02	0.162 ± .004	2520 ± 40

Slope ages and µ values calculated on the basis of a two-stage lead evolution model for the three mineral isochrons are listed in Table 16. The parameters a_o, b_o, and t_o used for such calculations are the same as those used for the temperature isochrons.

The results of mineral and temperature isochrons indicate that both isochrons yield a consistent slope-age for a rock. If this consistency is general (for all types of rocks), the lead isotope dating procedure can be greatly simplified by employing the volatilization technique since no mineral separation is required.

7.3. Sulfide mineral isochron of the Yellowknife volcanics

To study the relationship in ages between the western granodiorite and the Yellowknife volcanics, twenty-three sulfide and five galena samples separated mostly from the Yellowknife volcanics (two sulfides and one galena from the Yellowknife sediments) were analysed. Sample collection, mineral separations and lead extractions on these samples were made by A. P. Leech of the Department of Geology. The writer made the mass spectrometric analyses and the results are shown in Tables 17 and 18.

Figure 35 shows the plot of ratios Pb^{206}/Pb^{204} versus Pb^{207}/Pb^{204} of the twenty-three sulfide samples. The data show very much scatter around the best fitting straight line which has a slope of 0.173 ± .0064. The scatter is believed mainly due to various sources of analytical error. These analyses were performed during the initial stage of this work and the precision is not as good as that obtained later. The µ value is calculated to be 8.90 ± .04.

Table 17. Pb ratios of sulfide samples from the Yellowknife volcanics

Sample ident.:	Pb^{206}/Pb^{204}	Pb^{207}/Pb^{204}	Pb^{208}/Pb^{204}
L-9, pyrite	13.843	14.801	33.386
	.013*	.014	.032
L-8, pyrite	13.870	14.858	33.522
	.020	.021	.048
L-8(+G), chalcopyrite	13.892	14.871	33.580
	.058	.062	.141
L-7, pyrite	13.900	14.885	33.619
	.009	.010	.022
L-8(-G), pyrite	13.901	14.893	33.622
	.010	.011	.026
	13.909	14.898	33.644
Ptarmigan pyrite	14.017	14.947	33.675
	.012	.013	.026
	14.033	14.964	33.718
	.014	.015	.035
L-26, pyrite	14.131	14.971	33.795
	.041	.044	.100
L-29, arsenopyrite	14.164	14.817	33.541
	.036	.037	.084
	14.173	14.879	33.646
	.061	.064	.146
Giant 15-8, pyrite	14.136	15.058	34.096
	.066	.071	.166
L-19, pyrite	14.282	15.026	34.347
	.013	.013	.032
Ptarmigan chalcopyrite	14.596	15.072	34.675
	.051	.052	.121

* Internal estimate of standard deviation.

Table 17 cont'd

Sample ident.:	Pb^{206}/Pb^{204}	Pb^{207}/Pb^{204}	Pb^{208}/Pb^{204}
K-97-117, pyrite	14.734	15.110	34.790
	.029*	.030	.069
L-6, pyrite	14.867	15.188	34.554
	.034	.035	.081
K-97-116, pyrite	14.990	15.150	34.797
	.045	.046	.106
L-21, pyrite	15.312	15.317	35.697
	.041	.042	.102
B-1143, pyrite	15.814	15.225	35.508
	.023	.022	.051
L-2, pyrite	15.977	15.532	34.430
	.030	.029	.067
	15.980	15.526	34.392
	.036	.035	.082
L-24, arsenopyrite	16.341	15.475	36.424
	.089	.084	.204
Crestaurum chalcopyrite	17.015	15.414	36.131
	.026	.023	.055
B-1269, pyrite	17.476	15.468	37.747
	.020	.018	.044
Akaithcho chalcopyrite	18.277	15.687	38.235
	.016	.014	.035
Akaithcho pyrite	17.937	15.530	37.626
	.011	.010	.024
L-20, pyrite	22.094	16.426	49.947
	.042	.031	.095
	22.119	16.441	49.796
	.063	.047	.143

* Internal estimate of standard deviation.

Table 18. Pb ratios of galena samples from the Yellowknife volcanics

Sample ident.:	Pb^{206}/Pb^{204}	Pb^{207}/Pb^{204}	Pb^{208}/Pb^{204}
Ptarmigan galena	13.844	14.891	33.773
	.030*	.032	.075
	13.870	14.915	33.846
	.028	.031	.070
L-8 Rycon galena	13.871	14.852	33.536
	.012	.013	.031
Con galena, 3300' level-Cambell shear	13.934	14.978	33.820
	.019	.021	.048
Con galena	13.937	14.977	33.818
	.016	.017	.039
Rycon galena, 3300' level-Campbell shear	13.944	14.971	33.870
	.014	.015	.034

* Internal estimate of standard deviation.

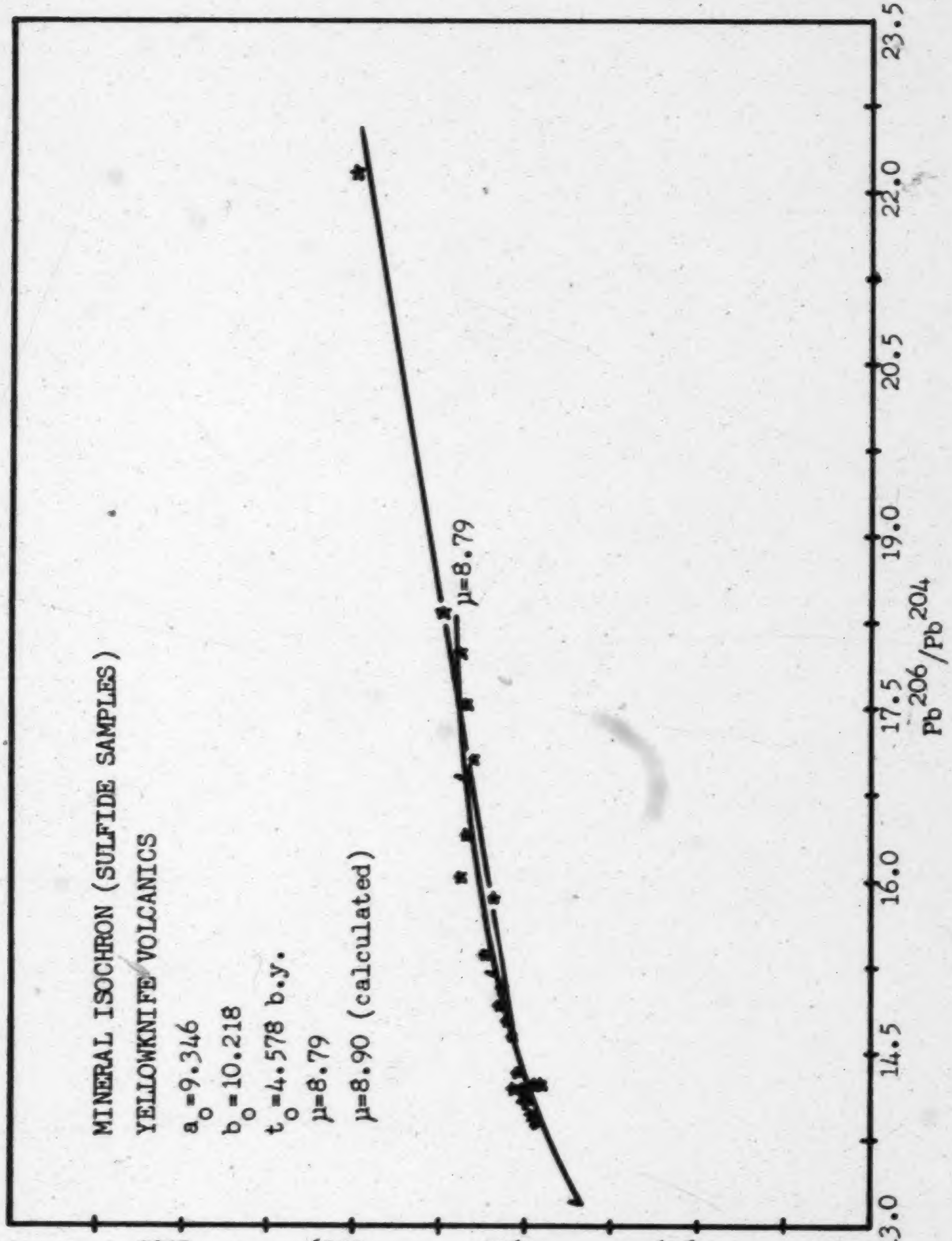
MINERAL ISOCHRON (SULFIDE SAMPLES)
YELLOWKNIFE VOLCANICS
a_o=9.346
b_o=10.218
t_o=4.578 b.y.
μ=8.79
μ=8.90 (calculated)
μ=8.79
Pb^{207}/Pb^{204}
12.0
13.5
15.0
16.5
18.0
Pb^{206}/Pb^{204}
13.0
14.5
16.0
17.5
19.0
20.5
22.0
23.5

Figure 35

The spread of ratios along a straight line is believed to be the result of less than perfect mineral separations, and the lead ratios observed are not representative of leads in pyrites (assorted sulphides) but are linear combinations of contributions from sulfides and different proportions of impurities remaining after mineral separation (possibly zircon, sphene, etc.). Microscopic examination of some of the samples indicated that various impurities were present (Cumming personal communication, 1973) and in many cases separation was extremely difficult due to the great range of minerals present. The best fitting straight line thus represents a mineral isochron of the volcanics or at least the mineralized rock in the ore zones.

Although the observed ratios are not representative of the sulfides, an age can still be derived from the mineral isochron and is found to be 2630 m.y. ± 70 m.y. from the slope of the line given above. If we take the least radiogenic lead from the sample L-9 to represent the lead in sulfide, the ratio lies on the conformable growth curve at 2630 m.y. identical to the slope-age of the mineral isochron.

Figure 36 shows the lead-lead diagram of the five galena samples. The ratios, which agree with each other within 0.5% lie slightly above the conformable growth curve at 2640 m.y., the same age as the pyrite. Thus the mineralization of galenas and pyrites (metallic sulphides) of the Yellowknife volcanics occurred contemporaneously at about 2630 m.y. ± 70 m.y. ago. The volcanics should then be at least this old.

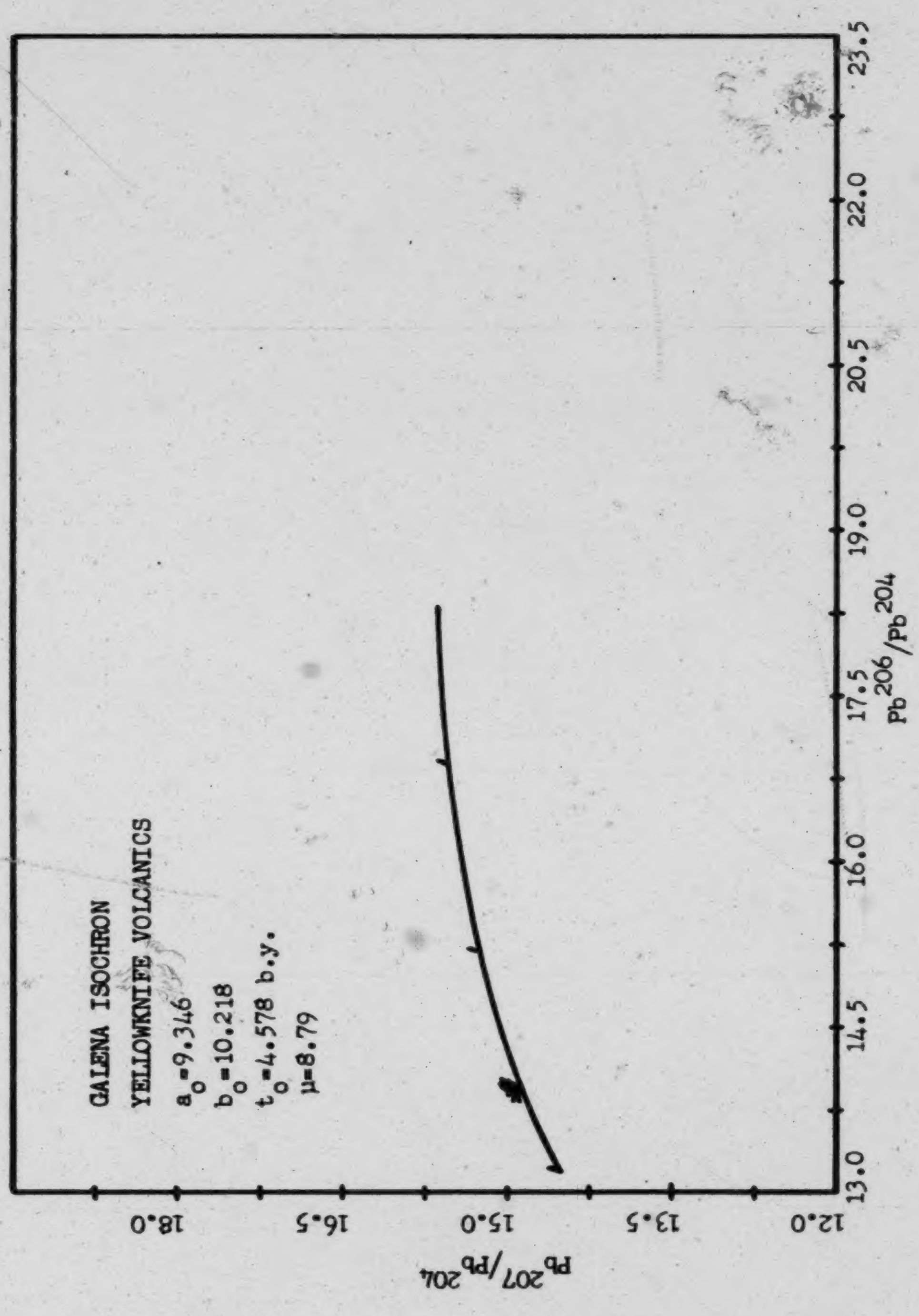
GALENA ISOCHRON
YELLOWKNIFE VOLCANICS
a_o=9.346
b_o=10.218
t_o=4.578 b.y.
μ=8.79
Pb^{207}/Pb^{204}
12.0
13.5
15.0
16.5
18.0
Pb^{206}/Pb^{204}
13.0
14.5
16.0
17.5
19.0
20.5
22.0
23.5

Figure 36

7.4. An indication of the age of the Yellowknife metasediments

Among the twenty-three sulfide and five galena samples analysed, two sulfides (Ptarmigan pyrite and Ptarmigan chalcopyrite) and one galena (Ptarmigan galena) are separated from the Yellowknife metasediments. Lead ratios from the two sulfide samples are not interpretable due to possible impurities from mineral separations. The Ptarmigan galena has ratios equal to those of the galenas from the volcanics which suggests that the age of the sediments should at least be as old as the galenas at about 2640 m.y..

CHAPTER VIII

SUMMARY AND CONCLUSIONS

8.1. Introduction

It has been pointed out by many workers that the U/Pb system has distinct advantages over other methods of dating because one can obtain useful information from the Pb isotope ratios alone without the necessity of chemical extraction of parent and daughter elements. In this work the advantages of the Pb/Pb method have been extended so that it is possible to obtain both whole rock and mineral isochron information on the same rock in a simple manner. The extra information can be interpreted geologically in a manner consistent with age measurements by other techniques.

8.2. Interpretation and comparison with other results

A whole rock lead-lead isochron age of 2700 m.y. ± 85 m.y. was derived from six western granodiorite samples based on a two stage model. Since the concordia plot of Figure 17 indicates that a two stage model cannot account for the observed ratios, it is necessary to consider those three stage models which yield rectilinear plots. For our data, the best straight line passes through the intersection of the zero isochron and the conformable growth curve, so if we interpret the data in terms of a three stage f_1=constant model, the lower intercept must correspond to t_2 and therefore there would have been an earlier event at the time t_1, with an age greater than 2700 million years. There is no support in the present data for such an event although Robertson and Cumming (1968) obtained a lead-lead model age of about 4000 m.y. based on analyses of some anomalous leads from galena samples.

The other three stage model which yields a linear lead-lead plot is the case where f_2=constant for which the lower intercept yields t_1 regardless the value of f_2 and it is impossible to test this particular model any further from the lead-lead data alone.

From the concordia plot of Figure 17, the best line through the data points intersects the normal concordia curve at 1540 ± 200 m.y. and if a three stage model applies, this time is an upper limit to t_2 for the f_2=constant case or equal to t_2 if f_1=constant, i.e. $t_2 \leq 1540 \pm 200$ m.y.. The only indication of an event at this time is a poorly defined Rb/Sr isochron on dyke set III. Gates and Hurley (1973) obtained an age of 1370 m.m. $< t <$ 1730 m.y. for these rocks. It is possible that the intrusion of these dykes may have been related to the end of a second stage of the lead-uranium system in the western granodiorite.

The lead-lead mineral isochron age of 2530 m.y. ± 20 m.y. (S.D. of the weighted mean of the rocks YKWG #2, #3, #4, #5, #7, and #8) cannot correspond to t_2 in these three stage models since $t_2 \leq 1540$ m.y. ± 200 m.y., therefore it must represent some event which is not reflected in the whole rock data.

Figure 37 summarizes the pertinent age measurements of the major geological units of the Yellowknife area. Upon comparison of the

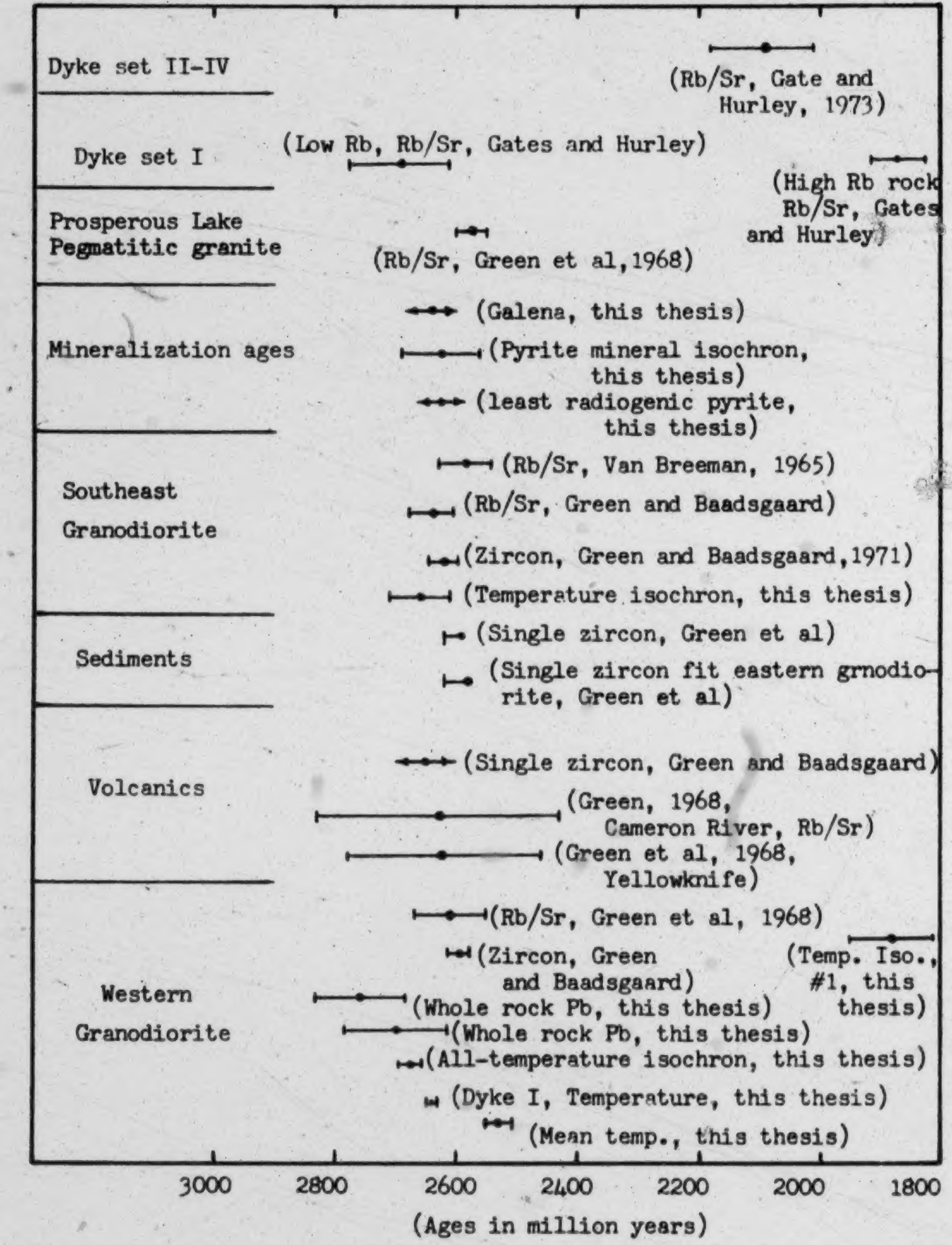

Figure 37. Age measurements of the Yellowknife area

data shown in Figure 37, some of the features noted are;

(1). The lead-lead whole rock isochron age of the western granodiorite agrees reasonably well with the Rb/Sr age obtained by Green et al (1968).

(2). The mineral age of the western granodiorite is about 150 m.y. less than the whole rock age. This difference of ages agrees with the cooling interval of 140 m.y. deduced from K/Ar mica ages by Green and Baadsgaard (1971).

(3). The age of the pegmatite dyke based on the mineral isochron (temperature isochron) is less than the whole rock age of the country rock. The age of the pegmatite dyke apparently has not been updated by the process which altered the country rock at 2530 m.y..

(4). Lead data from fractional heating of a southeast granodiorite rock sample confirmed the Rb/Sr analyses that this granodiorite is older than the western granodiorite.

(5). The much younger mineral age of YKWG #1 agrees remarkably well with the Rb/Sr data from Gates and Hurley (1973) on the high Rb rocks of dyke set I (age and error shown in Figure 37 are recalculated values using five rocks which have the highest Rb/Sr ratios).

(6). The mineralization age of 2630 m.y. derived from galena and and pyrite (metallic sulphide) samples from the Yellowknife group suggests that the formation of volcanics, intrusion of granite and ore formation must have taken place in a short period of time, no more than a few tens of million of years.

(7). An apparent conflict in age relationships appears in the data of Gates and Hurley (1973) for the dyke set I. The dyke which they sampled cuts the Prosperous Lake granite and yet appears to have an older age. It amy be that the Rb/Sr mineral isochron age on the granite corresponds to the younger lead-lead mineral age and that the rock is actually older.

8.3. Mass discrimination

Discrimination in a mass spectrometer is always a serious problem in precise measurements of isotopic abundances. It has been shown that different filament positions between runs in a single filament solid-source mass spectrometer may introduce mass dependent errors in the isotope ratios. Some evidence of possible focusing effects on the isotope ratios were also demonstrated.

The solution to this problem seems to be to ensure that the source geometry is maintained as constant as possible so that significant changes of focusing parameters are not required between runs.

REFERENCES CITED

AMIEL, S. (1962). Analytical application of delayed neutron emission in fissionable element. Anal. Chem. 34, pp. 1683-1692.

AUSTIN, C.F., SLAWSON, W.F. (1961). Isotopic analyses of single galena crystals. Amer. Mineralogist 46, pp. 1132-1140.

BAADSGAARD, H. (1965). Geochronology. Saertryk af Meddelelser fra Dansk Geologisk Forening Bd. 16, Hefte 1. København.

BLACK, L.P., GALE, N.H., MOORBATH, S., PANKHURST, R.J. (1971). Isotope dating of very early precambrian amphibolite gneisses from the Godthaab district, West Greenland. Earth Planet. Sci. Letters 12, pp. 245-259.

BURWASH, R.A., BAADSGAARD, H. (1962). Yellowknife-Nonacho age and structural relations. Roy. Sco. Canada Spec. Pub. 4, pp. 22-29.

CARTANZARO, E.J., MURPHY, T.J., SHIELDS, W.R., GARNER, E.I. (1968). Absolute isotope abundance ratios of common, Equal Atom and radiogenic lead isotope standards. J. Res. Natl. Bur. Stand. 72A, pp. 261-267.

COMPSTON, W., OVERSBY, V.M. (1969). Lead isotope analysis using a double-spike. J. Geophys. Res. 74, p. 4338.

COOPER, J.A., RICHARDS, J.R. (1966). Lead isotopes and volcanic magmas. Earth Planet. Sci. Letters 1, pp. 259-269.

COOPER, J.A., RICHARDS, J.R. (1966). Solid-source isotope measurements and isotopic fractionation. Earth Planet. Sci. Letters 1, pp. 58-64.

COOPER, J.A., GREEN, D.H. (1969). Lead isotope measurements on ilerzolite inclusions and host basanites from western Victoria, Australia. Earth Planet. Sci. Letters 6, pp. 69-76.

COOPER, J.A., REYNOLDS, P.H., RICHARDS, J.R. (1969). Double spike calibration of the Broken Hill standard lead. Earth Planet. Sci. Letters 6, p. 467.

CUMMING, G.L., BURKE, M.D., TSONG, F., McCULLOUGH, H. (1971). A digital mass spectrometer. Can. J. Phys. 49, pp. 956-965.

CUMMING, G.L., TSONG, F., GUDJURGIS, P.J. (1970). Fractional removal of lead from rocks by volatilization. Earth Planet. Sci. Letters 9, pp. 49-54.

CUMMING, G.L., WILSON, J.T., FARQUHAR, R.M., RUSSELL, R.D. (1955). Some dates and subdivisions of the Canadian shield. Proc. Geol. Assoc. Can. 7, pp. 27-79.

DOE, B.R., TILTON, G.R., HOPSON, C.A. (1965). Lead isotopes in feldspars from selected granitic rocks associated with regional metamorphism. J. Geophys. Res. 70, pp. 1947-1966.

DOE, B.R., TATSUMOTO, M. (1972). Volatilized lead from Apollo 12 and 14 soils. Pro. third Lunar Sci. Conf.. Geochim. Cosmochim. Acta Suppl. 3, vol. 2, pp.1981-1989. MIT Press.

EDWARDS, G., UREY, H.C. (1955). Determination of alkali metals in meteorites by a distillation process. Geochim. Cosmochim. Acta 7, pp.154-168.

EDWARDS, G., HESS, D.C. (1956). Determination of lead in meteorites by a distillation process. Natl. Research Council Publ. 400, p. 100.

FISHER, D.E. (1970). Homogenized fission track determination of uranium in whole rock geologic samples. Anal. Chem. 42, pp. 414-416.

FOLINSBEE, R.E. (1955). Archaean monazite in beach concentrates, Yellowknife geologic province, Northwest Territories, Canada. Trans. Royal Soc. Canada. 3rd. ser. 49, pp.7-24.

FOLINSBEE, R.E.,LIPSON, J., REYNOLDS, J.H. (1956). Potassium-Argon dating. Geochim. Cosmochim. Acta 10, pp. 60-68.

GALE, N.H. (1967). Development of delayed neutron technique as rapid and precise method for determination of uranium and thorium at trace levels in rocks and minerals, with applications to isotope geochronology. Radioactive dating and methods of low-level counting. International Atom. Energy Agen. Publ., Vienna, 1967, pp. 431-452

GALE, N.H., MUSSETT, A.E. (1973). Episodic uranium-lead models and the interpretation of variations in the isotopic composition of lead in rocks. J. Geophys. and Space Phys. 11, pp. 37-85.

GATES, T.M., HURLEY, P.M. (1973). Evaluation of Rb/Sr dating method apply to the Matachewan, Abitibi, Mackenzie and Sudbury dyke swarms in Canada. Can. J. of Earth Sci. 10, pp. 900-919.

GREEN, D.C., BAADSGAARD, H., CUMMING, G.L. (1968). Geochronology of the Yellowknife area, Northwest Territories, Canada. Cana. J. of Earth Sci. 5, pp.725-735.

GOLES, G.G., ANDERS, E. (1962). Abundances of iodine, tellurium and uranium in meteorites. Geochim. Cosmochim. Acta 26, pp. 251-262.

GREEN, D.C. (1968). Precambrian geology and geochronology of the Yellowknife area, Northwest Territories, Canada. Ph. D thesis, University of Alberta, Edmonton, Alberta, Canada.

GREEN, D.C., BAADSGAARD, H. (1972). Temporal evolution and petrogenesis of an Archaean crustal segment at Yellowknife, N.W.T., Canada. J. of Petrogy vol. 12, No. 1, pp. 177-217.

HAMILTON, E.I. (1965). The isotopic composition of lead in igneous rocks. Earth Planet. Sci. Letters 1, pp. 30-37.

HUEY, J.M., IHOCHI, H., BLACK, L.P., OSTIC, R.G., KOHMAN, T.P. (1971). Lead isotopes and volatile transfer in the lunar soil. Pro. Second Lunar Sci. Conf., Geochim. Cosmochim. Acta Suppl. 2, p. 1547. MIT Press.

INGHRAM, M.G., HAYDEN, R.J. (1954). Mass spectrometry. Natl. Res. Coun. Natl. Acad. Sci. (U.S.), Nucl. Sci. Ser. Report 14.

KANASEWICH, E.R. (1968). The interpretation of lead isotopes and their geological significance. Interscience Pub. 1968, pp.147-223.

KEEVIL, N.B., JOLLIFE, A.W., LARSEN, E.S. (1942). Distribution of helium and radioactivity in rocks. Pt. IV. Helium age investigations of diabase and granodiorite from Yellowknife, Northwest Territories, Canada. Amer. J. Sci., 4th Series, 240, pp. 831-846.

KROGH, T.E. (1972). A low-contamination method for hydrothermal decomposition of zircon and extraction of U and Pb for isotopic age determinations. Geochim. Cosmochim. Acta 37, pp. 485-494.

MARSHALL, R.R., HESS, D.C. (1960). Determination of very small quantities of lead. Anal. Chem. 32, pp. 960-966.

MARSHALL, R.R. (1962). Mass spectrometric study of lead in carbonaceous chondrites. J. Geophys. Res. 67, pp.2005-2015.

MASUDA, A. (1964). Lead isotope composition in volcanic rocks of Japan. Geochim. Cosmochim. Acta 28, pp. 291-303.

MATTINSON, J.M. (1971). Preparation of ultrapure HF, HCl and HNO_3. Carnegie Inst. Washington Yearb. 70, pp. 266-268.

MATTINSON, J.M. (1972). Preparation of hydrofluoric and nitric acids at ultralow lead levels. Anal. Chem. 44, pp. 1715-1716.

MOORBATH, S., WELKE, H. (1968). Lead isotope studies on igneous rocks from the Isle of Skye, Northeast Scotland. Earth Planet. Sci. Letters 5, pp. 217-230.

MORGAN, J.W., LOVERING, J.F. (1963). The determination of uranium and thorium in rocks by neutron activation analysis. Anal. Chem. 28, pp. 405-417.

MORGAN, J.W. (1968). Uranium and thorium in chondritic meteorites. Talanta 15, pp. 1079-1095.

PAYNE, A.V., BAADSGAARD, H., BURWASH, R.A., CUMMING, G.L., EVANS, C.R., FOLINSBEE, R.E. (1965). A line of evidence supporting continental drift. Upper Mantle Sym. New Delhi, 1964 of the International Union of Geophys. Sci. Copenhagen 1965. pp. 83-93.

ROBERTSON, D.K., CUMMING, G.L. (1968). Lead and sulphur isotope ratios from the Great Slave area, Canada. Can. J. Earth Sci. 5, pp. 1269-1276.

RUSSELL, R.D., CUMMING, G.L. (1955). Lead isotope abundance. (Abstr.) Program, 36th Annual Meeting. American Geophys. Union, Washington, D.C., May, 1955. p. 526.

RUSSELL, R.D., FARQUHAR, R.M. (1960). Lead isotope in Geology. Intersci. Pub. Inc., New York.

SINHA, A.K. (1969). Removal of radiogenic lead from potassium feldspars by volatilization. Earth Planet. Sci. Letters 7, pp. 109-118.

SILVER, L.T. (1970). U-Th-Pb isotopes in some Tranquility base samples and their implications for lunar history. Proc. Apollo 11 Lunar Sci. Conf. Geochim. Cosmochim. Acta Suppl. 2, p. 1533. Pergamon.

SILVER, L.T. (1971). U-Th-Pb isotope systems in Apollo 11 and 12 regolithic materials and a possible age for the Copernicus impact event. (Abstr.) Trans. Amer. Geophys. Union 52, p. 534.

STACEY, J.S., DELEVAUX, M.E., ULRYCH, T.J. (1969). Some triple-filament lead isotope ratio measurements and an absolute growth curve for a single-stage leads. Earth Planet. Sci. Letters 6, pp. 15-25.

STARIK, I.E., SOBOTOVICH, E.V., LOVTSYUS, G.P., LOVTSYUS, A.V., AVDZEIKO, G.V. (1957). Modes of lead occurence in nature. Geokhimiya 2, pp. 683-692.

TATSUMOTO, M. (1969). New method for preparing ultrapure hydrofluoric acid. Anal. Chem. 41, pp. 2088-2089.

TILTON, G.R., PATTERSON, C., BROWN, H., INGHRAM, M., HAYDEN, R., HESS, D., LARSEN, E. JR. (1955). Isotopic composition and distribution of lead, uranium and thorium in a Precambrian granite. Bull. Geo. Soc. Amer. 66, pp.1131-1148.

TILTON, G.R. (1956). Interpretation of lead age discrepancies by acid washing experiments. Trans. Amer. Geophys. Union 37, pp. 224-230.

TILTON, G.R. (1960). Volume diffusion as a mechanism for discordant lead ages. J. Geophys. Res. 65, pp. 2933-2945.

ULRYCH, T.J. (1967). Oceanic basalt leads, a new interpretation and an independent age for the earth. Science 158, p. 252.

ULRYCH, T.J., REYNOLDS, P.H. (1966). Whole-rock and mineral leads from the Llano uplift, Texas. J. Geophys. Res. 71, pp. 3089-94.

VAN BREEMAN, O. (1965). Thermally induced relocation of strontium and rubidium in a granodiorite. M. Sc. Thesis, University of Alberta, Edmonton, Canada. (unpublished).

WELKE, H., MOORBATH, S., CUMMING, G.L., SIGURDSSON, H. (1968). Lead isotope studies on igneous rock from Iceland. Earth Planet. Sci. Letters 4, pp. 221-231.

WETHERILL, G.W. (1956). Discordant uranium-lead ages, I. Trans. Amer. Geophys. Union 37, pp. 320-326.

WHITTLES, A.B.L. (1964). Trace lead studies with gas source mass spectrometry. Ph. D. Thesis, University of British Columbia, Vancouver, Canada.

APPENDIX I

SOME FORMULAS ON VECTOR DIFFERENTIATION

Let x and y be column vectors and x^T, y^T be the transpose of x and y respectively, let A be a square matrix and A^T be the transpose of A. Then,

$$\frac{\partial}{\partial x}(x^T A y) = Ay$$

$$\frac{\partial}{\partial x^T}(x^T A y) = y^T A^T$$

$$\frac{\partial}{\partial y}(x^T A y) = A^T x$$

$$\frac{\partial}{\partial y^T}(x^T A y) = x^T$$ [illegible]

For a symmetric matrix, B, we have

$$\frac{\partial}{\partial x}(x^T B x) = 2Bx$$

$$\frac{\partial}{\partial x^T}(x^T B x) = 2x^T B^T$$

APPENDIX II

COMPUTER PROGRAMS FOR DATA REDUCTION BY IBM 360

```
      DIMENSION DATA(1024),IDATA(1024),XCOR(1024),C(9),D(9),W(50),
     1PHITES(100),PTIMES(100),ANAME(20),IPIV(10),L(25),M(25)
      REAL*8 DAT(25,4),DAB(25,4),FMAT(2000),RHS(100),X(100),TRFMAT(2000)
     1,R(700),A(25),RES(25),AUX(25),LSRES(100),FR,CALC,TD,H,ESP,S1,S2,
     2 S3,RHO12,RHO13
      INTEGER EOFC,TBC,GBC,BARY(30)
C     SET CONTROL PARAMETERS
 2000 EOFC=1
      TBC=0
      GBC=0
      NEQ=0
      JEND=0
      NPEAKS=4
      IRG=4
C     EOFC = END OF FILE COUNT
C     TBC = TOTAL BLOCK SCAN COUNTS
C     GBC = NO. OF BLOCKS IN  THE SPECTRUM
C     IRG =NO. OF POINT MISSING DUE TO INTER-RECORD GAP AND FLYBACK
C     NPEAKS = NO. OF PEAKS IN THE DIDIVIDUAL SCAN
C     READ IN TILE AND CONTROL PARAMETERS
      READ(5,1000) (ANAME(I),I=1,20)
 1000 FORMAT(20A4)
      READ(5,1001) LENGTH,LFILT,LCOR,IDENT,IDG,DIS
 1001 FORMAT(5I5,F5.0)
C     LENGTH = NO. OF DATA POINTS IN A BLOCK OR SCAN
C     LFILT = NO. OF POINTS TO BE SMOOTHED BY THE INPUT FILTER
C     LCOR = LENGHT OF SQUARE WINDOW USED TO FIND PEAKS
C     IDG =   ORDER OF POLYNOMIAL TO BE USED FOR FITTING THE PEAKS
C     DIS = DISCRIMINATION LEVEL TO NEGLECT UNWANTED SMALL PEAKS
```

```
C     IDENT = IDENTIFICATION NO. CARRIED AS TWO LEAST SIGNIFICANT DIGITS
C        ABOVE ARE HALF LENGHT FILTERS
      WRITE(6,1002)
1002  FORMAT(1H1)
      IF(LENGTH.EQ.0) GO TO 100
      NSKIP=LFILT+LCOR-2
C     NSKIP = THE APPROXIMATE NUMBER OF REDUNDANT POINTS AT THE BEGINNIN
C     AND END OF EACH FILTERED SCAN
      WRITE(6,1012) (ANAME(I),I=1,20)
      EOFC=0
C     COUNTERS FOR SORTING DATA INTO PROPER BINS.
  100 TBC=TBC+1
      LGTH=LENGTH
      ICODE=0
      ISKIP=0
C     ISKIP IS NUMBER OF SCANS TO BE SKIPPED WHEN RECORDING ERRORS
C     WERE NOTICED.  SET TO ZERO BUT MAY BE CHANGED.
      CALL GDATA(IDATA,LGTH,ICODE,ISKIP)
C     ICODE NOT ZERO ON RETURN FROM THE SUBROUTINE GDATA MEANS
C     A FAULT IN SCAN.
      IF(ICODE.EQ.0) GO TO 102
      IF(ICODE.EQ.6) GO TO 101
      WRITE(6,1003) TBC,LGTH
1003  FORMAT(5X,'BLOCK',I3,' FAILED TO READ,',I5,' BYTES PRESENT'/)
      BARY(TBC)=0
      GO TO 100
  101 BARY(TBC)=2
      EOFC=EOFC+1
      WRITE(6,1004) TBC
 1004 FORMAT('0    READ END OF FILE AT BLOCK',I3/)
      IF(EOFC.EQ.2) GO TO 20
      GO TO 103
  102 WRITE(6,1005) TBC
 1005 FORMAT(5X,'GDATA READ BLOCK',I3/)
      GBC=GBC+1
      BARY(TBC)=1
      DO 1 I=1,LENGTH
      NUMBER=IDATA(I)/100
      NSTRIP=NUMBER*100
      NIDENT=IDATA(I)-NSTRIP
      DATA(I)=FLOAT(NUMBER)/100000.0
    1 CONTINUE
      CALL SEC DIF(DATA,XCOR,LENGTH,0.15)
C     REMOVE ERROR SPIKES FROM DATA WHEN ERROR IS IN FIRST DECIMAL
C     PLACE. FILTER  AND CROSSCORRELATE THE BLOCK (SCAN) OF DATA
C     FIRST SMOOTH
      CALL BOX(W,LFILT)
      CALL CONSYM(LENGTH,DATA,LFILT,W,XCOR)
      CALL TIDY(XCOR,LENGTH,LFILT)
      CALL MOVE(XCOR,DATA,LENGTH)
C     SECOND SMOOTH
      CALL BOX(W,LCOR)
      CALL CONSYM(LENGTH,DATA,LCOR,W,XCOR)
      CALL TIDY(XCOR,LENGTH,LCOR)
      NFLAG=0
C     FIND THE TIMES WHEN PEAKS OCCUR.
      CALL TIMES(NPEAKS,LENGTH,DATA,XCOR,C,D,DIS,NFLAG)
      IF(NFLAG.EQ.0) GO TO 3
      WRITE(6,1006) NFLAG,TBC,(D(I),I=1,NFLAG)
 1006 FORMAT(5X,I3,' PEAKS FOUND IN BLOCK',I3,5X,'PEAKS OCCUR AT',7F7.0/
     1)
      IF(NFLAG.GT.5) GO TO 333
      IF(NFLAG.LE.3) GO TO 333
      IF(D(5).GT.350.0) GO TO 33
      GO TO 333
   33 IF(C(5).LT.C(4)*0.20) GO TO 3
  333 BARY(TBC)=0
      GBC=GBC-1
      GO TO 100
    3 NEQ=NEQ+NPEAKS
      WRITE(6,1007) (C(I),D(I),I=1,NPEAKS)
 1007 FORMAT(5X,5(F8.6,2X,F4.0,5X))
      WRITE(6,1008) NIDENT
 1008 FORMAT(1X,'PEAK HEIGHTS AND TIMES. CORRECTED FOR BASELINE BELOW.
     1                 I.D.=',I2)
C     CORRECT FOR BASELINE.
      CALL FINBAS(C,D,NSKIP,XCOR,DATA,NPEAKS,LENGTH)
      WRITE(6,1007) (C(I),D(I),I=1,NPEAKS)
      WRITE(6,1009)
 1009 FORMAT('0')
      ADD=FLOAT((TBC-1)*(LENGTH+IRG))
C     INCREASE TIMES TO CORRESPOND TO ACTURAL POSITION ON
C     RECORD.
      DO 2 I=1,NPEAKS
    2 D(I)=D(I)+ADD
C     PUT TIMES AND PEAK HEIGHTS IN PROPER POSITION IN ARRAYS.
      DO 4 I=1,NPEAKS
      J=JEND+I
      PHITES(J)=C(I)
    4 PTIMES(J)=D(I)
      JEND=JEND+NPEAKS
      GO TO 100
  103 CONTINUE
      IF(GBC.GE.2) GO TO 104
      WRITE(6,1010)
 1010 FORMAT(5X,'INSUFFICIENT NUMBER OF SCANS'/)
      GO TO 2000
C     SCALF TIMES TO RANGE -1 TO + 1.
  104 CALL SCAL 1 1(PTIMES,NEQ)
C     SORT DATA READY FOR FORMING MATRIX.
C     NOTE THAT |DAT| ABD DAB| ARE DOUBLE PRECISION, THIS IS REQUIRED.
C     CONVERT ALL NUMBERS TO DOUBLE PRECISION AT THIS POINT.
      DO 7 I=1,GBC
      DO 7 J=1,NPEAKS
      K=J+(I-1)*NPEAKS
      DAT(I,J)=DBLE(PTIMES(K))
    7 DAB(I,J)=DBLE(PHITES(K))
C     FORM MATRIX.
      CALL MARMAT(DAT,DAB,FMAT,RHS,NPEAKS,GBC,IDG,IRFMAT)
      NVAR=IDG+NPEAKS
      IWN=NEQ*NVAR
      IFR=NVAR*NVAR
      IQ=0
      CALL MATA(FMAT,R,NEQ,NVAR,IQ)
C     SOLVE MATRIX.
C     OBTAIN (FMAT TRANSPOSE FMAT) WHICH IS IN UPPER TRIANGULAR FORM
C     AND IS MADE TO GENERAL FORM BY THE SUBROUTINE TSONG.
C     TO OBTAIN THE INVERSE OF (FMAT TRANSPOSE FMAT) BY  'MINV'.
```

```
      CALL TSONG(R,NVAR)
      CALL MINV(R,NVAR,PR,L,M)
      IF(PR.EQ.0.0D0) GO TO 8
      GO TO 9
C     RHS = RIGHT HAND SIDE VECTOR.
    8 WRITE(6,1011)
 1011 FORMAT(5X,'SINGULARITY IN MATRIX R, NO INVERSE CAN BE FOUND'/)
      GO TO 2000
C     TO OBTAIN PRODUCT OF (FAMT TRANSPOSE ) AND (RHS) AND STORE
C     AT POSITIONS  AUX(NVAR).
    9 CALL SOLS(TRFMAT,RHS,NVAR,IWN,AUX)
C     TO OBTAIN FINAL SOLUTION VECTOR
      CALL SOLS(R,AUX,NVAR,IER,X)
C     TO OBTAIN VARIANCE AND COVARIANCE MATRIX BY CALLING PAUL AND ERROR
C     LSRES IS THE LEAST SQUARE RESIDUALS.
      CALL PAUL(FMAT,X,NVAR,IWN,NEQ,LSRES)
      H=0.0D0
      DO 10 I=1,NEQ
   10 H=H+(LSRES(I)-RHS(I))**2
      SIGMA=H/(NEQ-NVAR)
      DO 110 I=1,IER
  110 R(I)=R(I)*SIGMA
      LSRES(1)=R(1)
      LSRES(2)=R(NVAR+2)
      LSRES(3)=R(2*NVAR+3)
      LSRES(4)=R(2)
      LSRES(5)=R(3)
      RHO12=R(2)/DSQRT(R(1)*R(NVAR+2))
      RHO13=R(3)/DSQRT(R(1)*R(2*NVAR+3))
C     TO OBTAINRATIOS AS 206/204,207/204,208/204 AS R(I),R(3),R(4).
```

```
      NP1=NPEAKS-1
      DO 11 I=1,NP1
   11 R(I+1)=1.0D0/X(I)
      R(1)=1.0D0
      IDG1=IDG+1
      DO 12 I=1,IDG1
      J=I+NP1
C     TO SORT OUT RATIOS AND POLYNOMIAL COEFFICIENTS.
   12 A(I)= X(J)
      WRITE(6,1002)
      WRITE(6,1012) (ANAME(I),I=1,20)
 1012 FORMAT(5X,20A4//)
      WRITE(6,1013)
 1013 FORMAT('  LENGTH  NO.OF BLOCKS  FILTER HALF WIDTHS  IDENT.NOS. POL
     1Y.DEG. DIS'/)
      WRITE(6,1014) LENGTH,TBC,LFILT,LCOR,IDENT,NIDENT,IDG,DIS
 1014 FORMAT(2X,I4,7X,I3,9X,I3,4X,I3,9X,I3,2X,I3,5X,I3,5X,F4.3//)
      WRITE(6,1015)
 1015 FORMAT(2X,'SUMMARY OF BLOCK STATUS   0-BAD DATA  1-GOOD DATA  2-E
     1D OF FILE'/)
      WRITE(6,1016) (BARY(I),I=1,TBC)
 1016 FORMAT(9X,30(2X,I1)/)
      WRITE(6,1017)
 1017 FORMAT('0 POLYNOMIAL COEFFICIENTS')
      WRITE(6,1018) (A(I),I=1,IDG1)
 1018 FORMAT(2X,10D13.5)
C     OBTAIN DEVIATIONS IN RATIOS AS AUX(1),AUX(2),AUX(3).
      DO 16 J=1,NPEAKS
      NADD=203
      IF(J.GT.1) NADD=NADD+1
      DO 15 I=1,GBC
C     CALCULATE RESIDUALS OF PEAKS BY SUBROUTINE CHEBEV.
C     CALC  COME OUT IN TERMS OF 204 PEAK HEIGHTS AND MUST BE
C     ADJUSTED TO ACTUAL HEIGHTS.
      CALL CHEBEV(A,IDG1,DAT(I,J),CALC)
      CALC=CALC*R(J)
   15 RES(I)=CALC-DAB(I,J)
      JPEAK=J+NADD
      WRITE(6,1019) JPEAK
 1019 FORMAT('0 RESIDUALS FOR ',I3,' PEAKS')
      WRITE(6,1020) (RES(I),I=1,GBC)
 1020 FORMAT(1X,10F11.6)
   16 CONTINUE
C     CALCULATE CORRELATION COEFFICIENTS RHO 12, RHO 13.
      RA7=R(3)/R(2)
      RA8=R(4)/R(2)
      AUX(1)=(DSQRT(LSRES(1))/X(1))*R(2)
      AUX(2)=(DSQRT(LSRES(2))/X(2))*R(3)
      AUX(3)=(DSQRT(LSRES(3))/X(3))*R(4)
      S1=AUX(1)/R(2)
      S2=AUX(2)/R(3)
      S3=AUX(3)/R(4)
      AUX(4)=RA7*DSQRT(S1**2+S2**2-2.0D0*RHO12*S1*S2)
      AUX(5)=RA8*DSQRT(S1**2+S3**2-2.0D0*RHO13*S1*S3)
      WRITE(6,1009)
      WRITE(6,2021)
 2021 FORMAT('0',26X,'206/204',5X,'207/204',5X,'208/204',5X,'207/206',5X
     1,'208/206')
      WRITE(6,1021) R(2),R(3),R(4),RA7,RA8
 1021 FORMAT('0 RATIOS OBTAINED ARE ',5F12.4/)
```

```
      WRITE(6,1022)  (AUX(I),I=1,5)
1022  FORMAT('  STANDARD DEVIATIONS ',5F12.4/)
C     MULTIPLY BY THE NORMALIZED CORRECTION FACTORS.
      R(2)=R(2)*.99815
      R(3)=R(3)*.99723
      R(4)=R(4)*.99630
      WRITE(6,1023)  R(2),R(3),R(4)
1023  FORMAT('  CORRECTED RATIOS ARE',3F12.4//)
      WRITE(6,1024)  RHO12,RHO13
1024  FORMAT('  CORRELATION COEFFS.        ',2F12.4)
      GO TO 2000
   20 CONTINUE
      WRITE(6,1025)
1025  FORMAT(5X,'END OF DATA SET'//)
      STOP
      END





      SUBROUTINE BOX(W,N)
C     PRODUCES A HALF WIDTH FILTER WITH NORMALIZED UNIT WEIGHTS
C    FOR USE IN SMOOTHING DATA
      DIMENSION W(1)
      NN = N+N-1
      DO 1 I=1,N
    1 W(I) = 1.0/FLOAT(NN)
      RETURN
      END
      SUBROUTINE CONSYM(N,DATA,L,FILT,OUTPUT)
C   THIS SUBROUTINE PERFORMS A CONVOLUTION AFTER THE SUBROUTINE OF
C   ROBINSON BUT SHIFTS THE OUTPUT BY HALF THE WIDTH OF THE FILTER
C   IN ORDER TO PRESERVE THE TIMING OF THE POINTS IN THE BLOCK.
      DIMENSION DATA(1),FILT(1),OUTPUT(1)
      LAGS = N-L-L+2
      DO 10 I=1,LAGS
      J = I+L-1
      CALL SYMDOT(DATA(I),FILT,L,OUTPUT(J))
   10 CONTINUE
      RETURN
      END





      SUBROUTINE SYMDOT (Y,F,N,D)
C   SYMMETRICAL DOT PRODUCT.  COMPUTES DOT PRODUCT WITH A FILTER
C   WHICH IS SYMMETRICAL AND HAS BEEN SPECIFIED OVER HALF ITS RANGE
C   PLUS THE CENTER POINT.
      DIMENSION Y(1),F(1)
      D = 0.0
      M = N-1
      K = N+M
      DO 10 J=1,M
      D = F(J)*(Y(J)+Y(K))+D
      K = K-1
   10 CONTINUE
      D = D+F(N)*Y(N)
      RETURN
      END
      SUBROUTINE TIDY(X,N,M)
C   FILLS IN THE END OF THE ARRAY WITH FIRST AND LAST POINT REPEATED
C   SO THAT LENGTH IS MAINTAINED. THIS PRESERVES THE TIMING OF THE BLOCK
C   DATA.
      DIMENSION X(1)
C   N IS THE LENGTH OF ARRAY
C   M IS THE LENGTH OF FILTER THAT WAS USED
C   I.E. ONE LOBE PLUS CENTER POINT
      IM = M-1
      DO 1 I=1,IM
    1 X(I) = X(M)
      M2 = N+1-M
      M1 = M2+1
      DO 2 I=M1,N
    2 X(I) = X(M2)
      RETUPN
      END




      SUBROUTINE MOVE(X,Y,LX)
C   TRANSFERS THE FIRST ARRAY INTO THE SECOND WITHOUT DESTROYING
C   THE FIRST
      DIMENSION X(2),Y(2)
      DO 1 I=1,LX
    1 Y(I) = X(I)
      RETURN
      END
      SUBROUTINE SEC DIF(A,B,LA,ALEV)
C    FINDS SECOND DIFFERENCES AND TESTS TO CHECK FOR ERRORS
C    IN THE FIRST SIGNIFICANT FIGURE
      DIMENSION A(1),B(1),W(2)
      W(1) = 1.0
      W(2) = -2.0
      CALL CONSYM(LA,A,2,W,B)
      CALL TIDY(B,LA,2)
      TEST = ABS(B(1))
      IF(TEST.GE.ALEV) GO TO 2
      GO TO 3
    2 B(1) = ALEV/2.0
    3 CONTINUE
      DO 1 I=1,LA
      TEST = ABS(B(I))
      IF(TEST.LT.ALEV) GO TO 1
      A(I) = (A(I+1)+A(I-1))/2.0
    1 CONTINUE
      RETURN
      END





      SUBROUTINE SCAL 1 1(T,N)
      DIMENSION T(100)
      T ONE=T(1)
      T N=T(N)
      TFACT= 2.0 / (T N-T ONE)
      DO 1 I=1,N
    1 T(I) = (T(I) - T ONE) * TFACT -1.0
      RETURN
      END
      SUBROUTINE MAKMAT(DAT,DAB,PMAT,RHS,NIG,NGP,IDG,TRFMAT)
      REAL*8 DAT(25,4),DAB(25,4),PMAT(2000),RHS(100),WA,WB,S,
     1BMAT(150,40),TRFMAT(2000)
      IEQ=0
      IDP=IDG+1
      DO 4 IGP=1,NGP
      IEQ=IEQ+1
      RHS(IEQ)= DAB(IGP,1)
      DO 1 J=2,NIG
      BMAT(IEQ,J-1)=0.0D0
    1 CONTINUE
C     CHEBYSHEV INSERT FOR MAKMAT
      WA=1.0D0
      WB=DAT(IGP,1)
      K=NIG
      DO 2 J=1,IDP
      BMAT(IEQ,K)=WA
      S=WA
      WA=2.0D0*DAT(IGP,1)*WA-WB
      WB=S
      K=K+1
    2 CONTINUE
      DO 4 IG=2,NIG
      IEQ=IEQ+1
      RHS(IEQ)= 0.0D0
      DO 3 J=2,NIG
      BMAT(IEQ,J-1)=0.0D0
    3 CONTINUE
      BMAT(IEQ,IG-1)=-DAB(IGP,IG)
C     CHEBYSHEV INSERT FOR MAKMAT
      WA=1.0D0
      WB=DAT(IGP,IG)
      K=NIG
      DO 4 J=1,IDP
      BMAT(IEQ,K)=WA
      S=WA
      WA=2.0D0*DAT(IGP,IG)*WA-WB
      WB=S
      K=K+1
    4 CONTINUE
      NVAR=NIG+IDG
      NEQ=NGP*NIG
      L=0
      DO 7 I=1,NVAR
      DO 7 J=1,NEQ
      L=L+1
    7 FMAT(L)=BMAT(J,I)
      IM=0
      DO 8 I=1,NEQ
      DO 8 J=1,NVAR
      IM=IM+1
    8 TRFMAT(IM)=BMAT(I,J)
      RETURN
      END
      SUBROUTINE MINV(A,N,D,L,M)
C    PURPOSE OF THIS SUBROUTINE IS TO INVERT A MATRIX
C    A IS INPUT MATRIX, DESTROVED IN COMPUTATION AND REPLACED BY THE RESL
C    N IS THE ORDER OF MATRIX A
C    D IS THE RESULTANT DETERMINANT
C    L IS THE WORK VECTOR OF LENGTH N
C    M IS THE WORK VECTOR OF LENGTH N
C    MATRIX A MUST BE A GENERAL MATRIX
C    STANDARD GAUSS-JORDAN METHOD IS USED, DETERMINANT ALSO CALCULATED.
      DIMENSION A(1),L(1),M(1)
      DOUBLE PRECISION A,D,BIGA,HOLD
C     SERACH FOR LARGEST ELEMENT
      D=1.0D0
      NK=-N
      DO 80 K=1,N
      NK=NK+N
      L(K)=K
      M(K)=K
      KK=NK+K
      BIGA=A(KK)
      DO 20 J=K,N
      IZ=N*(J-1)
      DO 20 I=K,N
      IJ=IZ+I
   10 IF(DABS(BIGA)-DABS(A(IJ)))15,20,20
   15 BIGA=A(IJ)
      L(K)=I
      M(K)=J
   20 CONTINUE
C     INTERCHNNGE ROWS
      J=L(K)
      IF (J-K)35,35,25
   25 KI=K-N
      DO 30 I=1,N
      KI=KI+N
      HOLD=-A(KI)
      JI=KI-K+J
      A(KI)=A(JI)
   30 A(JI)=HOLD
C     INTERCHANPE COLUMNS
   35 I=M(K)
      IF(I-K)45,45,38
   38 JP=N*(I-1)
      DO 40 J=1,N
      JK=NK+J
      JI=JP+J
      HOLD=-A(JK)
      A(JK)=A(JI)
   40 A(JI)=HOLD
C     DIVIDE COLUMN BY MINUS PIVOT ( CONTAINED IN BIGA)
   45 IF(BIGA)48,46,48
   46 D=0.0D0
      RETURN
   48 DO 55 I=1,N
      IF(I-K)50,55,50
   50 IK=NK+I
      A(IK)=A(IK)/(-BIGA)
   55 CONTINUE
C     REDUCE MATRIX
      DO 65 I=1,N
      IK=NK+I
      IJ=I-N
      DO 65 J=1,N
      IJ=IJ+N
      IF(I-K)60,65,60
   60 IF(J-K)62,65,62
   62 KJ=IJ-I+K
      A(IJ)=A(IK)*A(KJ)+A(IJ)
   65 CONTINUE
C     DIVIDE ROW BY PIVOT
      KJ=K-N
      DO 75 J=1,N
      KJ=KJ+N
      IF(J-K)70,75,70
   70 A(KJ)=A(KJ)/BIGA
   75 CONTINUE
C    PRODUCT OF PIVOT
      D=D*BIGA
C    REPLACE PIVOT BY RECIPROCAL
      A(KK)=1.0D0/BIGA
   80 CONTINUE
C    FINAL ROW AND COULUMN INTERCHANGE
      K=N
  100 K=(K-1)
      IF(K) 150,150,105
  105 I=L(K)
      IF(I-K) 120,120,108
  108 JQ=N*(K-1)
      JR=N*(I-1)
      DO 110 J=1,N
      JK=JQ+J
      HOLD=A(JK)
      JI=JR+J
      A(JK)=-A(JI)
  110 A(JI)=HOLD
  120 J=M(K)
      IF(J-K)100,100,125
  125 KI=K-N
      DO 130 I=1,N
      KI=KI+N
      HOLD=A(KI)
      JI=KI-K+J
      A(KI)=-A(JI)
  130 A(JI)=HOLD
      GO TO 100
  150 RETURN
      END
      SUBROUTINE LDC(I,J,IR,N,M,MS)
C    PURPOSE OF THIS SUBROUTINE IS COMPUTE A VECTOR SUBSCRIPT FOR AN
C    ELEMENT IN A MATRIX OF SPECIFIED STORAGE MODE
C    I  IS THE ROW NUMBER OF ELEMENT
C    J IS COLUMN NUMBER OF THE ELEMENT
C    IR RESULTANT VECTOR SUBSCRIPT
C    N IS NUMBER OF ROW IN MATRIX
C    M NUMBER OF COLUMNS IN MATRIX
C    MS IS ONE DIGIT NUMBER; 0 FOR GENERAL, 1 FOR SYMMETRIC,2 FOR DIAGINA
      IX=I
      JX=J
      IF(MS-1) 10,20,30
   10 IRX=N*(JX-1)+IX
      GO TO 36
   20 IF(IX-JX)22,24,24
   22 IRX=IX+(JX*JX-JX)/2
      GO TO 36
   24 IRX=JX+(IX*IX-IX)/2
      GO TO 36
   30 IRX=0
      IF(IX-JX)36,32,36
   32 IRX=IX
   36 IR=IRX
      RETURN
      END
```

```
         SUBROUTINE MATA(A,R,N,M,MS)
C   PURPOSE OF THIS IS  PREMULTIPLY A MATRIX BY ITS TRANSPOSE TO FORM
C   A SYMMETRIC MATRIX
C   A IS THE INPUT MATIRX
C   R IS THE OUTPUT MATRIX
C   N IS NUMBER OF ROWS IN A
C   M IS THE NUMBER OF COLUMNS IN A , ALSO NUMBER OF ROWS AND NUMBER OF
C   COULUMNS IN R
C   MS IS ONE DIGIT NUMBER FOR STORAGE MIDE OF MATRIX A;0 FOR GENERAL, 1
C   SYMMETRIC, AND 2 FRO DIAGONAL
C   MATRIX R CANNOT BE IN THE SAME POSITION AS MATRIX A
C   MATRIX R IS ALWAYS A SYMMETRIC MATRIX WITH A STORAGE MIDE=1
C   REGARDLESS THE STORAGE MODE OF THE INPUT MATRIX A. A IS NOT CHANGED
C   SUBROUTINE LDC IS REQUIRED
      DIMENSION A(1),R(1)
      DOUBLE PRECISION A,R
      DO 60 K=1,M
      KX=(K*K-K)/2
      DO 60 J=1,M
      IF(J-K)10,10,60
   10 IR=J+KX
      R(IR)=0.0D0
      DO 60 I=1,N
      IF(MS)20,40,20
   20 CALL LDC(I,J,IA,N,M,MS)
      CALL LDC(I,K,IB,N,M,MS)
      IF(IA)30,60,30
   30 IF(IB)50,60,50
   40 IA=N*(J-1)+I
      IB=N*(K-1)+I
   50 R(IR)=R(IR)+A(IA)*A(IB)
   60 CONTINUE
      RETURN
      END
      SUBROUTINE TSONG(R,NVAR)
C  THIS PROGRAM FILLS UP ALL ELEMENTS OG THE SYMMETRICAL MATRIX OF (A TB
C   A) FOUND BY SUBROUTINE (MATA) AND WERE STORED IN COMPACT FORM OF MOD
C  THIS SUBROUTINE IS NECESSARY FOR OBTAINING THE INVERSE OF (A TRANSPOS
C  SUBROUTINE (MINV) OF PAGE 55 , SCIENTIFIC SUBROUTINE PACKAGES.
C  R IS THE INPUT UPPER TRIANGULAR MATRIX , REPLACED BY THE RESULTANT SC
C  SYMMETRICAL MATRIX
      REAL*8 R(700),B(30,30)
      N=0
      DO 1 J=1,NVAR
      DO 1 I=1,J
      N=N+1
      B(I,J)=R(N)
      B(J,I)=R(N)
    1 CONTINUE
      L=0
      DO 2 I=1,NVAR
      DO 2 J=1,NVAR
      L=L+1
      R(L)=B(J,I)
    2 CONTINUE
      RETURN
      END
      SUBROUTINE SOLS(A,W,NVAR,N,C)
      REAL*8 A(700),W(100),B,C(25)
      DO 1 I=1,NVAR
      B=0.0D0
      K=0
      DO 1 J=I,N,NVAR
      K=K+1
      B=B+A(J)*W(K)
      C(I)=B
    1 CONTINUE
      RETURN
      END
```

```
      SUBROUTINE ERROR(R,LSRES,IER)
      REAL*8 R(700),LSRES(100)
      DO 1 I=1,IER
      R(I)=R(I)*LSRES(1)
    1 CONTINUE
      RETURN
      END
      SUBROUTINE CHEBEV(A,N,X,S)
C    COMPUTES THE SUM OF 'N' TERMS OF THE CHEBYSHEV POLYNOMIAL
C    AFTER "MODERN COMPUTING METHODS" PAGE 77, USING DOUBLE
C    PRECISION ARITHMETIC.
C
      REAL *8 A(1),X,S,B,B2,BPLUS1,BPLUS2
      BPLUS1 = 0.0D0
      BPLUS2 = 0.0D0
      DO 10 I=1,N
      J = N-I
      B = 2.0D0*X*BPLUS1-BPLUS2+A(J+1)
      BPLUS2 = BPLUS1
      BPLUS1 = B
      IF(J.EQ.2) B2=B
   10 CONTINUE
      S = (B+A(1)-B2)/2.0D0
      RETURN
      END



      SUBROUTINE PAUL(A,W,NVAR,M,NEQ,C)
      REAL*8 A(2000),W(100),B,C(25)
      DO 1 I=1,NEQ
      B=0.0D0
      K=0
      DO 1 J=I,M,NEQ
      K=K+1
      B=B+A(J)*W(K)
      C(I)=B
    1 CONTINUE
      RETURN
      END
      SUBROUTINE TIMES    ( NP, MAX, A, B, C, D, DIS, NFLAG)
C    ENTER WITH NFLAG EQUAL ZERO, CHANGE ONLY IF WRONG NUMBER OF PEAKS
C    ARE FOUND.
      DIMENSION A(1), B(1), C(1), D(1)
C      NP - THE NUMBER OF PEAKS IN THE BLOCK
C      MAX - THE NUMBER OF STEPS PER SCAN (I.E. PER BLOCK)
C      A - FILTERED DATA
C      B - THE XCOR FUNCTION
C      C - THE PEAK HEIGHTS
C      D - THE TIMES OF THESE
C      L - THE PEAK COUNTER
C      J - THE DATA POINT COUNTER
      L = 1
      J = 38
C    SKIPS THE FIRST 38 POINTS TO AVOID SPURIOUS FLYBACK PEAKS.
    1 J = J + 1
      IF ( J .GT. MAX ) GO TO 2
      IF ( B(J) .LT. DIS ) GO TO 1
      IF ( B(J) .LE. B(J-1)) GO TO 1
      IF ( B(J+1) .GT. B(J)) GO TO 1
      C(L) = (A(J-2) +A(J-1) +A(J) +A(J+1) +A(J+2))/5.0
C     AVERAGE 5 POINTS ABOUT THE PEAK CENTER
      D(L) = FLOAT(J)
      L = L + 1
      GO TO 1
    2 IF(NP.NE.(L-1)) NFLAG = (L-1)
C     IF THE NUMBER OF PEAKS FOUND IS NOT EQUAL TO THE NUMBER EXPECTED
C     SET NFLAG EQUAL TO THE NUMBER FOUND, OTHERWISE LEAVE IT AS ZERO
      RETURN
      END
      SUBROUTINE FINBAS(C,D,NSKIP,XCOR,DATA,NPEAKS,LENGTH)
      DIMENSION C(1),D(1),XCOR(1),DATA(1)
      IT1=IFIX(D(1))
C     END OF FIRST SWEEP FOR MINIMUM IS AT TIME OF FIRST PEAK.
      H1=XCOR(1)
      ITB1=1
C     SET INITIAL VALUE OF BASELINE HEIGHT AND ITS POSITION.
      DO 1 I=1,IT1
      IF(XCOR(I).LE.H1) GO TO 2
      GO TO 1
    2 H1=XCOR(I)
      ITB1=I
    1 CONTINUE
      TB1=FLOAT(ITB1)
C
C     SET END OF SECOND SWEEP
      IT2=IFIX(D(2))
      H2=XCOR(IT1)
      ITB2=IFIX(D(1))
      DO 3 I=IT1,IT2
      IF(XCOR(I).LE.H2) GO TO 4
      GO TO 3
    4 H2=XCOR(I)
      ITB2=I
    3 CONTINUE
      TB2=FLOAT(ITB2)
```

```
C
      NEND=LENGTH-NSKIP
      IT3=IFIX(D(4))
      H3=XCOR(IT3)
      ITB3=IFIX(D(4))
      DO 5 I=IT3,NEND
      IF(XCOR(I).LE.H3) GO TO 6
      GO TO 5
    6 H[illegible]=XCOR(I)
      ITB3=I
    5 CONTINUE
      TB3=FLOAT(ITB3)
C
C     FIND SLOPE OF BASELINE FOR INTERPOLATION
C
      SLP1=(H2-H1)/(TB2-TB1)
      SLP2=(H3-H2)/(TB3-TB2)
C
      BAS204=H1+(D(1)-TB1)*SLP1
      BAS206=H2+(D(2)-TB2)*SLP2
      BAS207=H2+(D(3)-TB2)*SLP2
      BAS208=H2+(D(4)-TB2)*SLP2
C
      C(1)=C(1)-BAS204
      C(2)=C(2)-BAS206
      C(3)=C(3)-BAS207
      C(4)=C(4)-BAS208
      RETURN
      END
```

APPENDIX III

DITHIZONE EXTRACTION PROCEDUES

All chemical ware was initially cleaned with distilled water and placed in hot HNO_3 for several hours or overnight before a final rinsing with pure water before being used. The following is an outline of the procedures used in purifing the leads for mass spectrometer analysis.

(1). Adjust the pH of the lead containing solution of 3N HNO_3 with ammonium hydroxide (28%) to about 10 in a separatory funnel.

(2). Add 1c.c. of KCN (in 2% NH_4OH) and 1 c.c. of 30% ammonia citrate to the solution to form complexes of other reacting metals.

(3). Shake the solution with some dithizone (0.1% in Chloroform). The reaction of dithizone with lead gives a brilliantly colored pink solution. Transfer the chloroform-dithizone solution containing lead into a smaller separatory funnel.

(4). Repeat step (3) until the solution no longer shows pink color indicating all the lead has been taken up.

(5). Add 1.5 c.c. of 2% HNO_3 into the pink solution and shake it, the lead is redissolved in the 2% HNO_3. Discard the dithizone.

(6). Wash the 2% HNO_3 solution containing the lead with about 5 c.c. of chloroform at least twice by adding the chloroform into the solution and vigorously shake the combined solution. Discard the chloroform.

(7). Transfer the washed 2% solution from the top of the separatory funnel into a 2 c.c. centrifuge tube and adjust the pH of this solution to about 4.5 and bubble it with H_2S gas causing PbS sample to be precipitated.

(8). Centrifuge the precipitated PbS ready for loading onto the filament for mass spectrometer analysis.

VITA

NAME: Tsong, Chin-Fong (Frank)

PLACE OF BIRTH: Kaohsiung, Taiwan, Republic of China

YEAR OF BIRTH: 1936

POST-SECONDARY EDUCATION AND DEGREES:

Taiwan Normal University
Taipei, Taiwan
1955-1959 B.Sc.

Dalhousie University
Halifax, Nova Scotia, Canada
1962-1965 M.Sc.

HONOURS AND AWARDS:

Dalhousie Graduate Scholarship
Dalhousie University
1962-1964

Medicine Hat College Employment Bursary
Medicine Hat College
1964-1965

Graduate Teaching Assistantship
University of Alberta
1968-1969

University of Alberta Dissertation Fellowship
University of Alberta
1969-1970